

Interplay between superconductivity and non-Fermi liquid at a quantum-critical point in a metal.

I: The γ model and its phase diagram at $T = 0$. The case $0 < \gamma < 1$.

Artem Abanov¹ and Andrey V. Chubukov²

¹*Department of Physics, Texas A&M University, College Station, USA*

²*School of Physics and Astronomy and William I. Fine Theoretical Physics Institute, University of Minnesota, Minneapolis, MN 55455, USA*

(Dated: May 9, 2022)

Abstract

Near a quantum-critical point in a metal a strong fermion-fermion interaction, mediated by a soft boson, acts in two different directions: it destroys fermionic coherence and it gives rise to an attraction in one or more pairing channels. The two tendencies compete with each other. We analyze a class of quantum-critical models, in which momentum integration and the selection of a particular pairing symmetry can be done explicitly, and the competition between non-Fermi liquid and pairing can be analyzed within an effective model with dynamical electron-electron interaction $V(\Omega_m) \propto 1/|\Omega_m|^\gamma$ (the γ -model). In this paper, the first in the series, we consider the case $T = 0$ and $0 < \gamma < 1$. We argue that tendency to pairing is stronger, and the ground state is a superconductor. We argue, however, that superconducting state is highly non-trivial as there exists a discrete set of topologically distinct solutions for the pairing gap $\Delta_n(\omega_m)$ ($n = 0, 1, 2, \dots, \infty$). All solutions have the same spatial pairing symmetry, but differ in the time domain: $\Delta_n(\omega_m)$ changes sign n times as a function of Matsubara frequency ω_m . The $n = 0$ solution $\Delta_0(\omega_m)$ is sign-preserving and tends to a finite value at $\omega_m = 0$, like in BCS theory. The $n = \infty$ solution corresponds to an infinitesimally small $\Delta(\omega_m)$, which oscillates down to the lowest frequencies as $\Delta(\omega_m) \propto |\omega_m|^{\gamma/2} \cos(2\beta \log(|\omega_m|/\omega_0))$, where $\beta = O(1)$ and ω_0 is of order of fermion-boson coupling. As a proof, we obtain the exact solution of the linearized gap equation at $T = 0$ on the entire frequency axis for all $0 < \gamma < 1$, and an approximate solution of the non-linear gap equation. We argue that the presence of an infinite set of solutions opens up a new channel of gap fluctuations. We extend the analysis to the case where the pairing component of the interaction has additional factor $1/N$ and show that there exists a critical $N_{cr} > 1$, above which superconductivity disappears, and the ground state becomes a non-Fermi liquid. We show that all solutions develop simultaneously once N gets smaller than N_{cr} .

I. INTRODUCTION.

The interplay between superconductivity and pairing near a quantum-critical point (QCP) in a metal is a fascinating subject, which attracted substantial attention in the correlated electron community after the discovery of superconductivity (SC) in the curates, heavy-fermion and organic materials, and, more recently, Fe-pnictides and Fe-chalcogenides. (see, e.g., Refs.^{1–12}). Itinerant QC models, analyzed analytically in recent years include, e.g., models of fermions in spatial dimensions $D \leq 3$ (Refs.^{13–18}), 2D models near a spin-density-wave (SDW) and charge-density-wave (CDW) instabilities (Refs. ^{19–35}), $2k_F$ density-wave instability (Refs.³⁶), pair-density-wave instability ^{37,38}, $q = 0$ instabilities towards a Pomeranchuk order instability^{39–49} and towards circulating currents⁵⁰, 2D fermions at a half-filled Landau level⁵¹, generic QC models with different critical exponents^{52–60}, SYK and SYK-Yukawa models^{61–65}, strong coupling limit of electron-phonon superconductivity,^{66–70}, and even color superconductivity of quarks, mediated by gluon exchange⁷¹. These problems have also been studied using various numerical techniques^{35,72–75}

From theory perspective, the key interest in the pairing near a QCP is due to the fact that an effective dynamic electron-electron interaction, $V(q, \Omega)$, mediated by a critical collective boson, which condenses at a QCP, provides strong attraction in one or more pairing channels and, at the same time, gives rise to non-Fermi liquid (NFL) behavior in the normal state. The two tendencies compete with each other: fermionic incoherence, associated with NFL behavior, destroys Cooper logarithm and reduces the tendency to pairing, while the opening of a SC gap eliminates the scattering at low energies and reduces the tendency to NFL. To find the winner (SC or NFL) one needs to analyze the set of integral equations for the fermionic self-energy, $\Sigma(\mathbf{k}, \omega)$, and the gap function, $\Delta(\mathbf{k}, \omega)$, for fermions with momentum/frequency (\mathbf{k}, ω) and $(-\mathbf{k}, -\omega)$.

We consider the subset of models in which collective bosons are slow modes compared to dressed fermions, for one reason or the other. In this situation, which bears parallels with Eliashberg theory for electron-phonon interaction⁷⁶, the self-energy and the pairing vertex can be approximated by their values at the Fermi surface (FS) and computed within one-loop approximation. The self-energy on the FS, $\Sigma(\mathbf{k}, \omega)$ is invariant under rotations from the point group of the underlying lattice. The rotational symmetry of the gap function $\Delta(\mathbf{k}_F, \omega)$ and the relation between the phases of $\Delta(\mathbf{k}_F, \omega)$ on different FS's in multi-band

systems are model specific. Near a ferromagnetic QCP, the pairing interaction mediated by a soft boson is attractive in the p-wave channel. Near an antiferromagnetic QCP, the strongest attraction is in d -wave channel for the case of a single FS and fermionic density near half-filling. For a nearly compensated metal with hole and electron pockets, as in Fe-based superconductors, the two attractive channels near an antiferromagnetic QCP are s^{+-} and d -wave. Near a $q = 0$ nematic QCP, the pairing interaction, mediated by soft nematic fluctuations, is attractive in all channels: s -wave, p -wave, d -wave, etc. In each particular case, one has to project the pairing interaction into the proper irreducible channel, find the strongest one, and solve for the pairing vertex within a given pairing symmetry. In principle, even after projection, one has to solve an infinite set of coupled equations in momentum space as in a lattice system each irreducible representation contains an infinite set of eigenfunctions. However, near a QCP the pairing is often confined to a narrow range on the FS around special "hot spots". In this situation, the momentum integration near the FS can be carried out exactly, and the set of coupled equations for the self-energy and the gap function reduce to two 1D equations for $\Sigma(\omega)$ and $\Delta(\omega)$, each with frequency-dependent effective "local" interaction $V(\Omega)$ (Ref.²² The same holds for the cases of s-wave pairing by a soft optical phonon, when momentum-dependencies of Σ and Δ are not crucial and can be neglected, of non-s-wave pairing, when one eigenfunction gives the dominant contribution to the gap (e.g., $\cos k_x - \cos k_y$ for d -wave pairing in the cuprates), and for the case when the fermionic density of states is peaked at particular \mathbf{k}_F due to, e.g. van-Hove singularities (see e.g., 4 and references therein).

Away from a QCP, the effective $V(\Omega)$ tends to a finite value at $\Omega = 0$. In this situation, the fermionic self-energy has a FL form at the smallest frequencies, the equation for $\Delta(\omega)$ is similar to that in a conventional Eliashberg theory for phonon-mediated superconductivity, and the only qualitative distinction for electronically-mediated pairing is that $V(\Omega)$ by itself changes below T_c due to feedback from fermionic pairing on collective modes.

At a QCP, the situation becomes qualitatively different because the effective interaction $V(\Omega)$, mediated by a critical massless boson, becomes a singular function of frequency: on Matsubara axis $V(\Omega_m) \propto 1/|\Omega_m|^\gamma$ (Fig. 1). The exponent $\gamma > 0$ depends on the model, ranging from small $\gamma = 0(\epsilon)$ in models in $D = 3 - \epsilon$ to $\gamma \leq 1$ in 2D models at SDW, CDW, and nematic QCP and in Yukawa-SYK model^{4,62,63,70,77}. The case $\gamma = 2$ corresponds to fermions, interacting with a critical Einstein phonon. The set of models with $V(\Omega_m) \propto 1/|\Omega_m|^\gamma$ has

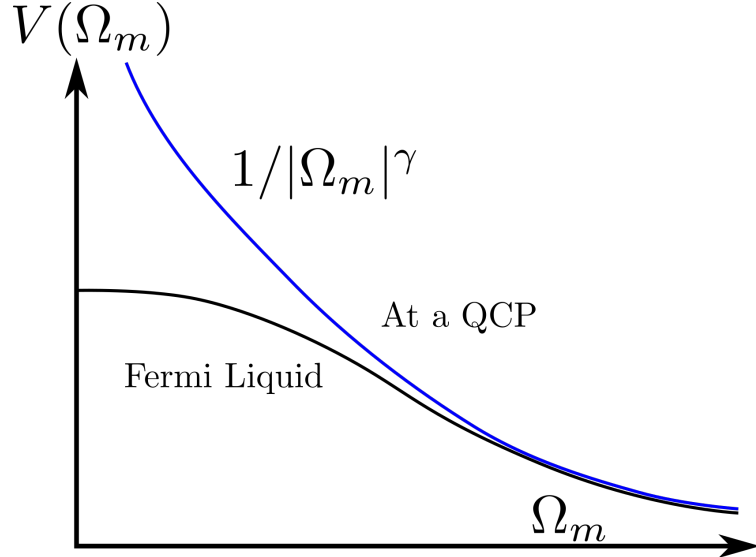


FIG. 1. Frequency dependence of the effective interaction $V(\Omega_m)$, mediated by a soft boson, at $T = 0$. Away from a QCP, $V(\Omega_m)$ tends to a finite value at $\Omega_m = 0$. Right at a QCP, the boson becomes massless, and $V(\Omega_m)$ diverges as $1/|\Omega_m|^\gamma$.

been nicknamed the γ -model, and we will use this notation. We present an (incomplete) set of models in Tables I and II.

In this and subsequent papers we present comprehensive analysis of the competition between NFL and SC within the γ -model. We define the dimensionless $V(\Omega_m)$ as $V(\Omega_m) = (\bar{g}/|\Omega_m|)^\gamma$, where \bar{g} is the effective fermion-boson coupling. This \bar{g} is the only parameter in the model with the dimension of energy, and we will see that it determines both the magnitude of the gap function $\Delta(\omega_m)$ and the upper limit of NFL behavior in the normal state, i.e., the scale below which $\Sigma(\omega_m) > \omega_m$. We show that the competition between NFL and SC holds for all values of γ , but the physics and the computational analysis are different for the models with $\gamma < 1$, $\gamma = 1$, $1 < \gamma < 2$, $\gamma = 2$, and $\gamma > 2$, which we consider separately. We show that for all γ , a NFL self-energy in the normal state does not prevent the formation of bound pairs of fermions at a non-zero onset temperature T_p . However, we argue that T_p is generally higher than the actual superconducting T_c , and at $T_c < T < T_p$ bound pairs remain incoherent. In this T range various observables, e.g., the spectral function and the density of states, display pseudogap behavior. This holds for all γ , but the width of the pseudogap phase increases with γ . We relate the pseudogap behavior to strong gap fluctuations, but

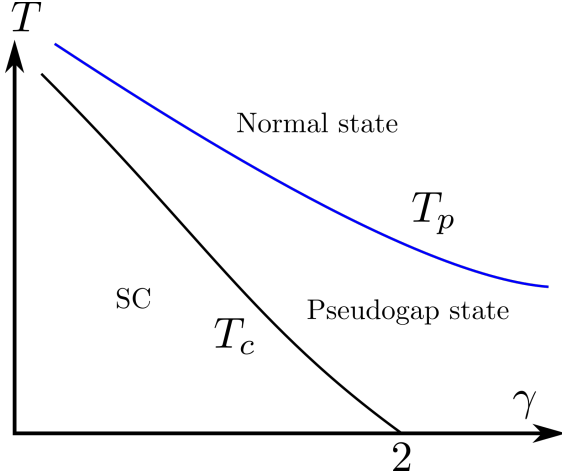


FIG. 2. The phase diagram of the γ -model. In this and subsequent papers we argue that for the pairing near a QCP the onset temperatures for the pairing and for long-range superconducting order, T_p and T_c , differ. In between T_p and T_c the system displays pseudogap behavior. The width of the pseudogap region increases with increasing γ and extends to $T = 0$ for $\gamma \geq 2$.

argue that these fluctuations can be viewed as long-wavelength phase fluctuations only in some range $\bar{T}_p < T < T_p$. At smaller $T_c < T < \bar{T}_p$, pseudogap behavior is predominantly due to the existence of low-energy "longitudinal" gap fluctuations, which change the functional form of $\Delta(\omega)$ and cause phase slips. We argue that longitudinal gap fluctuations develop a zero mode at $\gamma = 2$ in which case SC order gets destroyed already at $T = 0$. Specifically, the presence of a zero mode implies that there exists an infinite number of solutions for $\Delta(\omega)$, all with the same condensation energy. In this situation, the ground state is a mixture of different $\Delta(\omega)$, each with its own phase. We will argue that T_c gradually vanishes at $\gamma \rightarrow 2$ and remains zero at larger γ , while T_p and \bar{T}_p stay finite. We show the phase diagram in Fig. 2. Our results present the novel scenario for the pseudogap, which holds even if for a given solution for $\Delta(\omega)$ SC stiffness is larger than T_c , i.e., conventional phase fluctuations are weak. This scenario is complimentary to the one in which the smallness of the superfluid stiffness is caused by the closeness to a Mott transition (see e.g. Ref.⁷⁸ and references therein).

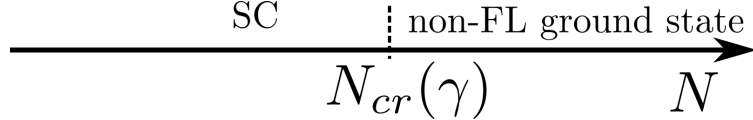


FIG. 3. The $T = 0$ phase diagram of the γ -model for $0 < \gamma < 1$ as a function of N . At smaller $N < N_{cr}$ the ground state is a superconductor. At larger $N > N_{cr}$ it is a NFL with no superconducting order. The value of N_{cr} is larger than one.

A. A brief summary of the results of this work

In this paper, the first in the series, we analyze the γ -model at $T = 0$ at $0 < \gamma < 1$. For definiteness we focus on spin-singlet pairing. The analysis of spin-triplet pairing is more involved because of different spin factors in the self-energy and the pairing vertex⁴⁷ In this paper we discuss even frequency pairing. The analysis of odd-frequency pairing⁷⁹ is more involved and requires a separate consideration.

Our key goal is to understand the interplay between the competing tendencies towards pairing and towards NFL behavior. The first comes from the interaction in the particle-particle channel, the second from the interaction in the particle-hole channel. In the original γ -model, both interactions are given by the same $V(\Omega_m)$. In order to separate the two tendencies we extend the model and introduce the knob to vary the relative strength of the interaction in the two channels. Specifically, we multiply the pairing interaction by $1/N$ and treat N as a parameter. For $N > 1$ ($N < 1$) the tendency towards pairing decreases (increases) compared to the one towards NFL ground state. The extension to integer $N > 1$ can be formally justified by extending the model from $SU(1)$ to an $SU(N)$ global symmetry⁵². In our analysis, we use the extension to arbitrary $N \neq 1$ just as a computational trick to better understand what happens in the physical case of $N = 1$.

The $T = 0$ phase diagram of the γ -model for $N \geq 1$ has been studied before^{52,56}. It was argued that for any $\gamma < 1$ there exists a critical $N_{cr} > 1$, separating a SC ground state at $N < N_{cr}$ and a normal, NFL ground state at $N > N_{cr}$ (see Fig. 3). The physical case $N = 1$ falls into the SC region. A similar result has been recently found in the study of the pairing in the SYK-type model⁶⁴.

The conventional wisdom holds that $\Delta(\omega) = 0$ for $N > N_{cr}$, is infinitesimally small for $N = N_{cr}$, and has a finite value for $N < N_{cr}$, i.e., that the linearized gap equation has the

solution at $N = N_{cr}$, and the non-linear gap equation has the solution for $N < N_{cr}$. We argue that in our case the conventional wisdom fails. Namely, we prove that the linearized equation has a solution not only for $N = N_{cr}$, but also for all $N < N_{cr}$, including the physical case of $N = 1$. We obtain the exact solution of the linearized gap equation, $\Delta(\omega_m)$, for all $N < N_{cr}$ and all $0 < \gamma \leq 1$. This $\Delta(\omega_m)$ oscillates at small $\omega_m \ll \bar{g}$ as $\Delta(\omega_m) \propto |\omega_m|^{\gamma/2} \cos(\beta_N \log(|\omega_m|/\bar{g})^\gamma + \phi_N)$, where β_N and ϕ_N are particular functions of N (for a given γ), e.g., $\beta_N \propto (N_{cr} - N)^{1/2}$ for $N \lesssim N_{cr}$. At large $\omega_m \gg \bar{g}$, $\Delta(\omega_m)$ decreases as $1/|\omega_m|^\gamma$ (see Fig. 11).

At small γ , when $\Delta(\omega_m)$ is a smooth function of frequency, the integral equation for $\Delta(\omega_m)$ can be approximated by second-order differential equation, whose solution, $\Delta_{\text{diff}}(\omega_m)$, also exists for all $N \leq N_{cr}$ and can be expressed analytically as a combination of two complex-conjugated hypergeometric functions. This $\Delta_{\text{diff}}(\omega_m)$ also oscillates at small ω_m and decays as $1/|\omega_m|^\gamma$ at large frequencies (see Fig. 9). We show that $\Delta_{\text{diff}}(\omega_m)$ coincides with the exact $\Delta(\omega_m)$ to leading order in γ .

We then analyze the non-linear gap equation. We argue that it has an infinite, discrete set of solutions, specified by integer n , which ranges between 0 and ∞ . All solutions have the same spatial gap symmetry (i.e., s -wave, d -wave ...). A solution $\Delta_n(\omega_m)$ changes sign n times as a function of frequency. Each $\Delta_n(\omega_m)$ tends to a finite value at $\omega_m = 0$, but the magnitude of $\Delta_n(0)$ progressively decreases with increasing n . At $n = \infty$, $\Delta_\infty(\omega_m)$ is the solution of the linearized gap equation, which has an infinite number of sign changes due to $\cos(\beta_N \log(|\omega_m|/\bar{g})^\gamma + \phi_N)$ oscillations running down to the smallest ω_m . The $n = 0$ solution yields sign-preserving $\Delta_0(\omega)$.

The existence of an infinite set of $\Delta_n(\omega)$, each representing a local minimum of the Luttinger-Ward (LW) functional, opens up a new channel of longitudinal gap fluctuations, which cause phase slips. As long as the set is discrete, there is a single global minimum of the LW functional. In our case, it corresponds to $n = 0$. Then, at $T = 0$ the system should display a SC order. Still, the existence of the infinite set of $\Delta_n(\omega_m)$ is a non-trivial aspect of the pairing at a QCP. In the next paper we analyze the γ -model for $0 < \gamma < 1$ at a finite T and show explicitly that for any $N < N_{cr}$ there exists a discrete, infinite set of onset temperatures for the pairing, $T_{p,n}$, and the corresponding eigenfunctions $\Delta_n(\omega_m)$ change sign n times as a function of Matsubara frequency. We argue that at $T \rightarrow 0$, each $\Delta_n(\omega_m)$ approaches the n -th solution of the non-linear integral gap equation at $T = 0$. We

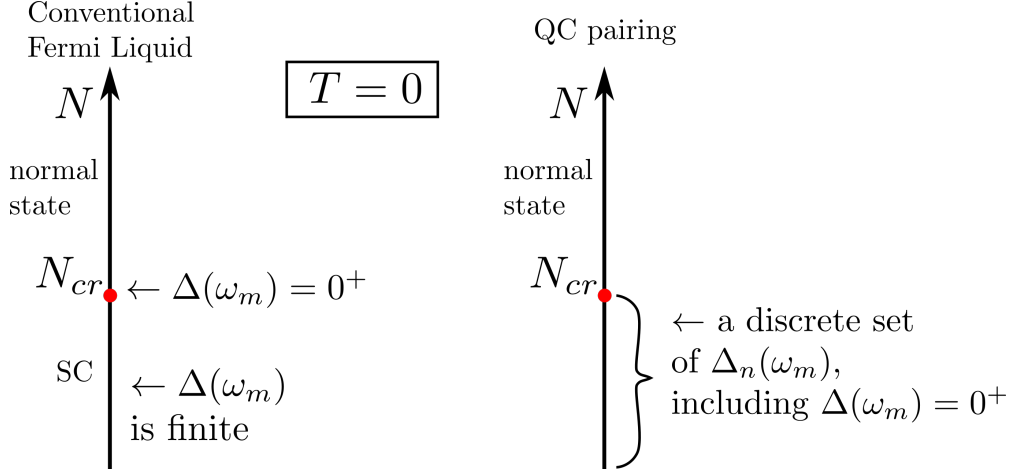


FIG. 4. A phase diagram away from a QCP (left) and at a QCP (right). Away from a QCP, the gap equation has a solution for infinitesimally small $\Delta(\omega_m)$ at $N = N_{cr}$, and for a finite $\Delta(\omega_m)$ at $N < N_{cr}$. At a QCP, a solution with infinitesimally small gap function exists for all $N \leq N_{cr}$, and for $N < N_{cr}$ there is a discrete set of solutions for a finite $\Delta_n(\omega_m)$. A gap $\Delta_n(\omega_m)$ changes sign n times as a function of ω_m .

show that away from a QCP, only solutions with $n < n_{max}$ remain, where n_{max} decreases with the deviation from a QCP.

We note in passing that a discrete set of solutions for the gap function at $T = 0$, with different *momentum* dependencies along the FS, has been detected in the analysis of $\Delta(\mathbf{k}_F)$ near a nematic QCP, Refs.^{49,80} There, however, the physics is different, and the number of solutions is finite at a QCP. This is similar to our case away from a critical point.

B. Relevance of the exact solution of the linearized gap equation

The existence of an infinite set of solutions of the non-linear gap equation is a direct consequence of a highly unusual result that at a QCP the linearized gap equation has a solution not only at $N = N_{cr}$, but also for any $N < N_{cr}$ (see Fig. 4). This does not away from a QCP, where the linearized gap equation as a solution only at $N = N_{cr}$. The proof of the existence of the solution for infinitesimally small $\Delta(\omega_m)$ for all $N \leq N_{cr}$, including the original $N = 1$, is, therefore, the central element of our analysis.

The linearized gap equation can be analyzed at frequencies much smaller and much

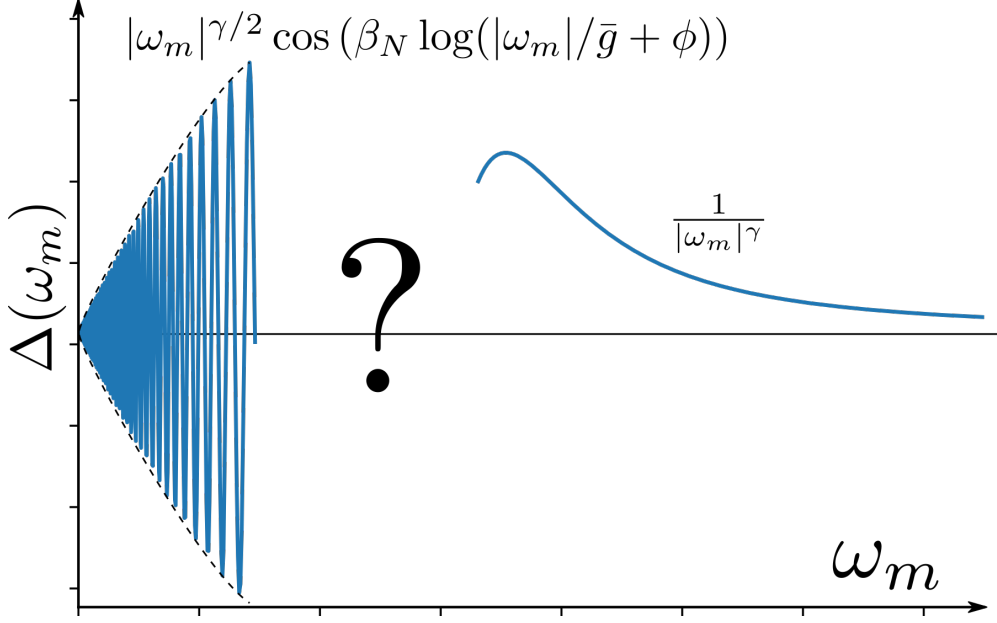


FIG. 5. The gap equation for infinitesimally small $\Delta(\omega_m)$. The solution can be found separately at large and small frequencies. There is no guarantee, however, that for any $N \leq N_{cr}$ there exists the solution, which interpolates between the two limiting forms.

larger than \bar{g} . In these two limits one can truncate the gap equation by keeping only leading terms either in ω_m/\bar{g} or in \bar{g}/ω_m . The truncated equation can be solved and yields $\Delta(\omega_m) \propto 1/|\omega_m|^\gamma$ at large ω_m and $\Delta(\omega_m) \propto |\omega_m|^{\gamma/2} \cos(\beta_N \log((|\omega_m|/\bar{g})^\gamma + \phi))$ at small ω_m , where the phase factor ϕ is a free parameter. The generic task is then to verify whether by fixing ϕ one can find $\Delta(\omega_m)$, which smoothly interpolates between small and large ω_m (see Fig. 5). The verification would be straightforward if there was a finite frequency range where both forms were valid and could be made equal by fixing ϕ . In our case, however, the low-frequency and the high-frequency regimes do not overlap, so the only option is to solve the full equation. We present the exact solution $\Delta_{\text{ex}}(\omega_m)$ and show that at small and large frequencies it reduces to known forms. The analytic expression for $\Delta_{\text{ex}}(\omega_m)$ is rather complex, but one can straightforwardly plot $\Delta_{\text{ex}}(\omega_m)$ for any input parameters (see Fig. 11).

At small γ , where the interaction $V(\Omega_m) \propto 1/|\Omega_m|^\gamma$ is a slowly varying function of frequency, the actual, integral gap equation can be approximated by a differential equation. The latter can be solved analytically, and the solution, $\Delta_{\text{diff}}(\omega_m)$, is a hypergeometric function of ω . Using the properties of a hypergeometric function at small and large value of the

argument one can explicitly verify that $\Delta_{\text{diff}}(\omega_m)$ does interpolate between the known forms at small and large ω_m if one properly chooses the value of the phase ϕ .

We show that $\Delta_{\text{ex}}(\omega_m)$ and $\Delta_{\text{diff}}(\omega_m)$ coincide at small γ and use the analytic form of $\Delta_{\text{diff}}(\omega_m)$ to analyze the structure of the gap function at different $N \leq N_{cr}$. We demonstrate by the direct comparison that at larger γ , $\Delta_{\text{ex}}(\omega_m)$ and $\Delta_{\text{diff}}(\omega_m)$ differ qualitatively. We argue that the series for the exact $\Delta_{\text{ex}}(\omega_m)$ contain non-local terms, not present for $\Delta_{\text{diff}}(\omega_m)$. These non-local terms are negligible at small γ , but must be kept for $\gamma = O(1)$, particularly near $\omega_m = \omega_{max}$, which separates oscillating behavior at smaller ω_m and $1/|\omega_m|^\gamma$ decay at larger ω_m .

C. The structure of the paper

The paper is organized as follows. In Sec. II we briefly review the γ -model and extend it to $N \neq 1$. We present the set of coupled Eliashberg equations for the pairing vertex $\Phi(\omega_m)$ and the fermionic self-energy $\Sigma(\omega_m)$ and combine them into the equations for the gap function $\Delta(\omega_m)$ and the inverse quasiparticle residue $Z(\omega_m)$.

In Secs. III- IV we study the linearized gap equation with infinitesimally small $\Delta(\omega_m)$. In Sec. III we analyze the truncated gap equation at small and large ω_m and obtain the solutions, valid in the corresponding limits. Here we identify N_{cr} and show that the solution at small frequencies changes qualitatively between $N > N_{cr}$ and $N < N_{cr}$. In Sec. IV we consider the limit of small γ and approximate the actual integral gap equation by second-order differential equation. We solve the differential equation for all ω_m and explicitly show how one can match low-frequency and high-frequency forms by fixing a single phase factor. We show that this only holds for $N \leq N_{cr}$, while for $N > N_{cr}$ the potential solution does not satisfy the condition of normalizability. In Sec. V we obtain the exact solution $\Delta_{\text{ex}}(\omega_m)$ of the full linearized gap equation. We show that it exists for all $N < N_{cr}$. The solution, $\Delta_{\text{ex}}(\omega_m)$, oscillates at small frequencies and decays as $1/|\omega_m|^\gamma$ at large $|\omega_m|$. In Sec. V A we analyze the structure of $\Delta_{\text{ex}}(\omega_m)$ and compare it with $\Delta_{\text{diff}}(\omega_m)$. We show that the two coincide at the smallest γ , but differ at $\gamma = O(1)$. We argue that the difference is due to the fact that $\Delta_{\text{ex}}(\omega_m)$ contain non-local terms, not present in $\Delta_{\text{diff}}(\omega_m)$. In Sec. VI we consider the non-linear gap equation. We first analyze the non-linear differential equation and argue that it has an infinite, discrete set of solutions $\Delta_{\text{diff},n}(\omega_m)$ for any $N < N_{cr}$. The

index $n = 0, 1, 2, \dots$ specifies the number of times $\Delta_{\text{diff},n}(\omega_m)$ changes sign as a function of frequency. The solution with $n = 0$ is sign-preserving. The solution $n \rightarrow \infty$ coincides with the solution of the linearized differential equation. We conjecture that the actual, non-linear integral gap equation also possesses an infinite, discrete set of topologically distinct solutions $\Delta_n(\omega_m)$. Sec. VII presents the summary of our results.

D. Brief outline of subsequent papers

In the next paper in the series (paper II) we consider the linearized gap equation for the same range $0 < \gamma < 1$ at a finite T and show that there exists an infinite discrete set of critical temperatures $T_{p,n}$ for the pairing instability, all within the same pairing symmetry. The corresponding eigenfunction $\Delta_n(\omega_m)$ changes sign n times as a function of discrete Matsubara frequency $\omega_m = \pi T(2m + 1)$. We argue that at $T \rightarrow 0$ these finite T solutions become $\Delta_n(\omega_m)$, which we find here in the $T = 0$ analysis.

For $\gamma < 1$, the sign-preserving solution $\Delta_0(\omega_m)$ has the largest condensation energy and the largest $T_{p,0}$. Still, the presence of an infinite set of $\Delta_n(\omega_m)$ at $T = 0$ is not only highly unusual, but creates a new channel of "longitudinal" gap fluctuations. In subsequent papers we will focus on the physical case $N = 1$ and extend the analysis at $T = 0$ to $\gamma > 1$. We will show that the set $\Delta_n(\omega)$ becomes more dense with increasing γ and eventually becomes continuous at $\gamma = 2$. For this special γ , all solutions of the non-linear gap equation have equal condensation energy, and long-range superconducting order at $T = 0$ gets destroyed upon averaging over different solutions, each with its own phase. We will argue that this also holds for larger γ . We will corroborate this by the analysis of the gap equation for the same γ at finite T and obtain the phase diagram, shown in Fig. 2.

II. THE γ -MODEL.

We consider itinerant fermions at the onset of a long-range order in either spin or charge channel. At the critical point the propagator of a soft boson becomes massless and mediates singular interaction between fermions. We follow earlier works^{1,13,14,22,23,27,43,52,53,56,57,81} and assume that this interaction is attractive in at least one pairing channel and that a pairing boson can be treated as slow mode compared to a fermion, i.e., at a given momentum q ,

typical fermionic frequency is much larger than typical bosonic frequency. This is the case for a conventional phonon-mediates superconductivity, where for $q \sim k_F$ a typical fermionic frequency is of order E_F , while typical bosonic frequency is of order Debye frequency ω_D . The ratio $\delta_E = \omega_D/E_F$ is the small parameter for Eliashberg theory of phonon-mediated superconductivity. This theory allows one to obtain a set of coupled integral equations for frequency dependent fermionic self-energy and the pairing vertex. By analogy, the theory of electronic superconductivity, mediated by soft collective bosonic excitations in spin or charge channel, is also often called Eliashberg theory. We will use this convention.

Justification of Eliashberg theory for electronically mediated superconductivity is case specific and sometimes a small parameter for Eliashberg approximation can be found only by extending a model to, e.g., large number of fermionic flavors. Furthermore, for several 2D models, the corrections to Eliashberg approximation for the self-energy in the normal state are logarithmically singular and in the absence of the pairing would change the system behavior at the smallest frequencies. Here we assume that the onset temperature for the pairing, T_p , is larger, at least numerically, than the scale at which corrections to Eliashberg approximation become relevant, and stick with the Eliashberg theory.

Within the Eliashberg approximation, one can explicitly integrate over the momentum component perpendicular to the Fermi surface (for a given pairing symmetry) and reduce the pairing problem to a set of coupled integral equations for frequency dependent self-energy $\Sigma(\omega_m)$ and the pairing vertex $\Phi(\omega_m)$ with effective frequency-dependent dimensionless interaction $V(\Omega) = (\bar{g}/|\Omega|)^\gamma$. This interaction gives rise to NFL form of the self-energy in the normal state and, simultaneously, gives rise to the pairing.

At $T = 0$, the coupled Eliashberg equations for the pairing vertex and the fermionic self-energy are, in Matsubara formalism

$$\begin{aligned} \Phi(\omega_m) &= \frac{\bar{g}^\gamma}{2} \int d\omega'_m \frac{\Phi(\omega'_m)}{\sqrt{\tilde{\Sigma}^2(\omega'_m) + \Phi^2(\omega'_m)}} \frac{1}{|\omega_m - \omega'_m|^\gamma}, \\ \tilde{\Sigma}(\omega_m) &= \omega_m + \frac{\bar{g}^\gamma}{2} \int d\omega'_m \frac{\tilde{\Sigma}(\omega'_m)}{\sqrt{\tilde{\Sigma}^2(\omega'_m) + \Phi^2(\omega'_m)}} \frac{1}{|\omega_m - \omega'_m|^\gamma} \end{aligned} \quad (1)$$

where $\tilde{\Sigma}(\omega_m) = \omega_m + \Sigma(\omega_m)$. In these equations both $\Sigma(\omega_m)$ and $\Phi(\omega_m)$ are real functions. Observe that we define $\Sigma(\omega_m)$ with the overall plus sign and without the overall factor of

ⁱ⁸² In the normal state ($\Phi \equiv 0$),

$$\tilde{\Sigma}(\omega_m) = \omega_m + \omega_0^\gamma |\omega_m|^{1-\gamma} \operatorname{sgn} \omega_m \quad (2)$$

where $\omega_0 = \bar{g}/(1-\gamma)^{1/\gamma}$. At small γ , $\omega_0 = \bar{g}/e$.

The superconducting gap function $\Delta(\omega_m)$ is defined as a real function

$$\Delta(\omega_m) = \omega_m \frac{\Phi(\omega_m)}{\tilde{\Sigma}(\omega_m)} = \frac{\Phi(\omega_m)}{1 + \Sigma(\omega_m)/\omega_m} \quad (3)$$

The equation for $\Delta(\omega_m)$ is readily obtained from (1):

$$\Delta(\omega_m) = \frac{\bar{g}^\gamma}{2} \int d\omega'_m \frac{\Delta(\omega'_m) - \Delta(\omega_m) \frac{\omega'_m}{\omega_m}}{\sqrt{(\omega'_m)^2 + \Delta^2(\omega'_m)}} \frac{1}{|\omega_m - \omega'_m|^\gamma}. \quad (4)$$

This equation contains a single function $\Delta(\omega_m)$, but for the cost that $\Delta(\omega_m)$ appears also in the r.h.s., which makes Eq. (4) less convenient for the analysis than Eqs. (1).

Eqs. (1)-(4) describe color superconductivity⁷¹ and pairing in 3D ($\gamma = 0_+$, $V(\Omega_m) \propto \log |\omega_m|$), spin- and charge-mediated pairing in $D = 3 - \epsilon$ dimension^{13,14,52} and superconductivity in graphene⁸³ ($\gamma = O(\epsilon) \ll 1$), a 2D pairing³⁶ with interaction peaked at $2k_F$ ($\gamma = 1/4$), pairing at a 2D nematic/Ising-ferromagnetic QCP^{39,44,47} ($\gamma = 1/3$), pairing at a 2D (π, π) SDW QCP^{19,22,23,26} and an incommensurate CDW QCP^{31,32,84} ($\gamma = 1/2$), dispersionless fermions randomly interacting with an Einstein phonon⁶²⁻⁶⁴ and a spin-liquid model for the cuprates²⁷ ($\gamma = 0.7$) a 2D pairing mediated by an undamped propagating boson ($\gamma = 1$), pairing in several Fe-based superconductors⁷⁴ ($\gamma = 1.2$) and even the strong coupling limit of phonon-mediated superconductivity for either dispersion-full⁶⁶⁻⁶⁹ or dispersion-less^{62,63} fermions ($\gamma = 2$). The pairing models with parameter-dependent γ have been analyzed as well (Refs. 24 and 53). The case $\gamma = 0$ describes a BCS superconductor. We list some of the model in Tables I and II

In this paper we consider the set of γ -models with $0 < \gamma < 1$. The analysis for $\gamma \geq 1$ requires separate consideration because of divergencies in the r.h.s. of both equations in (1) (but not in (4)) and will be presented in subsequent papers.

Notice that for any $\gamma > 0$ the pairing interaction $V(\Omega)$ decays at large frequencies as $1/|\Omega|^\gamma$. A simple experimentation shows that the integrals in (1) and (4) are then convergent in the ultraviolet. The only exceptions are the BCS case $\gamma = 0$, when $V(\Omega)$ is just a constant, and the case $V(\Omega_m) \propto \log |\omega_m|$, i.e., $\gamma = 0_+$ (color superconductivity/pairing in

TABLE I. Examples of the pairing near Quantum-critical point in 2D.

Model/Order	$V(q, \Omega_m)$	$V(\Omega_m) = \int dq V(q, \Omega_m)$	γ
Ising-nematic order, Ising FM, fermions at 1/2 filled Landau level	$\frac{1}{q^2 + \Gamma \frac{ \Omega_m }{q}}$	$\frac{1}{ \Omega_m ^{2/3}}$	2/3
SDW/CDW order, hot-spot models	$\frac{1}{q^2 + \Gamma \Omega_m }$	$\frac{1}{ \Omega_m ^{1/2}}$	1/2
Undamped fermions	$\frac{1}{q^2 + \Omega_m^2}$	$\frac{1}{ \Omega_m }$	1
Pairing by a soft Einstein phonon	$\frac{1}{\Omega_m^2}$	$\frac{1}{\Omega_m^2}$	2
SYK-model with phonons. Weak coupling	$\frac{1}{ \Omega_m ^{0.6}}$	$\frac{1}{ \Omega_m ^{0.6}}$	0.6
<i>Fe</i> -based superconductors		$\frac{1}{ \Omega_m ^{1.2}}$	1.2

TABLE II. Examples of the pairing near Quantum-critical point in 3D.

Model/Order	$V(q, \Omega_m)$	$V(\Omega_m) = \int d^2q V(q, \Omega_m)$	γ
Ising-nematic order, Ising FM,	$\frac{1}{q^2 + \Gamma \frac{ \Omega_m }{q}}$	$\log \frac{1}{ \Omega_m }$	0+
SDW/CDW order, hot-spot models	$\frac{1}{q^2 + \Gamma \Omega_m }$	$\log \frac{1}{ \Omega_m }$	0+
Anisotropic Ising-nematic	$\frac{1}{q^{2+\epsilon} + \Gamma \frac{ \Omega_m }{ q }}$	$\frac{1}{ \Omega_m ^{3+\epsilon}}$	$\frac{\epsilon}{3+\epsilon}$
Anisotropic SDW/CDW	$\frac{1}{q^{2+\epsilon} + \Gamma \Omega_m }$	$\frac{1}{ \Omega_m ^{2+\epsilon}}$	$\frac{\epsilon}{2+\epsilon}$

3D, Refs.^{14,71}). For these two cases one needs to set the upper cutoff of frequency integration at some Λ to cut ultra-violet divergence. We discuss the limit $\gamma \rightarrow 0$ in Appendix A.

The full set of Eliashberg equations for electron-mediated pairing contains also the equation describing the feedback from the pairing on the bosonic propagator. This feedback is small by δ_E in the case of electron-phonon interaction, but is generally not small when the pairing is mediated by a collective mode because the dispersion of a collective mode may change qualitatively below T_p . The most known example of this kind is the transformation of

Landau overdamped spin collective mode in the normal state to a propagating mode (often called a resonance mode) below the onset of d -wave pairing mediated by antiferromagnetic spin fluctuations (see, e.g., Refs.^{85–88}). To avoid additional complications, we do not include this feedback into our consideration. In general terms, the feedback from the pairing makes bosons less incoherent and can be modeled by assuming that γ moves towards a larger value as $\Phi(\omega)$ increases.

The coupled equations for Φ and $\tilde{\Sigma}$, Eq. (1), describe the interplay between the two competing tendencies – one towards superconductivity, specified by Φ , and the other towards incoherent non-Fermi liquid behavior, specified by $\tilde{\Sigma}$. The competition between the two tendencies is encoded in the fact that $\tilde{\Sigma}$ appears in the denominator of the equation for Φ and Φ appears in the denominator of the equation for $\tilde{\Sigma}$. In more physical terms a self-energy $\tilde{\Sigma}$ is an obstacle to Cooper pairing, while if Φ is non-zero, it reduces the strength of the self-energy and moves the system back into a FL regime.

In Eq. (1) the couplings in the particle-particle and particle-hole channels have the same magnitude \bar{g} . To study the interplay, it is convenient to have a parameter, which would increase either the tendency towards NFL or towards pairing. With this in mind, we multiply the coupling in the particle-particle channel by a factor $1/N$, i.e., set it to be \bar{g}^γ/N instead of \bar{g}^γ , and keep the coupling in the particle-hole channel intact. For $N < 1$, the tendency towards pairing is enhanced, for $N > 1$ the tendency towards NFL effectively gets larger. We will treat N as a free parameter, but use the extension as just a way to see the relevant physics more clearly, as our ultimate goal is to understand system behavior in the physical case of $N = 1$. We note in passing that the extension to integer $N > 1$ can be formalized by extending the original model to matrix $SU(N)$ model.

The modified equations for $\Phi(\omega_m)$ and $\tilde{\Sigma}(\omega_m)$ are

$$\Phi(\omega_m) = \frac{\bar{g}^\gamma}{2N} \int d\omega'_m \frac{\Phi(\omega'_m)}{\sqrt{\tilde{\Sigma}^2(\omega'_m) + \Phi^2(\omega'_m)}} \frac{1}{|\omega_m - \omega'_m|^\gamma}, \quad (5)$$

$$\tilde{\Sigma}(\omega_m) = \omega_m + \frac{\bar{g}^\gamma}{2} \int d\omega'_m \frac{\tilde{\Sigma}(\omega'_m)}{\sqrt{\tilde{\Sigma}^2(\omega'_m) + \Phi^2(\omega'_m)}} \frac{1}{|\omega_m - \omega'_m|^\gamma}, \quad (6)$$

and the equation for $\Delta(\omega_m)$ becomes

$$\Delta(\omega_m) = \frac{\bar{g}^\gamma}{2N} \int d\omega'_m \frac{\Delta(\omega'_m) - N\Delta(\omega_m)\frac{\omega'_m}{\omega_m}}{\sqrt{(\omega'_m)^2 + \Delta^2(\omega'_m)}} \frac{1}{|\omega_m - \omega'_m|^\gamma}. \quad (7)$$

Below we will occasionally refer to the equation for $\Phi(\omega_m)$ as the gap equation, notwithstanding that the gap equation is given by Eqs. (7) and (12), (13). Indeed, once we know $\Phi(\omega_m)$ and $\tilde{\Sigma}(\omega_m)$, we also know $\Delta(\omega_m) = \Phi(\omega_m)\omega_m/\tilde{\Sigma}(\omega_m)$.

We will be searching for normalized solutions for $\Phi(\omega_m)$ and $\Delta(\omega_m)$. Physically, the normalizability of a solution follows from the requirement that the Free energy of a superconductor should be free from divergencies. The Free energy F_{sc} is given by^{59,76,89,90}

$$\frac{F_{sc}}{N_0} = - \int d\omega_m \frac{\omega_m^2}{\sqrt{\omega_m^2 + \Delta^2(\omega_m)}} - \frac{\bar{g}^\gamma}{4} \int d\omega_m d\omega'_m \frac{\omega_m \omega'_m + \frac{1}{N} \Delta(\omega_m) \Delta(\omega'_m)}{\sqrt{\omega_m^2 + \Delta^2(\omega_m)} \sqrt{(\omega'_m)^2 + \Delta^2(\omega'_m)}} \frac{1}{|\omega_m - \omega'_m|^\gamma}. \quad (8)$$

The gap equation (7) is obtained from the condition $\delta F_{sc}/\delta \Delta(\omega_m) = 0$.

The condensation energy E_c is the difference between F_{sc} and F_n (the free energy for $\Delta = 0$). Using Eq. (8) and the gap equation (7) we obtain

$$\frac{E_c}{N_0} = - \int d\omega_m \frac{|\omega_m|}{\sqrt{1 + D^2(\omega_m)}} \left(\sqrt{1 + D^2(\omega_m)} - 1 \right)^2 - \frac{\bar{g}^\gamma}{4} \int \frac{d\omega_m d\omega'_m}{\sqrt{1 + D^2(\omega_m)} \sqrt{1 + D^2(\omega'_m)}} \times \left(\sqrt{1 + D^2(\omega_m)} - \sqrt{1 + D^2(\omega'_m)} \right)^2 \left(\frac{1}{|\omega_m - \omega'_m|} - \frac{1}{|\omega_m + \omega'_m|} \right) \quad (9)$$

where $D(\omega_m) = \Delta(\omega_m)/\omega_m$. Note that both terms in the r.h.s. of (9) are negative, hence the condensation energy is negative for *any* solution of the gap equation $\Delta(\omega_m)$.

To understand whether or not the ground state at $T = 0$ is a NFL state or a superconducting state, we first consider infinitesimally small $\Phi(\omega_m)$. The corresponding equation is obtained by neglecting Φ in the denominator of Eq. (5) and using (2) for $\tilde{\Sigma}$:

$$N\Phi(\omega_m) = \frac{1 - \gamma}{2} \int d\omega'_m \frac{\Phi(\omega'_m)}{|\omega'_m|^{1-\gamma} |\omega_m - \omega'_m|^\gamma} \frac{1}{1 + \left(\frac{|\omega'_m|}{\omega_0} \right)^\gamma} \quad (10)$$

This is an equation for an eigenfunction of a linear operator, in which N plays a role of the eigenvalue. Observe that the fermion-boson coupling \bar{g} appears only in the last term in the denominator, via $\omega_0 \propto \bar{g}$. Without this term, the r.h.s. of (10) is marginal by power counting (the total exponent in the denominator is $1 - \gamma + \gamma = 1$). Then, once we rescale frequency to $\bar{\omega}_m = \omega_m/\omega_0$, the equation for $\Phi(\bar{\omega}_m)$ becomes fully universal:

$$\Phi(\bar{\omega}_m) = \frac{1 - \gamma}{2N} \int d\bar{\omega}'_m \frac{\Phi(\bar{\omega}'_m)}{|\bar{\omega}'_m|^{1-\gamma} |\bar{\omega}_m - \bar{\omega}'_m|^\gamma} \frac{1}{1 + |\bar{\omega}'_m|^\gamma} \quad (11)$$

The same is true for the linearized equation for $\Delta(\omega_m)$:

$$\Delta(\omega_m) = \frac{\bar{g}^\gamma}{2N} \int d\omega'_m \frac{\Delta(\omega'_m) - N\Delta(\omega_m)\frac{\omega'_m}{\omega_m}}{|\omega'_m|} \frac{1}{|\omega_m - \omega'_m|^\gamma}. \quad (12)$$

Using $\bar{g}^\gamma = \omega_0^\gamma(1 - \gamma)$ and introducing again $\bar{\omega}_m = \omega_m/\omega_0$, we re-express (12) as

$$\Delta(\bar{\omega}_m) = \frac{1 - \gamma}{2N} \int d\bar{\omega}'_m \frac{\Delta(\bar{\omega}'_m) - N\Delta(\bar{\omega}_m)\frac{\bar{\omega}'_m}{\bar{\omega}_m}}{|\bar{\omega}'_m|} \frac{1}{|\bar{\omega}_m - \bar{\omega}'_m|^\gamma}. \quad (13)$$

For infinitesimal Φ and Δ , $\Delta(\omega_m) = \Phi(\omega_m)/(1 + (\omega_0/|\omega_m|)^\gamma)$, or, equivalently, $\Delta(\bar{\omega}_m) = \Phi(\bar{\omega}_m)/(1 + |\bar{\omega}_m|^{-\gamma})$.

A conventional wisdom, borrowed from BCS theory, would imply that Eqs. (11) and (13) must have solutions at a single critical N_{cr} , separating NFL and superconducting states, assuming that such critical N_{cr} exists. By the same logic, the full non-linear gap equation has no solution at $N > N_{cr}$, while at $N < N_{cr}$, the solution $\Phi(\omega_m)$ (or $\Delta(\omega_m)$) has a finite magnitude, which increases with $N_{cr} - N$.

We show below that the situation in the γ -model is different. Specifically, we show that critical N_{cr} exists, but the linearized gap equation has a solution not only at $N = N_{cr}$, but for all $N < N_{cr}$. Furthermore, $N = N_{cr}$ turns out to be a multi-critical point of the γ -model (for $0 < \gamma < 1$), below which there exists an infinite number of solutions of the full non-linear gap equation, $\Delta_n(\omega_m)$. The magnitude of the n th solution initially increases as $e^{-A_n/\sqrt{N_{cr}-N}}$, where the factor A_n depends on the number n of the solution.

In the next four sections we discuss the linearized gap equation, Eqs. (11) and (13). We return to non-linear gap equation in Sec. VI.

To verify that a potential solution of the linearized gap equation is normalizable, we will need to analyze the Free energy (8) order Δ^2 . Expanding in (8) we obtain

$$F_{sc} = F_{norm} + \frac{N_0}{2N} J(\Delta, N) \quad (14)$$

$$J(\Delta, N) = N \int d\bar{\omega}_m \frac{\Delta^2(\bar{\omega}_m)(1 + |\bar{\omega}_m|^\gamma)}{|\bar{\omega}_m|^{1+\gamma}} - \frac{1 - \gamma}{2} \int d\omega_m d\bar{\omega}'_m \frac{\Delta(\omega_m)\Delta(\bar{\omega}'_m)}{|\bar{\omega}_m||\bar{\omega}'_m|} \frac{1}{|\bar{\omega}_m - \bar{\omega}'_m|^\gamma}.$$

The linearized gap equation (13) is obtained by varying this F_{sc} over $\Delta(\omega_m)$. A solution is normalizable if the variation $\delta J(\Delta, N)/\delta N$ is finite, i.e., if

$$\int d\bar{\omega}_m \frac{\Delta^2(\bar{\omega}_m)(1 + |\bar{\omega}_m|^\gamma)}{|\bar{\omega}_m|^{1+\gamma}} \quad (15)$$

is non-divergent. In terms of $\Phi(\bar{\omega}_m)$, the same integral is

$$\int d\bar{\omega}_m \frac{\Phi^2(\bar{\omega}_m)}{|\bar{\omega}_m|^{1-\gamma}(1 + |\bar{\omega}_m|^\gamma)} \quad (16)$$

III. THE LIMITS OF SMALL AND LARGE ω_m .

We begin with the analysis of the truncated gap equation at small and large frequencies. The analysis can be done most straightforwardly for the equation (11) for the pairing vertex. At large $|\bar{\omega}_m| \gg 1$, we can pull out the external $\bar{\omega}_m$ from the integral in the r.h.s. of (10) and obtain

$$\Phi(\bar{\omega}_m) = \frac{1}{|\bar{\omega}_m|^\gamma} \frac{1-\gamma}{N} \int_0^{O(|\bar{\omega}_m|)} d\bar{\omega}'_m \frac{\Phi(\bar{\omega}'_m)}{|\bar{\omega}'_m|^{1-\gamma}} \frac{1}{1+|\bar{\omega}'_m|^\gamma}. \quad (17)$$

Substituting $\Phi(\bar{\omega}'_m) \propto 1/|\bar{\omega}_m|^\gamma$ into the r.h.s of (17) we find that the integral converges at $|\bar{\omega}'_m| = O(1)$. This shows that pulling out $\bar{\omega}_m$ from the integral is justified when $|\bar{\omega}_m| \gg 1$. The outcome is that at large frequencies

$$\Phi(\bar{\omega}_m) = \frac{C_\infty}{|\bar{\omega}_m|^\gamma} \quad (18)$$

In this limit, $\Phi(\bar{\omega}_m) = \Delta(\bar{\omega}_m)$, hence we also have

$$\Delta(\bar{\omega}_m) = \frac{C_\infty}{|\bar{\omega}_m|^\gamma} \quad (19)$$

In the opposite limit of small $\bar{\omega}_m$ we assume and then verify that one can truncate (11) by replacing $1/(1+|\bar{\omega}'_m|^\gamma)$ in the r.h.s. by the upper cutoff at $|\bar{\omega}'_m| = O(1)$. The precise value of the cutoff frequency will play no role, and we set the cutoff at $|\bar{\omega}'_m| = 1$. The equation for the pairing vertex then becomes

$$\Phi(\bar{\omega}_m) = \frac{1-\gamma}{2N} \int_{-1}^1 d\bar{\omega}'_m \frac{\Phi(\bar{\omega}'_m)}{|\bar{\omega}'_m|^{1-\gamma} |\bar{\omega}_m - \bar{\omega}'_m|^\gamma} \quad (20)$$

Below we analyze this equation for different N .

A. Large N .

We first consider the limit of large N . The effective coupling constant in (20) scales as $1/N$, hence the solution with a non-zero $\Phi(\omega_m)$ emerges only if the smallness of the coupling is compensated by a large value of the frequency integral in the r.h.s. of (20). This is what happens in a BCS superconductor (the case $\gamma = 0$). There the pairing kernel scales as $1/|\bar{\omega}_m|$, $\Phi(\bar{\omega}_m) = \Phi$ is independent of the running fermionic frequency, and the integral $\int_{-1}^1 d\bar{\omega}'_m \Phi/|\bar{\omega}'_m|$ is logarithmically singular. The logarithm compensates for the smallness of the coupling $1/N$, and superconductivity emerges already for arbitrary weak attraction. A

way to see this is to compute the pairing vertex in the presence of an infinitesimally small initial Φ_0 . At $T = 0$ this has to be done at a non-zero total incoming bosonic frequency $\Omega_{tot} = \bar{\Omega}_{tot}/\omega_0$ to avoid divergencies. The result for a BCS superconductor is well known: to logarithmic accuracy

$$\Phi(\bar{\Omega}_{tot}) = \Phi_0 \left(1 + \frac{1}{N} \log \frac{1}{|\bar{\Omega}_{tot}|} + \frac{1}{N^2} \log^2 \frac{1}{|\bar{\Omega}_{tot}|} + \dots \right) = \frac{\Phi_0}{1 - \frac{1}{N} \log \frac{1}{|\bar{\Omega}_{tot}|}} \quad (21)$$

The ratio $\Phi(\bar{\Omega}_{tot})/\Phi_0$ (the pairing susceptibility) diverges at $|\Omega_{tot}| = \omega_0 e^{-N}$ and becomes negative at smaller $|\Omega_{tot}|$, indicating that the normal state is unstable towards pairing. (In a more accurate description, the pole in $\Phi(\Omega_{tot})$ moves from the lower to the upper half-plane of complex frequency⁹¹).

For a non-zero γ , the pairing kernel is the function of both internal $\bar{\omega}'_m$ and external $\bar{\omega}_m$

$$K(\bar{\omega}, \bar{\omega}'_m) = \frac{1}{|\bar{\omega}'_m|^{1-\gamma} |\bar{\omega}_m - \bar{\omega}'_m|^\gamma} \quad (22)$$

If we set the external $\bar{\omega}_m$ to zero, we find that $K(0, \bar{\omega}'_m) = 1/|\bar{\omega}'_m|$ is marginal, like in BCS theory. Then if we add Φ_0 and compute $\Phi(\bar{\omega}_m)$ perturbatively, the series will be logarithmical, like in BCS case. In distinction to BCS, however, each logarithmical integral $\int d\bar{\omega}'_m/|\bar{\omega}'_m|$ runs between the upper cutoff at $|\bar{\omega}'_m| = 1$ and the lower cutoff at $|\bar{\omega}'_m| \sim |\bar{\omega}_m|$. Because the lower cutoff is finite at a finite $\bar{\omega}_m$, we can safely set $\Omega_{tot} = 0$. Summing up logarithmical series we then obtain

$$\Phi(\bar{\omega}_m) = \Phi_0 \left(1 + \frac{1-\gamma}{N} \log \frac{1}{|\bar{\omega}_m|} + \frac{(1-\gamma)^2}{2N^2} \log^2 \frac{1}{|\bar{\omega}_m|} + \dots \right) = \Phi_0 \left(\frac{1}{|\bar{\omega}_m|} \right)^{\frac{1-\gamma}{N}} \quad (23)$$

We see that the pairing susceptibility remains finite and positive for all finite ω_m , even when $\Omega_{tot} = 0$. Re-doing calculations at a finite Ω_{tot} we find the same result as in (23), but with $|\bar{\omega}_m|$ replaced by $\max(|\bar{\omega}_m|, \bar{\Omega}_{tot})$. The implication is that at a finite γ , summing up logarithms does not give rise to the divergence of the pairing susceptibility, i.e., within a logarithmic approximation, the system at $T = 0$ remains in the normal state.

The difference between logarithmic approximation at $\gamma = 0$ and at a finite γ can be also understood by expressing the flow of $\Phi(\bar{\omega}_m, \bar{\Omega}_{tot})$ under external Φ_0 in terms of RG-type differential equation. In BCS theory one can re-sum logarithmical ladder series by selecting a cross-section in the middle with the smallest running frequency $\bar{\omega}_m$ and integrate over frequencies larger than $\bar{\omega}_m$ in the cross-sections on both sides of the selected one. One such integration gives $\Phi(\bar{\omega}_m)$, another gives the pairing susceptibility $\Phi(\bar{\omega}_m)/\Phi_0$. Combining and

differentiating over $L = \log 1/\bar{\Omega}_{tot}$, we obtain the RG equation $d\Phi(L)/dL = \Phi^2(L)/N\Phi_0$, with the boundary condition $\Phi(0) = \Phi_0$. The solution of this equation is Eq. (21). For a non-zero γ , the logarithmical integral in a given cross-section is cut not by an external bosonic $\bar{\Omega}_{tot}$, but by the external fermionic frequency in the neighboring cross-section. A simple experimentation shows that in this case the corresponding RG equation is $d\Phi(L)/dL = \Phi(L)/N$, where now $L = \log(1/|\bar{\omega}_m|)$. The solution of this equation is Eq. (23).

We now go beyond perturbation theory and analyze Eq. (20) without the Φ_0 term. Our first observation is that $\Phi(\bar{\omega}_m) \propto (1/|\bar{\omega}_m|)^{(1-\gamma)/N}$, which we found by summing up logarithms, does satisfy Eq. (20) at $|\bar{\omega}_m| \ll 1$. Indeed, substituting this form into (20) we find that it is satisfied, because to leading order in $1/N$,

$$\int_0^\infty \frac{dx}{|x|^{(1-\gamma)(N+1)/N}} \frac{1}{|1-x|^\gamma} = \frac{N}{1-\gamma} \quad (24)$$

We next observe that there is another possibility to compensate for the $1/N$ smallness of the coupling constant in (20), by choosing $\Phi(\bar{\omega}_m) \propto (1/|\bar{\omega}_m|)^{\gamma-(1-\gamma)/N}$, such that the integral over $\bar{\omega}'_m$ in the r.h.s. of (20) almost diverges at small $\bar{\omega}'_m$. Indeed, substituting this form into (20) we find that the equation is satisfied because to leading order in $1/N$,

$$\int_0^\infty \frac{dx}{|x|^{1-(1-\gamma)/N}} \frac{1}{|1-x|^\gamma} = \frac{N}{1-\gamma} \quad (25)$$

Note that the factor N now comes from small $|x| \ll 1$. This implies that this solution could not be obtained within a conventional logarithmic approximation, or, equivalently, from the RG equation, as the latter assumes that the logarithms, which sum up into the anomalous power-law form, come from internal frequencies, which are much larger than the external one.

The solution of (20) at large N is then the combination of the two power-law forms

$$\Phi(\bar{\omega}_m) = \frac{C_A}{|\bar{\omega}_m|^{(1-\gamma)/N}} + \frac{C_B}{|\bar{\omega}_m|^{\gamma-(1-\gamma)/N}}. \quad (26)$$

The overall factor doesn't matter because $\Phi(\omega_m)$ is defined up to a constant factor, but the ratio C_A/C_B is a free parameter at this moment.

We now argue that while both terms in (26) satisfy (20), only one component represents the normalized solution and should be kept. Indeed, substituting $\Phi(\bar{\omega}_m)$ into (16) and using the fact find that for large N , $(1-\gamma)/N \ll \gamma/2$, we find that the integral in (16) is finite for the first term in (26) but diverges for the second one. We then have to drop this term and keep only the C_A term in (26).

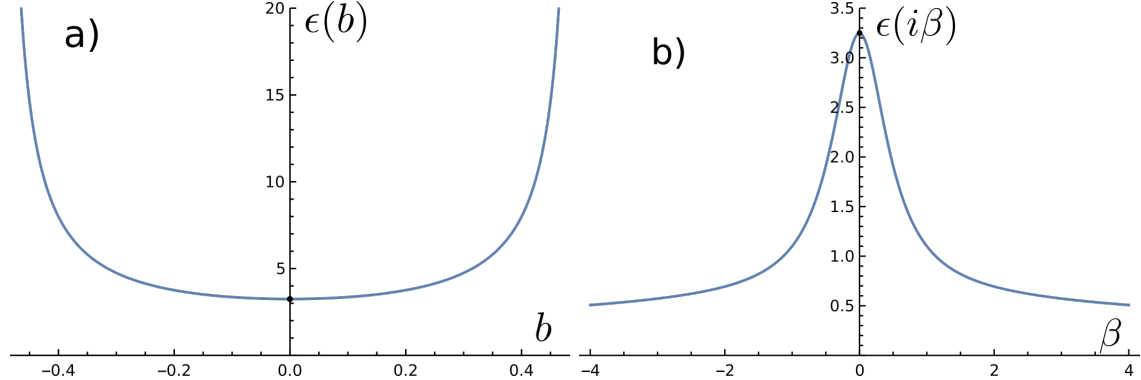


FIG. 6. The function $\epsilon(b)$ from Eq. 28 for real b (left panel) and imaginary b (right panel) for $\gamma = 0.6$. The solution of the truncated gap equation at small $\bar{\omega}$ exists if the equation $\epsilon(b) = N$ has a solution.

The full gap equation (11) has the solution if $\Phi(\bar{\omega}_m) = C_A/|\bar{\omega}_m|^{(1-\gamma)/N}$ at small $\bar{\omega}_m$ and $\Phi(\bar{\omega}_m) = C_\infty/|\bar{\omega}_m|^\gamma$ at large $\bar{\omega}_m$ can be smoothly connected (see Fig. 5). We show below that these two limiting forms cannot be connected, i.e., the linearized equation for the pairing vertex doesn't have a solution.

B. Arbitrary N .

The analysis of the truncated equation for the pairing vertex can be straightforwardly extended to arbitrary N . Like before, we use the fact that the kernel in (20) is marginal and search for power-law solution of (20) in the form $\Phi(\bar{\omega}_m) \propto 1/|\bar{\omega}_m|^{\gamma(1/2+b)}$, where b needs to be obtained self-consistently (we pulled out γ in the exponent for future convenience). Substituting into (20) and evaluating the integral we find that b is the solution of

$$\epsilon_b = N \tag{27}$$

where

$$\epsilon_b = \frac{1-\gamma}{2} \frac{\Gamma(\gamma/2 - \gamma b) \Gamma(\gamma/2 + \gamma b)}{\Gamma(\gamma)} \left(1 + \frac{\cos(\pi \gamma b)}{\cos(\pi \gamma/2)} \right) = N \tag{28}$$

The integral in the r.h.s. of (20) is evaluated using the identities

$$\begin{aligned}\int_0^\infty \frac{dy}{y^a(1+y)^\gamma} &= \frac{\Gamma(1-a)\Gamma(\gamma+a-1)}{\Gamma(\gamma)} \\ \int_0^1 \frac{dy}{y^a(1-y)^\gamma} &= \frac{\Gamma(1-a)\Gamma(1-\gamma)}{\Gamma(2-a-\gamma)} \\ \int_1^\infty \frac{dy}{y^a(y-1)^\gamma} &= \frac{\Gamma(a+\gamma-1)\Gamma(1-\gamma)}{\Gamma(a)}\end{aligned}\quad (29)$$

We plot ϵ_b in Fig. 6a. At small γ ,

$$\epsilon_b \approx \frac{4}{\gamma} \frac{1}{1-4b^2} \quad (30)$$

We see that ϵ_b is an even function of b , i.e., if b is a solution, then $-b$ is also a solution. This implies that

$$\Phi(\bar{\omega}_m) = \Phi(z) = \frac{C_A}{z^{1/2-b}} + \frac{C_B}{z^{1/2+b}}, \quad (31)$$

where

$$z = |\bar{\omega}_m|^\gamma = \left(\frac{|\omega_m|}{\omega_0} \right)^\gamma \quad (32)$$

At large N , $b \approx 1/2 - (1-\gamma)/(N\gamma)$ and (31) coincides with (26). As N increases, b gets smaller. As long as it remains positive, the second term in the r.h.s. of (31) has to be dropped as it does not satisfy the normalization condition (the integral in (16) diverges for $\Phi(\bar{\omega}_m) \propto 1/(z^{1/2+b})$). Then at small z ,

$$\Phi(z) = \frac{C}{z^{1/2-b}}, \quad \Delta(z) = Cz^{1/2+b}. \quad (33)$$

This is very similar to the case of large N .

We next observe that for any $0 < \gamma \leq 1$, there exists a critical N_{cr} , for which $b = 0$. It is given by

$$N_{cr} = \epsilon_0 = \frac{\frac{\pi}{2}(1-\gamma)}{\sin \frac{\pi}{2}(1-\gamma)} \frac{\pi}{\Gamma(\gamma)} \frac{\left(1-\cos \frac{\pi\gamma}{2}\right)^{-1}}{\Gamma^2(1-\gamma/2)} = \frac{1-\gamma}{2} \frac{\Gamma^2(\gamma/2)}{\Gamma(\gamma)} \left(1 + \frac{1}{\cos(\pi\gamma/2)}\right), \quad (34)$$

We plot N_{cr} vs γ in Fig. 7

We see that $N_{cr} > 1$ for all $\gamma < 1$. At small γ , we have from (30), $N_{cr} \approx 4/\gamma$. At $\gamma \rightarrow 1$, $N_{cr} \rightarrow 1$.

Right at $N = N_{cr}$, the two terms in (31) become equal, i.e., one solution of (20) is $\Phi(z) \propto 1/\sqrt{z}$. On a more careful look, we find that $\Phi(z) \propto \log z/\sqrt{z}$ is also the solution. Indeed, substituting this form into (20) and using $\int dy |y|^{\gamma/2-1} |y-1|^{-\gamma} \log |y| = 0$ and $((1-\gamma)/2N_{cr}) \int dy |y|^{\gamma/2-1} |y-1|^{-\gamma} = 1$, we find that this equation is satisfied, i.e.,

$$\frac{1-\gamma}{2N_{cr}} \int d\omega'_m \frac{\log |\omega'_m|}{|\omega'_m|^{1-\gamma/2} |\omega_m - \omega'_m|^\gamma} = \frac{\log |\omega_m|}{|\omega_m|^{\gamma/2}} \quad (35)$$

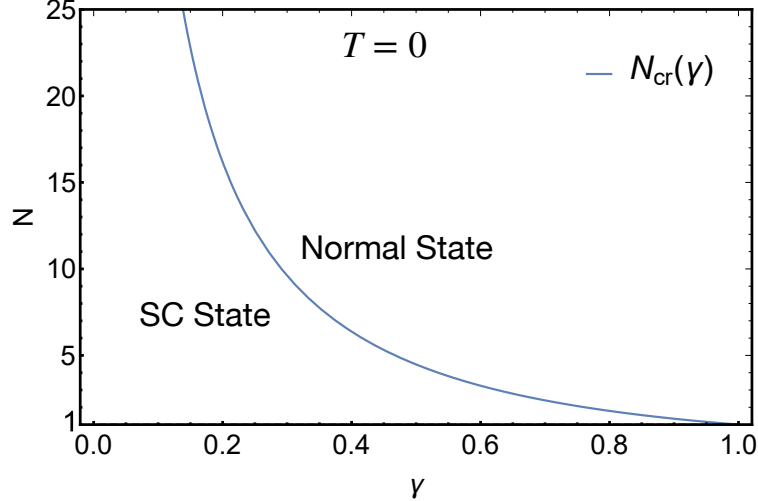


FIG. 7. The critical N_{cr} (for which Eq. (28) has a solution for $b = 0$) as a function of γ . At small γ , $N_{cr} \approx 4/\gamma$. At $\gamma \rightarrow 1$, $N_{cr} \rightarrow 1$.

The full solution of (20) at $N = N_{cr}$ is then

$$\Phi(z) = \frac{1}{\sqrt{z}} (C_A \log z + C_B) \quad (36)$$

or, equivalently,

$$\Phi(z) = \frac{C}{\sqrt{z}} (\log z + \phi), \quad \Delta(z) = C\sqrt{z} (\log z + \phi). \quad (37)$$

This $\Phi(z)$ contains two free parameters: C and ϕ . The overall factor C is irrelevant for the solution of the linearized equation, but ϕ is a free parameter, which we can vary in a hope that at a particular value of ϕ , $\Phi(z)$ and $\Delta(z)$ interpolate smoothly between small z and large z limits. This gives an indication that $N = N_{cr}$ may be the onset for superconductivity.

We now move to $N < N_{cr}$. There is no solution of (27) for real b , consistent with the conventional wisdom that the linearized gap equation has no solution inside the superconducting phase. However, it turns out that the solution of (20) still exists, but for imaginary $b = i\beta_N$, i.e., with complex exponents $1/2 \pm i\beta_N$. Indeed, for a generic $b = i\beta$,

$$\begin{aligned} \epsilon_\beta &= \frac{\frac{\pi}{2}(1-\gamma)}{\sin \frac{\pi}{2}(1-\gamma)} \frac{\pi}{\Gamma(\gamma)} \frac{(\cosh \pi\gamma\beta - \cos \pi\gamma/2)^{-1}}{\Gamma(1-\gamma/2(1+2i\beta)) \Gamma(1-\gamma/2(1-2i\beta))} \\ &= \frac{1-\gamma}{2} \frac{|\Gamma(\gamma/2(1+2i\beta))|^2}{\Gamma(\gamma)} \left(1 + \frac{\cosh(\pi\gamma\beta)}{\cos(\pi\gamma/2)} \right) \end{aligned} \quad (38)$$

is real, even, and monotonically decreases with increasing β from its maximum value $\epsilon_0 = N_{cr} > 1$ to 0, i.e., Eq. (27) has a solution for $N < N_{cr}$ at some non-zero $\beta = \beta_N$. We plot ϵ_β in Fig. 6b. At small γ ,

$$\epsilon_\beta \approx \frac{4}{\gamma} \frac{1}{1 + 4\beta^2} \quad (39)$$

and

$$\beta_N = \frac{1}{2} \sqrt{\frac{N_{cr} - N}{N}} \quad (40)$$

up to corrections of order γ . Solutions with complex exponents have been recently found in several other physics problems^{92–94}. For superconductivity, the solution with complex exponents has been found in Ref.²² for the γ model with $\gamma = 1/2$.

At N slightly below N_{cr} , $\beta_N \propto \sqrt{N_{cr} - N}$ for all $\gamma < 1$. For $N = 1$, $\beta_{N=1} \approx \gamma^{-1/2}(1 - ((15 - \pi^2)/24)\gamma + O(\gamma^2))$ for small γ , $\beta_{N=1} \approx 1.268$ for $\gamma = 1/2$, and $\beta_{N=1} \rightarrow 0.792$ for $\gamma \rightarrow 1$. For $N = O(1)$, but $N \neq 1$, the behavior at $\gamma < 1$ is very similar, but for $\gamma \rightarrow 1$, β_N diverges as $\beta_N \approx 0.561(1/N)^{1/(1-\gamma)}$.

Combining the contributions with β_N and $-\beta_N$, we obtain

$$\Phi(z) = \frac{C}{2} \frac{1}{\sqrt{z}} \left(\frac{e^{i\phi}}{z^{i\beta_N}} + \frac{e^{-i\phi}}{z^{-i\beta_N}} \right) = \frac{C}{\sqrt{z}} \cos(\beta_N \log z + \phi) \quad (41)$$

where ϕ is a free parameter. We see that $\Phi(z)$ oscillates on a logarithmical scale down to the lowest frequencies. Such an oscillating solution could not be obtained perturbatively, starting from $\Phi(z) = \Phi_0$, because within perturbation theory $\Phi(z)$ remains of the same sign as Φ_0 .

We also see that $\bar{\Phi} = \Phi(z)\sqrt{z} \propto e^{i(\beta_N \log z + \phi)} + c.c$ has the form of a wave function of a free fermion if we associate $x = \log z$ with the coordinate. In terms of x , the integral in (16) is expressed as $\int dx \bar{\Phi}(x)^2$, and is nothing but the norm of the eigenfunction of continuum spectrum. The norm can be made finite by adding infinitesimal $e^{-\delta|x|}$ to the integral, after which it converges. The addition of $e^{-\delta|x|}$ also makes the integral in (16) convergent for $\Phi(z)$ at $N = N_{cr}$, however for $N > N_{cr}$, the integral in (16) still diverges for one term in (31). We discuss the normalizability for $N > N_{cr}$ and $N \leq N_{cr}$ in more detail in Appendix C.

The gap function $\Delta(z)$ behaves as

$$\Delta(z) = C \sqrt{z} \cos(\beta_N \log z + \phi) \quad (42)$$

We see that the solution of the truncated equation for the pairing vertex at small z again has two free parameters. In Eq. (42) these are the overall factor C and the phase ϕ . The

overall factor is irrelevant, but the phase ϕ is a free parameter, which we can vary to verify whether at some particular ϕ , $\Delta(z)$ interpolates between (42) and (19).

We emphasize that a free parameter for $\Delta(z)$ at small z (or, equivalently, for $\Phi(z)$) exists both at $N = N_{cr}$ and $N < N_{cr}$. By conventional wisdom, one would expect that the linearized gap equation has the solution only for one value of N , which in our case is expectedly $N = N_{cr}$ (see Fig. 4). However, the presence of a free parameter for all $N \leq N_{cr}$ hints that our case may go against the conventional wisdom.

Matching the limiting forms of an integral equation is a non-trivial procedure as in general one should find a finite frequency range where the two forms coincide. This cannot be implemented in our case because the regions, where the integral equation can be truncated, do not overlap. Because of this, we will be searching for the solution of (11) without specifically looking at the limits of small and large $\bar{\omega}_m$.

IV. THE CASE $\gamma \ll 1$. THE LINEARIZED GAP EQUATION AS THE DIFFERENTIAL EQUATION.

We first consider the limit $\gamma \ll 1$, when the pairing interaction $(\bar{g}/|\Omega_m|)^\gamma$ is a shallow function of frequency, and reduce the linearized integral gap equation to the differential equation, for which we obtain the exact analytical solution, $\Delta_{\text{diff}}(\omega_m)$, which for convenience of notations we present below as a function of z , defined in (32). We show that a generic normalized solution exists for $N \leq N_{cr}$. At small ω_m , $\Delta_{\text{diff}}(z)$ coincides with the solution of the truncated gap equation. It oscillates as a function of $\beta_N \log z + \phi$. For arbitrary ϕ , $\Delta_{\text{diff}}(z)$ tends to a constant at large z , instead of decaying as $1/z$. However, for a certain value of ϕ the constant term cancels out, and the gap function has the correct asymptotic behavior at high frequencies. In other words, by fixing the phase in the oscillations of $\Delta_{\text{diff}}(z)$ at small z one recovers the correct form of sign-preserving $\Delta_{\text{diff}}(z)$ at large frequencies.

To obtain the differential equation we return to the linearized equation for the pairing vertex $\Phi(\omega_m)$, Eq. (11), and use the fact that for small γ , the integral in the r.h.s. of (10) comes from internal ω'_m , which are either substantially larger or substantially smaller than external ω_m . We then split the integral over ω'_m into two parts: in one we approximate

$|\omega_m - \omega'_m|$ by $|\omega'_m|$, in the other by $|\omega_m|$. The equation for $\Phi(\omega_m) = \Phi(z)$ then simplifies to

$$\Phi(z) = \frac{1-\gamma}{N\gamma} \left[\int_z^\infty dy \frac{\Phi(y)}{y(1+y)} + \frac{1}{z} \int_0^z dy \frac{\Phi(y)}{1+y} \right] \quad (43)$$

Differentiating this equation twice over z and replacing $\Phi(z)$ by $\Delta(z) = \Phi(z)z/(1+z)$, we obtain second order differential gap equation

$$(\Delta_{\text{diff}}(z)(1+z))'' = -\frac{N_{cr}}{4N} \frac{\Delta_{\text{diff}}(z)}{z^2}, \quad (44)$$

where $(\dots)'' = d^2(\dots)/dz^2$ and we used the fact that for small γ , $N_{cr} \approx 4/\gamma$. This $\Delta_{\text{diff}}(z)$ has to be real and satisfy the boundary conditions at small and large z . At large z we have from (19),

$$\lim_{z \rightarrow \infty} \Delta_{\text{diff}}(z) = C_\infty/z, \quad (45)$$

At small z we have from (33), (37) and (42)

$$\lim_{z \rightarrow 0} \Delta_{\text{diff}}(z) = \begin{cases} C_A z^{1/2+b}, & \text{for } N > N_{cr} \\ C z^{1/2} (\log z + \phi), & \text{for } N = N_{cr} \\ C z^{1/2} \cos(\beta_N \log z + \phi), & \text{for } N < N_{cr} \end{cases} \quad (46)$$

We recall that $\Delta_{\text{diff}}(z)$, which satisfies the boundary condition (46), is normalizable in the sense that the corresponding condensation energy is finite.

Before we proceed with the analysis of Eqs. (44), (45), and (46), a remark is in order. The integral equation (43) is “non-local” in the sense that the integrals in the r.h.s. are determined by all y , not only $y \approx z$. The differential equation (44), on the other hand, is local – both r.h.s. and l.h.s of (44) contain $\Delta_{\text{diff}}(z)$ with the same z . However, the boundary conditions (45) and (46) imply that once we fix the asymptotic form of $\Delta_{\text{diff}}(z)$ at $z \rightarrow 0$, we also determine the constant C_∞ in the asymptotic form at $z \rightarrow \infty$. Let’s take z large enough such that the asymptotic form of $\Delta_{\text{diff}}(z)$ holds. From Eq. (44) we obtain for such z , $C_\infty = \frac{N_{cr}}{4N} \int_0^\infty \Delta_{\text{diff}}(y) dy/y$. One can verify that the main contribution to this integral comes from $y \ll z$, i.e., the prefactor in $\Delta_{\text{diff}}(z)$ for $z \rightarrow \infty$ is determined by the form of $\Delta_{\text{diff}}(z)$ for much smaller z , roughly by $z \leq 1$, for which $\Delta_{\text{diff}}(z)$ is close to its form at small z . In this sense the non-locality of the initial integral equation (44) reflects itself in the boundary conditions (45), (46) for the local differential gap equation. We also emphasize that (44) is a second order differential equation, hence $\Delta_{\text{diff}}(z)$ is fully determined by the two boundary conditions (45) and (46)

We now analyze Eqs. (44), (45), (46) separately for $N < N_{cr}$, $N = N_{cr}$, and $N > N_{cr}$. We will show that the solution exists for all $N \leq N_{cr}$.

A. $N < N_{cr}$

We use Eq. (40) and re-express $N_{cr}/(4N)$ as $N_{cr}/(4N) = \beta_N^2 + 1/4$. Eq. (44) then becomes

$$(\Delta_{\text{diff}}(z)(1+z))'' = -\left(\beta_N^2 + \frac{1}{4}\right) \frac{\Delta_{\text{diff}}(z)}{z^2}, \quad (47)$$

At $z \ll 1$ (i.e., at $\omega \ll \omega_0$) Eq. (44) simplifies to

$$(\Delta_{\text{diff}}(z))'' = -\left(\beta_N^2 + \frac{1}{4}\right) \frac{\Delta_{\text{diff}}(z)}{z^2}, \quad (48)$$

The solution of this equation is the combination of two power-law functions $\Delta_{\text{diff}}(z) \propto z^{-1/2 \pm i\beta_N}$. Combining the two, we obtain the expected result

$$\Delta_{\text{diff}}(z) = Cz^{1/2} \cos(\beta_N \log z + \phi) \quad (49)$$

At $z \gg 1$, we have

$$(\Delta_{\text{diff}}(z)z)'' = -\frac{N_{cr}}{4N} \frac{\Delta_{\text{diff}}(z)}{z^2} \quad (50)$$

The solution of (50) is

$$\Delta_{\text{diff}}(z) = \frac{1}{\sqrt{z}} \left[A_1 J_1 \left(\sqrt{\frac{4\beta_N^2 + 1}{z}} \right) + A_2 Y_1 \left(\sqrt{\frac{4\beta_N^2 + 1}{z}} \right) \right], \quad (51)$$

where J_1 and Y_1 are Bessel and Neumann functions. At small value of the argument (or large z) $J_1(p) \approx p$ and $Y_1(p) \approx 1/p$. Substituting into (51) we find that to satisfy the boundary condition (45) we must set $A_2 = 0$.

At arbitrary z , the solution of (47) is expressed via Hypergeometric function

$$\Delta_{\text{diff}}(z) = C\sqrt{z} \times \text{Re} \left(e^{i\phi} z^{i\beta_N} {}_2F_1 \left[\frac{1}{2} + i\beta_N, \frac{3}{2} + i\beta_N, 1 + 2i\beta_N, -z \right] \right) \quad (52)$$

At small z , ${}_2F_1[..., -z] \approx 1$, and $\Delta_{\text{diff}}(z)$ is the same as in (49). At $z \gg 1$, we use large z asymptotic of the Hypergeometric function

$$\begin{aligned} {}_2F_1[1/2 + i\beta_N, 3/2 + i\beta_N, 1 + 2i\beta_N, -z] = \\ z^{-1/2 - i\beta_N} \left[\frac{\Gamma(1 + 2i\beta_N)}{\Gamma(3/2 + i\beta_N)\Gamma(1/2 + i\beta_N)} \left(1 + \left(\frac{1}{4} + \beta_N^2 \right) \frac{\log z}{z} \right) + O\left(\frac{1}{z}\right) \right] \end{aligned} \quad (53)$$

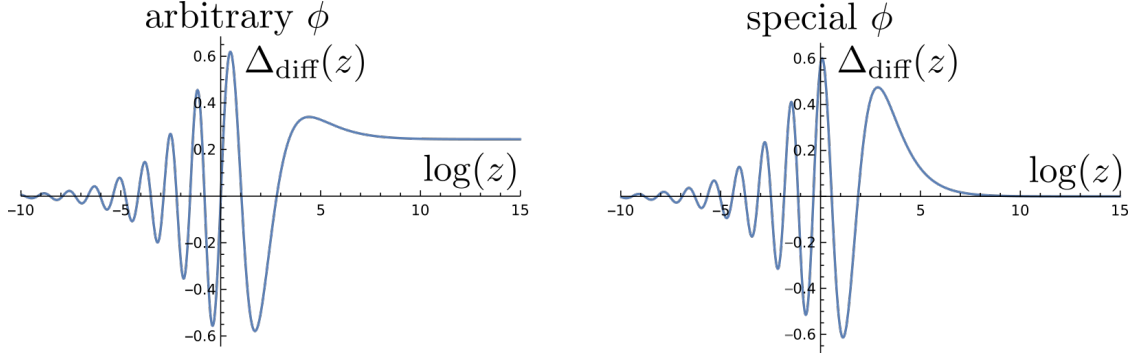


FIG. 8. The solution of the differential gap equation, Eq. (52) for arbitrary ϕ (left panel) and for particular $\phi = \phi_N$ given by Eq. (54) (right panel). In the last case $\Delta_{\text{diff}}(z)$ satisfies both boundary conditions at small and at large z .

and obtain that for arbitrary ϕ , $\Delta_{\text{diff}}(z)$ tends to a constant, which is inconsistent with the boundary condition (45) (see Fig. 8 left panel). However, for a particular $\phi = \phi_N$, where

$$\phi_N = \arctan \frac{\Re L}{\Im L}, \quad \text{where } L = \frac{\Gamma(1 + 2i\beta_N)}{\Gamma(1/2 + i\beta_N)\Gamma(3/2 + i\beta_N)}, \quad (54)$$

the constant term in $\Delta(z)$ vanishes (along with $\log z/z$ correction), and $\Delta_{\text{diff}}(z)$ does scale as $1/z$ at large z , consistent with (45) (see Fig. 8 right panel).

At small β_N , the solution of (54) is $\phi_N = \pi/2 - 0.77259\beta_N$. At $\beta_N = 1$, $\phi_N = \pi/2 - 0.93251$, and at large β_N , $\phi_N \approx 3\pi/4 - \beta_N \log 4$. Once $\phi = \phi_N$ is fixed, one can also express the prefactor A_1 in (51) in terms of C in (49), e.g., $A_1 = C(\pi\beta_N)^{1/2}$ for $\beta_N \gg 1$.

Analyzing Eq. (52) further, we note that both the location and the width of the crossover between small z and large z behavior of $\Delta_{\text{diff}}(z)$ depend on N (Fig. 9). For $N \leq N_{cr}$, $\beta_N \propto (N_{cr} - N)^{1/2}$ is small. In this situation $\Delta_{\text{diff}}(z)$ oscillates as a function of $\log z$ up to $z \sim e^{-1/\beta_N}$, then monotonically increases up to $z \sim 0.2$, passes through a maximum, and decays as $1/z$ at larger frequencies (Fig. 9a). For N such that $\beta_N = O(1)$, logarithmic oscillations extend to $z = O(1)$, and at larger z , $\Delta_{\text{diff}}(z) \propto 1/z$ (Fig. 9b). For $N = O(1)$, $\beta_N \approx 0.5(N_{cr}/N)^{1/2}$ is large because $N_{cr} \approx 4/\gamma \gg 1$. In this situation, logarithmic oscillations of $\Delta(z) = C\sqrt{z} \cos(\beta_N \log z/4 + 3\pi/4)$, persist up to $z = O(1)$, and at larger z there is a range $1 < z < \beta_N^2$, where $\Delta_{\text{diff}}(z)$ again oscillates as $\Delta_{\text{diff}}(z) \approx C \cos(3\pi/4 - 2\beta_N/\sqrt{z})/z^{1/4}$. These oscillations persist up to $z \sim (\beta_N)^2 \sim 1/\gamma$, i.e., up to $\omega = \omega_{max} \sim \bar{g}e^{|\log \gamma|/\gamma}$. At larger z , $\Delta_{\text{diff}}(z) \propto 1/z$ (Fig. 9c). Oscillations at small z are best seen if we use the logarithmical

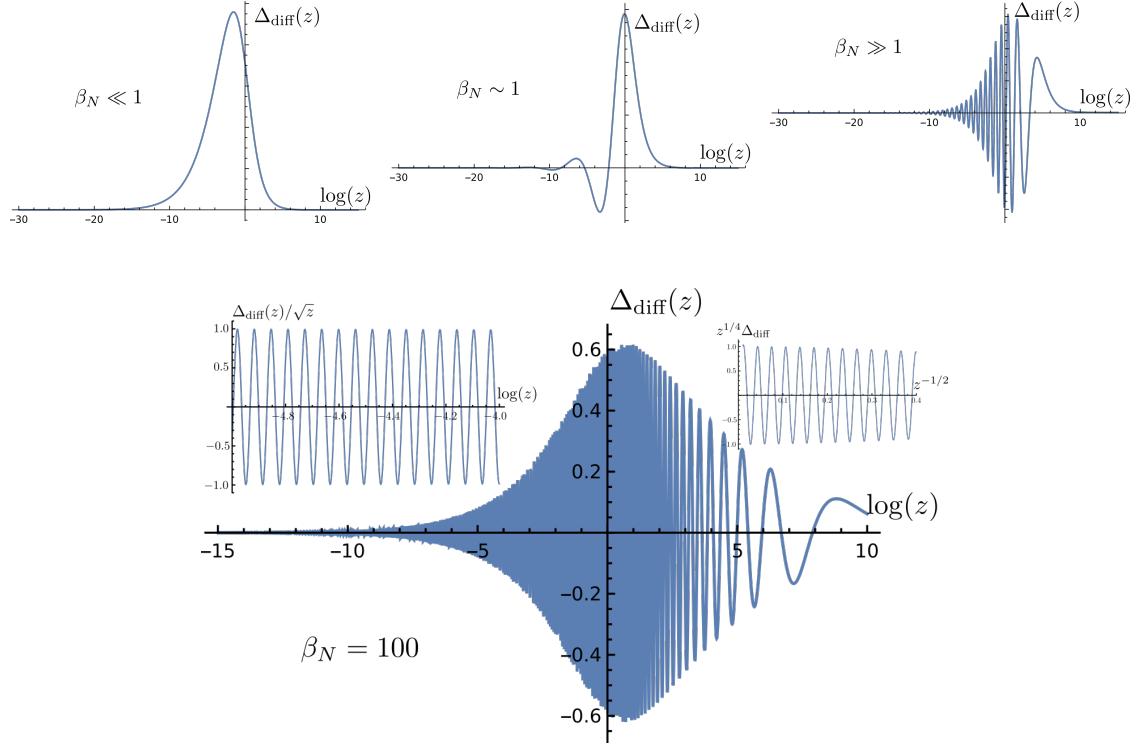


FIG. 9. The solution of the differential gap equation, Eq. (52) for various β_N . For $\beta_N \ll 1$ (panel a) $\Delta_{\text{diff}}(z)$ oscillates as a function of $\log z$ up to $z \sim e^{-1/\beta_N}$ and decays as $1/z$ at higher frequencies. For $\beta_N = O(1)$ (panel b) logarithmic oscillations extend to $z = O(1)$, and at larger z , $\Delta_{\text{diff}}(z) \propto 1/z$. For $\beta_N \gg 1$ (panel c) logarithmic oscillations persist up to $z = O(1)$, and at larger z $\Delta_{\text{diff}}(z)$ again oscillates as $\Delta_{\text{diff}}(z) \propto \cos(3\pi/4 - 2\beta_N/\sqrt{z})/z^{1/4}$. These oscillations persist up to $z \sim (\beta_N)^2 \gg 1$. At larger z , $\Delta_{\text{diff}}(z) \propto 1/z$. Panel d – a closer look at oscillations at $z \ll 1$ and $1 \ll z \ll \beta_N^2$ for large β_N (small γ).

variable

$$x = \log z = \log \left(\frac{|\omega_m|}{\bar{g}} \right)^\gamma \quad (55)$$

while oscillations at $z > 1$ are best seen if we plot $\Delta_{\text{diff}}(z)$ as a function of $1/\sqrt{z}$. We present both plots in Fig. 9d.

The existence of a large intermediate range $1 < z < \beta_N^2$ for $\beta_N^2 \gg 1$ can be inferred already from Eq. (51). Indeed, in this range the argument of the Bessel function $y = 2\beta_N/\sqrt{z}$ is large, $J_1(y) \propto y^{-1/2} \cos(y - 3\pi/4)$, and $\Delta(z)$ displays an oscillating behavior with the period set by $1/\sqrt{z}$ rather than by $\log z$.

The scale $z \sim \beta_N^2$ also shows up in the expansion of $\Delta_{\text{diff}}(z)$ in both $1/z$ and z . Expanding

in $1/z$, we find

$$\Delta_{\text{diff}}(z) \propto \frac{1}{z} \left(1 - \frac{\beta_N^2}{2z} + O\left(\frac{1}{z^2}\right) \right) \quad (56)$$

The expansion in z yields

$$\Delta_{\text{diff}}(z) \approx C \frac{\sqrt{z}}{(1+z)^{3/4}} \cos\left(\frac{3\pi}{4} + \beta_N Q(z)\right) f\left(\frac{z}{\beta_N^2}\right) \quad (57)$$

where $f(0) = 1$ and

$$Q(z) = \log \frac{z}{4} - \frac{z}{2} + \frac{3z^2}{16} - \frac{5z^3}{48} + \frac{19z^4}{256} + \dots, \quad (58)$$

We see that oscillations extend to $z > 1$. At $1 \ll z \ll \beta_N^2$, the form of $Q(z)$ is determined by comparison with (51). We have in this range $Q(z) \approx -2/\sqrt{z}$. Then $\beta_N Q(z)$ becomes of order one at $z \sim \beta_N^2$, where the argument of $f(z/\beta_N^2)$ also becomes of order one. This sets $z \sim \beta_N^2$ as the scale where Eqs. (57) and (56) match.

The scale $z \sim \beta_N^2$ (or, equivalently, $\omega_m \sim \omega_{\text{max}} \sim g(c/\gamma)^{1/\gamma}$, $c = O(1)$) is also the scale at which the boundary condition at $z \rightarrow \infty$ becomes relevant and the phase ϕ gets locked at $\phi = \phi_N$. To see this, we substituted $\Phi_{\text{diff}}(z) = \Delta_{\text{diff}}(z)(1+z)/z$ back into the r.h.s. of (43) and evaluated the integrals. We found that $\Phi_{\text{diff}}(z) \propto z^{-1/2} \cos(\beta_N \log z + \phi)$ at $z < 1$ and $\Phi_{\text{diff}}(z) \propto z^{-1/4} \cos(2\beta_N/\sqrt{z} + \phi)$ at $1 < z < \beta_N^2$ are reproduced for any ϕ , and the corresponding integrals are confined to internal $y \sim z$ in (43) (for $1 < z < \beta_N^2$ the integrals are expressed via Fresnel C-function, which have to be expanded to appropriate order). However, for $z > \beta_N^2$, Eq. (43) is reproduced only if we set $\phi = \phi_N$.

B. $\mathbf{N} = \mathbf{N}_{\text{cr}}$

We now analyze the form of $\Delta_{\text{diff}}(z)$ at $N = N_{\text{cr}}$, where, we expect, the normalized solution for Δ_{diff} first to appear. This analysis requires the same extra care as we exercised in Sec. III B, when we analyzed the truncated gap equation. Namely, we need to take the limit $\beta_N \rightarrow 0$ rather than just set $\beta_N = 0$. To take the limit properly, we re-express Eq. (52) as

$$\Delta_{\text{diff}}(z) = C_1 S(\beta_N, z) + C_2 S(-\beta_N, z) \quad (59)$$

where

$$S(\beta_N, z) = z^{i\beta_N - 1/2} {}_2F_1[1/2 + i\beta_N, 3/2 + i\beta_N, 1 + 2i\beta_N, -z], \quad (60)$$

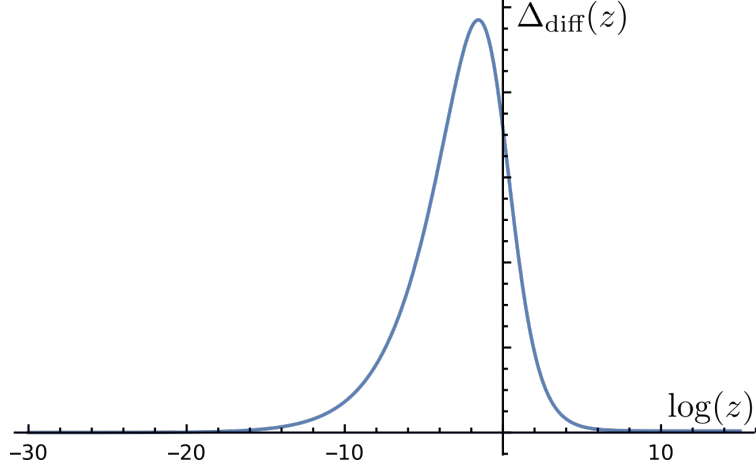


FIG. 10. The gap function $\Delta_{\text{diff}}(z)$ for $N = N_{cr} - 0$ ($\beta_N \rightarrow 0$). The function is sign-preserving. It scales as $\log z / \sqrt{z}$ at small z , passes through a maximum at $z \sim 0.2$, and decreases as $1/z$ at $z > 1$.

and C_1 and C_2 are two independent free parameters. Expanding to linear order in β_N , we obtain

$$\Delta_{\text{diff}}(z) = C_1^* S(0, z) + C_2^* S'(0, z) \quad (61)$$

where the derivative is with respect to $i\beta_N$. As long as β_N is non-zero, C_1^* and C_2^* are two independent parameters. The functions $S(0, z)$ and $S'(0, z)$ are expressed in terms of Meijer G-function and tend to finite values at large z , with subleading term of order $1/z$. Then $\Delta_{\text{diff}}(z) = a + b/z$ at large z . A constant a vanishes once we choose $C_2^*/C_1^* = 1.294$. For this particular C_2^*/C_1^* , $\Delta_{\text{diff}}(z)$ from (59) satisfies the boundary condition at $z \rightarrow \infty$. This implies that the solution does indeed exist at $N = N_{cr} - 0$. At small z , $S(0, z) \approx 1/\sqrt{z}$, $S'(0, z) \approx \log z / \sqrt{z}$, hence $\Delta(z) \propto \log z / \sqrt{z}$, consistent with (46). Computing the subleading terms and using $C_2^*/C_1^* = 1.294$, we obtain at $z < 1$,

$$\Delta_{\text{diff}}(z) = C\sqrt{z} \left(1 - \frac{3z}{4} \right) \left(\log \frac{z}{2.165} - \frac{z}{4} + O(z^2) \right) \quad (62)$$

In Fig. 10 we show $\Delta_{\text{diff}}(z)$ over the whole range of z . We see that $\Delta_{\text{diff}}(z)$ does not oscillate. It monotonically increases with z at small z , passes through a maximum at $z \sim 0.2$ and then decreases as $1/z$. We will study the consequences of this behavior in Sec. VI, where we analyze the non-linear gap equation.

C. $N > N_{cr}$

At $N > N_{cr}$, the exponent $b_N = ((N - N_{cr})/4N)^{1/2}$ is a real number, and the solution of (50) is

$$\Delta_{\text{diff}}(z) = C_1 S[b_N, z] + C_2 S[-b_N, z] \quad (63)$$

where

$$S[b_B, z] = x^{b_N+1/2} {}_2F_1 \left[\frac{1}{2} + b_N, \frac{3}{2} + b_N, 1 + 2b_N, -z \right]. \quad (64)$$

The boundary conditions at $z \gg 1$ and $z \ll 1$, Eqs. (45) and (46), set two conditions on the prefactors:

$$C_2 = 0 \quad \text{and} \quad \frac{C_2}{C_1} = -\frac{\Gamma(3/2 - b_N)\Gamma(1/2 - b_N)\Gamma(1 + 2b_N)}{\Gamma(3/2 + b_N)\Gamma(1/2 + b_N)\Gamma(1 - 2b_N)}. \quad (65)$$

These two conditions are incompatible for any b_N , hence there is no normalized solution of the gap equation for $N > N_{cr}$.

D. larger γ

At larger γ , the approximations used to reduce the integral equation for the pairing vertex to Eq. (43) is not justified. If we formally extend (43) to $\gamma \leq 1$, we still obtain Eq. (44), but with $N_{cr}^{\text{diff}} = 4(1 - \gamma)/\gamma$ instead of the actual N_{cr} given by (34). At small γ , $N_{cr}^{\text{diff}} \approx N_{cr} \approx 4/\gamma$, but for larger γ they differ. The difference becomes crucial for $\gamma \rightarrow 1$, where N_{cr}^{diff} tends to zero, while the actual N_{cr} approaches 1. This can be partly corrected by (i) expressing the differential equation in terms of β_N , as in (47), and using the correct expression for β_N in terms of γ and N , and (ii) modifying the derivation of the differential equation by adding the contribution from internal $\omega' \approx \omega$, as we show in Appendix (B). With this additional contribution, the differential equation for $N \leq N_{cr}$ remains the same as Eq. (47), but z is rescaled to $\bar{z} = z/d$, where $d = 4(1 - \gamma)/(N\gamma(4\beta_N^2 + 1))$. For small γ , $d \approx 1$, but for $\gamma \rightarrow 1$ and $N \rightarrow 1$, $d = (1 - \gamma)/(\beta_N^2 + 1/4)$. In this limit $z = (|\omega_m|/g)(1 - \gamma)$ vanishes, but $\bar{z} \approx (|\omega_m|/g)(\beta_N^2 + 1/4)$ remains finite.

Still, the assumption that the approximation of the actual integral gap equation by the differential one can be rigorously justified only for small γ , when the pairing interaction is

a weak function of frequency. At larger $\gamma = O(1)$ one must analyze the actual, integral gap equation. This is what we will do next.

V. THE EXACT SOLUTION OF THE LINEARIZED GAP EQUATION

In this section we prove that for any γ in the interval $0 < \gamma < 1$, the linearized gap equation has the solution for any $N \leq N_{cr}$. We obtain the exact analytical solution that satisfies Eq. (11) and the normalization condition, Eq. (15). The analysis is somewhat involved, so we discuss the details in Appendix C and here list the computational steps and present the final result.

We start by re-writing Eq. (11) as eigen-value/eigen-function equation of a linear integral operator

$$N\Phi(\bar{\omega}_m) = \frac{1-\gamma}{2} \int_{-\infty}^{\infty} \frac{\Phi(\bar{\omega}'_m) d\bar{\omega}'}{|\bar{\omega}_m - \bar{\omega}'_m|^{\gamma} |\bar{\omega}'_m|^{1-\gamma}} \frac{1}{1 + |\bar{\omega}'_m|^{\gamma}} \quad (66)$$

We then introduce a set of functions

$$\Phi_{\beta}(\Omega_m) \equiv \frac{|\Omega_m|^{i\beta\gamma + \delta_{\Omega_m}}}{|\Omega_m|^{\gamma/2}}, \quad (67)$$

which obey the orthogonality condition:

$$\int \frac{d\Omega_m}{|\Omega_m|^{1-\gamma}} \Phi_{\beta}^* \Phi_{\beta'} = \int dy e^{-i\gamma(\beta - \beta')y} = \frac{2\pi}{\gamma} \delta(\beta - \beta'), \quad (68)$$

and define the function b_{β} as

$$b_{\beta} = \frac{1}{2\epsilon_{\beta}} \int \frac{d\Omega_m}{|\Omega_m|^{1-\gamma}} \Phi_{\beta}(\Omega_m) \Phi(\Omega_m). \quad (69)$$

Multiplying both sides of Eq. (66) by $\Phi_{\beta}(\Omega_m)$ and integrating over $d\Omega_m/|\Omega_m|^{1-\gamma}$, we obtain the equation for b_{β} :

$$Nb_{\beta} = i \int_{-\infty}^{\infty} \frac{\epsilon_{\beta'}}{\sinh(\pi(\beta' - \beta + i0))} b_{\beta'} d\beta' \quad (70)$$

where ϵ_{β} is defined in (38). The normalizability condition for $\Phi(\bar{\omega}_m)$ for given N and γ is expressed in terms of b_{β} as the non-divergence of the integral

$$\int_{-\infty}^{\infty} \left[1 - \frac{1}{N} \epsilon_{\beta'} \right] \epsilon_{\beta'} b_{\beta'} b_{\beta'}^* d\beta'. \quad (71)$$

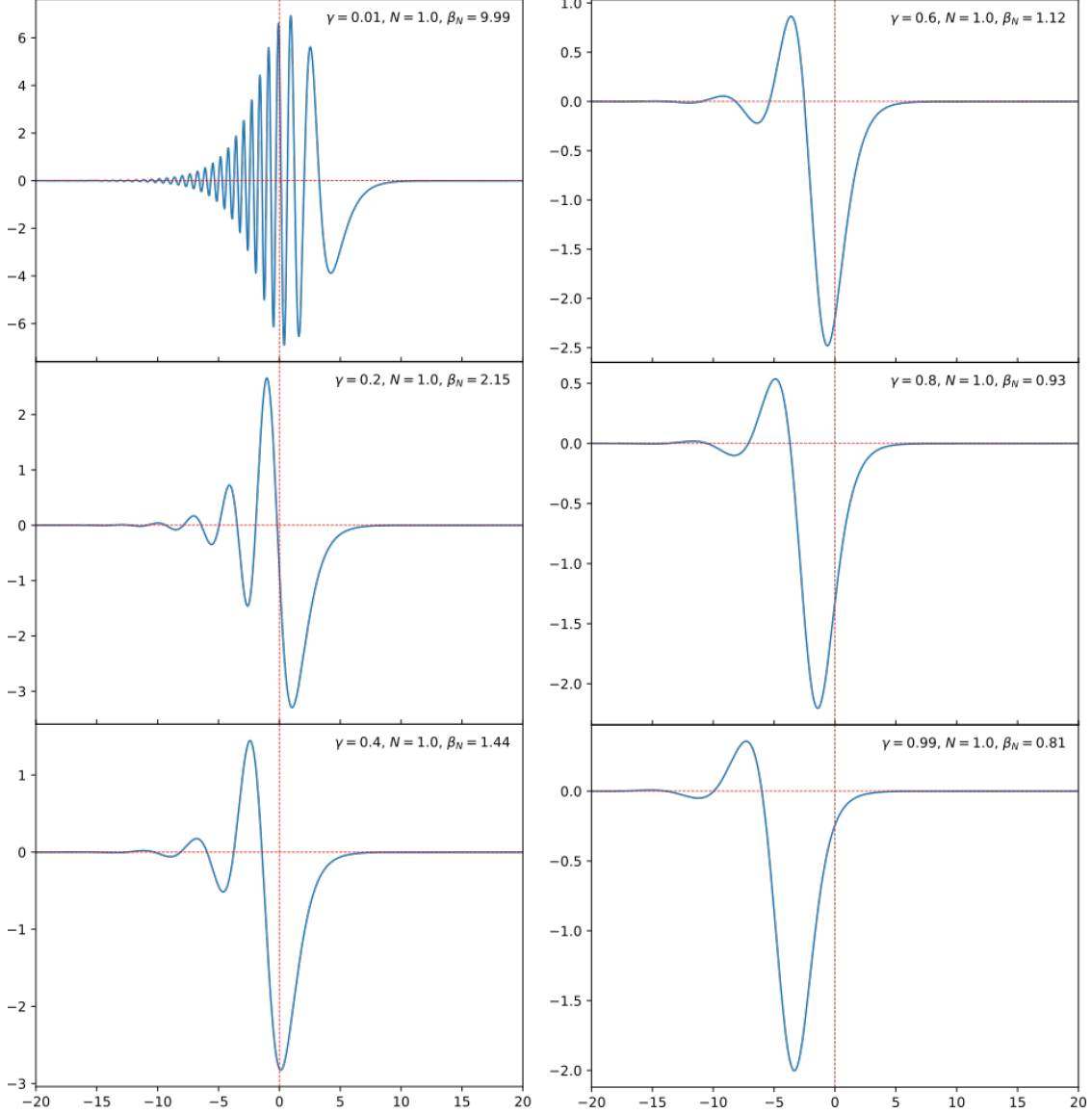


FIG. 11. The exact solution of the linearized gap equation, $\Delta_{\text{ex}}(x)$, as a function of $x = \log(|\omega_m|/\omega_0)^\gamma$ for $N = 1$ and various γ from the interval $0 < \gamma < 1$. For all γ , $\Delta_{\text{ex}}(x)$ oscillates at small frequencies with the period set by x , and decays as $(\omega_0/|\omega_m|)^\gamma = e^{-x}$ at large x .

We solve Eq. (70) subject to (71) in Appendix C and use (69) and (68) to extract $\Phi(\bar{\omega}_m)$ and $\Delta(\bar{\omega}_m) = \Phi(\bar{\omega}_m)/(1 + (\bar{\omega}_m)^{-\gamma})$. We find that there is no normalizable solution for $N > N_{cr}$, but for $N \leq N_{cr}$, the normalizable solution does exist. The solution $\Delta_{\text{ex}}(z)$ is expressed as

$$\Delta_{\text{ex}}(z) = \int_{-\infty}^{\infty} \frac{\sinh(\pi\beta_N) e^{-i\beta \log z - \frac{i}{2}I(\beta)} d\beta}{\sqrt{\cosh(\pi(\beta - \beta_N)) \cosh(\pi(\beta + \beta_N))}}. \quad (72)$$

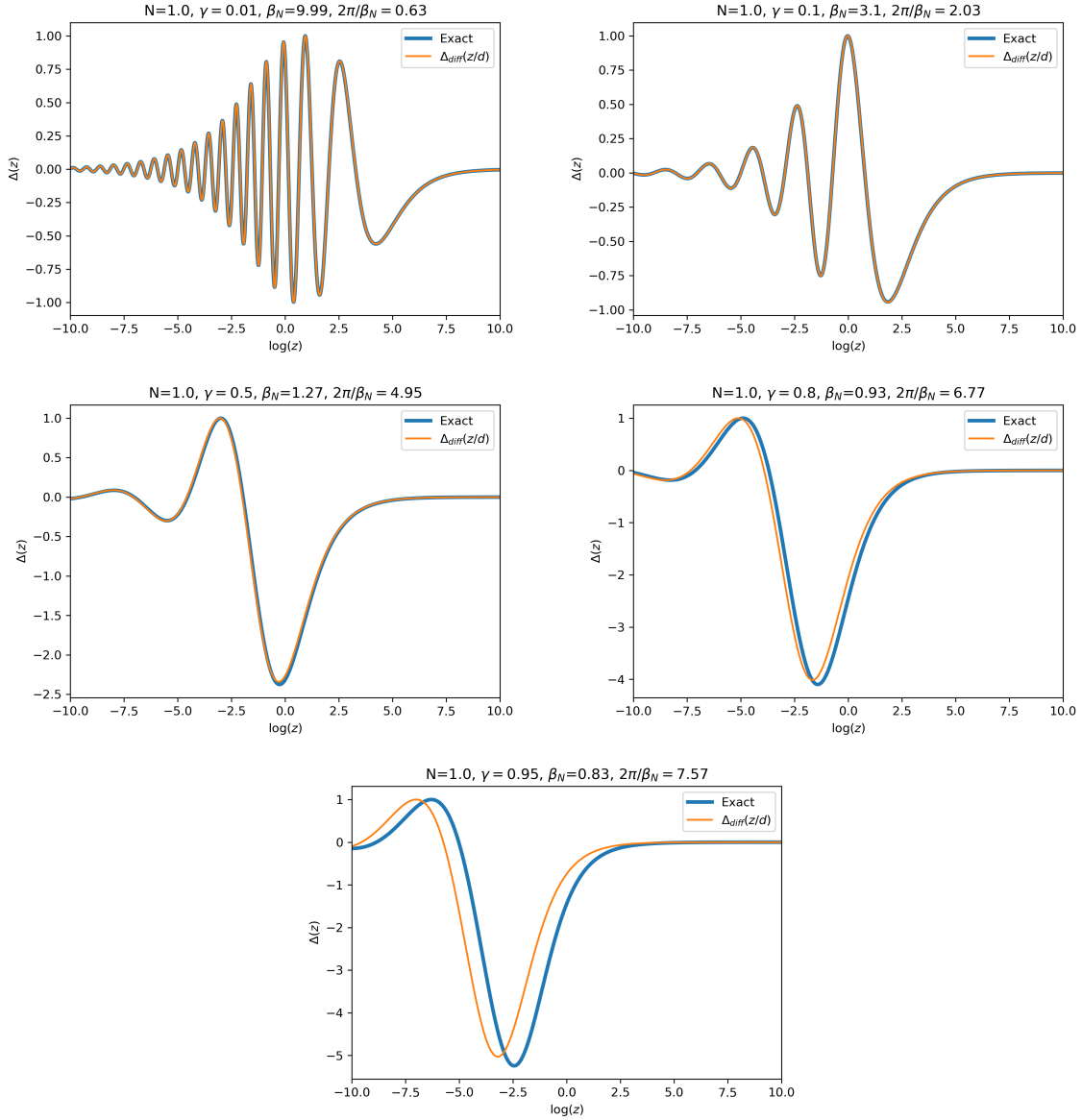


FIG. 12. The exact $\Delta_{\text{ex}}(x)$ and the solution of the differential gap equation $\Delta_{\text{diff}}(x)$ (Eq. (52)) as functions of $\log z = \log((|\omega_m|/\omega_0)^\gamma)$. For Δ_{diff} , we rescaled z to $\bar{z} = z/d$, where $d = 4(1 - \gamma)/(N\gamma(4\beta_N^2 + 1))$, see Appendix B.

Here β_N is the same as before (the solution of $\epsilon_{\beta_N} = N$), and the function $I(\beta)$ is given by

$$I(\beta) = \int_{-\infty}^{\infty} d\beta' \log \left| 1 - \frac{1}{N} \epsilon_{\beta'} \right| \left[\tanh(\pi(\beta' - \beta)) - \tanh(\pi\beta') \right]. \quad (73)$$

The gap function $\Delta_{\text{ex}}(z)$ likely cannot be represented by a simple analytical formula, but can be straightforwardly computed numerically. We plot $\Delta_{\text{ex}}(z)$ for different γ and $N = 1$ in Fig. 11. To show both the oscillations at small z and the power-law behavior at larger z ,

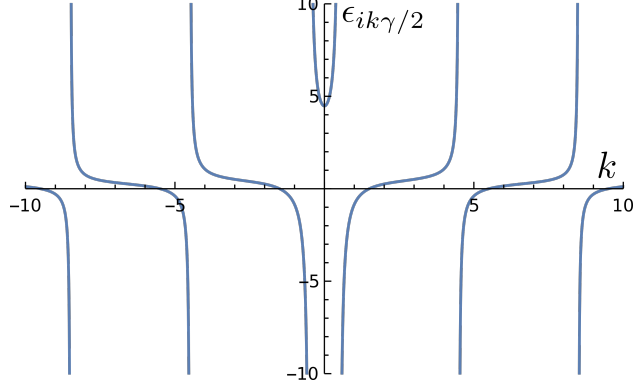


FIG. 13. The function $\epsilon_{\gamma b}$ for $\gamma = 0.5$

we use the logarithmical variable $x = \log(\bar{\omega}_m)^\gamma = \log z$, defined in (55).

A. The exact $\Delta_{\text{ex}}(z)$ vs $\Delta_{\text{diff}}(z)$

In Fig. 12 we compare the exact $\Delta_{\text{ex}}(z)$ for $N = 1$ and various γ with the solution of the differential equation $\Delta_{\text{diff}}(z)$ (both are expressed in terms of $x = \log z$). We see that the two essentially coincide for small γ and remain close to each other for $\gamma = O(1)$, but the discrepancy increases with increasing γ . To understand where the discrepancy comes from, we expanded the exact $\Delta_{\text{ex}}(z)$ in powers of z at small z and in powers of $1/z$ at large z and compared with the expansion of Δ_{diff} . We present the details of the calculations in Appendix D and here list the results. The expansion of $\Delta_{\text{ex}}(z)$ in z holds in

$$\Delta_{\text{ex}}(z) = \frac{1}{1+z} \text{Re} \sum_{n=0}^{\infty} e^{(i\beta_N \log z + \phi_N)} C_n^< z^{n+1/2} + \sum_{n,m=0}^{\infty} D_{n,m}^< z^{(n+b_m/\gamma+1/2)}. \quad (74)$$

The expansion of $\Delta_{\text{ex}}(z)$ in $1/z$ holds in

$$\Delta_{\text{ex}}(z) = \sum_{n=0}^{\infty} C_n^> z^{-(n+1)} + \sum_{n,m=0}^{\infty} D_{n,m}^> z^{-(n+2(m+1)/\gamma+1)} \quad (75)$$

The real b_m in (74) satisfy $\epsilon_{b_m/\gamma} = N$. There are no solutions for $|b_m| < \gamma/2$, but there are solutions for larger b , see Fig. 13. A given b_m is in the interval $\gamma/2 + 2m < b_m < \gamma/2 + 2(m+1)$. The crossover between the two regimes is at $z = z_{\text{max}} = (\omega_{\text{max}}/\omega_0)^\gamma$. This is the scale at which oscillating behavior of $\Delta_{\text{ex}}(z)$ crosses over to $1/z$ behavior.

The expansion of $\Delta_{\text{diff}}(z)$ yields

$$\Delta_{\text{diff}}(z) = \text{Re} \sum_{n=0}^{\infty} e^{(i\beta_N \log z + \phi_N)} \tilde{C}_n^< \frac{z^{n+1/2}}{1+z} \quad (76)$$

for the expansion in z , and

$$\Delta_{\text{diff}}(z) = \sum_{n=0}^{\infty} \tilde{C}_n^> z^{-(n+1)} \quad (77)$$

for the expansion in $1/z$.

We see that the expansion of $\Delta_{\text{diff}}(z)$ is a regular expansion in powers of either z or $1/z$. The coefficients $\tilde{C}_n^<$ and $\tilde{C}_n^>$ can be easily obtained by expanding the Hypergeometric function either in z or in $1/z$, see Eqs. (57) and (58).

The expansion of $\Delta_{\text{ex}}(z)$ is more complex and contains two types of terms – the C_n series and $D_{n,m}$ series. The $C_n^>$ series in (74) are local terms in the sense that in the direct perturbative expansion of the gap equation (7) they come from $\omega'_m \sim \omega_m$ in the integral in (7). The $D_{n,m}^<$ series describe non-local corrections, for which the integral over ω' is determined by $\omega_{\text{max}} \gg \omega_m$. Examining perturbation series, we find that the coefficients $C_n^<$ can be obtained analytically and are given by

$$C_n^< = C_0^< \left[I_n \prod_{m=1}^n \frac{1}{I_m - 1} \right] \quad (78)$$

where

$$I_m = \frac{1 - \gamma}{2N} Q(m, \gamma, \beta_N),$$

$$Q(m, \gamma, \beta_N) = \frac{\Gamma((m + 1/2)\gamma + i\beta_N\gamma)\Gamma((1/2 - m)\gamma - i\beta_N\gamma)}{\Gamma(\gamma)} +$$

$$\Gamma(1 - \gamma) \left(\frac{\Gamma((m + 1/2)\gamma + i\beta_N\gamma)}{\Gamma(1 - (1/2 - m)\gamma + i\beta_N\gamma)} + \frac{\Gamma((1/2 - m)\gamma - i\beta_N\gamma)}{\Gamma(1 - (m + 1/2)\gamma - i\beta_N\gamma)} \right) \quad (79)$$

The series do not converge absolutely because at large n , $C_n^< \propto 1/n$, but each term in the series can be easily calculated. At small γ and $N = 1$, when $\beta_N \approx (N_{\text{cr}}/4N) \gg 1$, the $C_n^<$ series in (74) reproduce, order by order, the expansion of $\Delta_{\text{diff}}(z)$, Eqs. (57) and (58). The same holds for the expansion in $1/z$ – the $C_n^>$ series in (75) reproduce the expansion in (56). The D terms are small for $\gamma \ll 1$ by a combination of two factors: (i) the prefactors are relatively small, e.g., $D_{0,0}^> \approx -C_0^> \gamma/4$, and (ii) $b_m \approx 2(m + 1)$, hence the non-local terms contain additional small factors $z^{2m/\gamma}$ in the expansion in z and $(1/z)^{-2m/\gamma}$ in the expansion in $1/z$. As the consequence, for small γ , $\Delta_{\text{ex}}(z)$ and $\Delta_{\text{diff}}(z)$ coincide, up to small corrections, as Fig. 12a demonstrates.

At larger $\gamma = O(1)$, the non-local terms become relevant, particularly near z_{max} , where $\Delta_{\text{ex}}(z)$ crosses over to $1/z$ behavior. Numbers-wise, $\Delta_{\text{diff}}(z)$ still agrees reasonably well with

$\Delta_{\text{ex}}(z)$, as Fig. 12 shows, but qualitatively, the exact $\Delta_{\text{ex}}(z)$ is different from $\Delta_{\text{diff}}(z)$.

We note in passing that for $\gamma \rightarrow 1$ and $N = 1$, Eq. (79) yields $I_n = 1 + (1 - \gamma)\bar{I}_n$, where

$$\begin{aligned}\bar{I}_n = & \frac{((-1)^n - 1)\pi}{2 \cosh(\pi\beta_N)} + \\ & \frac{1}{2} (\Psi(1/2 + i\beta_N) + \Psi(1/2 - i\beta_N) - \Psi(1/2 + n + i\beta_N) - \Psi(1/2 - n - i\beta_N))\end{aligned}\quad (80)$$

and $\beta_N \approx 0.79$. Hence $I_n - 1 \propto (1 - \gamma)$, and $C_n^< \propto (1/(1 - \gamma))^n$. This implies that the expansion in powers of $z = (|\omega_m|/\bar{g})^\gamma(1 - \gamma) \approx (|\omega_m|/\bar{g})(1 - \gamma)$ in the $C_n^<$ series in (74) actually holds in powers of $|\omega_m|/\bar{g}$. One can verify that the expansion in $D_{n,m}^<$ series also holds in powers of $|\omega_m|/\bar{g}$ instead of powers of z . As the consequence, ω_{max} and the period of oscillations at small ω_m remain finite at $\gamma \rightarrow 1$.

VI. THE NON-LINEAR GAP EQUATION

We now analyze the full non-linear gap equation, Eq. (7). We argue that it has an infinite, discrete set of solutions, which can be specified by topological index n , and the limit $n \rightarrow \infty$ corresponds to the solution of the linearized gap equation.

A. qualitative reasoning

We begin with qualitative reasoning. We assume that for any finite n , the gap function $\Delta_n(\omega_m)$ tends to a finite value at $\omega_m = 0$, while at $\omega_m > \omega_n^*$, $\Delta_n(\omega_m)$ is small and has the same dependence on ω_m as $\Delta_\infty(\omega_m) = \Delta_{\text{ex}}(\omega_m)$. We further assume that ω_n^* is the only relevant scale for $\Delta_n(\omega_m)$, i.e., $\Delta_n(\omega_m)$ saturates at $\omega_m < \omega_n^*$. This reasoning has two implications. First, $\Delta_n(\omega_n^*) \sim \omega_n^*$. Second, $\Delta_n(\omega_m)$ must satisfy the modified linearized gap equation, in which the lower limit of integration over positive and negative ω'_m is set at a frequency of order ω_n^* . Because $\Delta_{\text{ex}}(\omega_m)$ is the solution for $\omega_n^* = 0$, the modified linearized gap equation has a solution if

$$\int_0^{\omega_n^*} d\omega'_m \frac{\Delta_{\text{ex}}(\omega'_m)}{\omega'_m} = 0. \quad (81)$$

These two conditions determine ω_n^* and $\Delta_n(\omega_n^*)$. Below we use the variable z instead of ω_m and define $z_n^* = (\omega_n^*/\omega_0)^\gamma$.

For $N \leq N_{cr}$, $\Delta_{\text{ex}}(z)$ behaves at $z < 1$ as $C\sqrt{z} \cos(\beta_N \log z + \phi_N)$, where $\beta_N \propto (N_{cr} - N)^{1/2}$ is small and $\phi_N = \pi/2 - 0.773\beta_N$. Evaluating the integral in (81) and re-expressing the result in terms of z , we obtain

$$\sin(\beta_N (\log z^* - 2.77)) = 0, \quad (82)$$

This equation has a discrete set of solutions for $z^* \ll 1$: $\log z^* = 2.77 - \pi(n+1)/\beta_N$, where $n = 0, 1, 2, \dots$, i.e,

$$z_n^* \propto e^{-\pi(n+1)/\beta_N}, \quad (83)$$

All z_n^* , including z_0^* , are exponentially small at small β_N . The gap functions $\Delta_n(0) \sim \Delta_n(z_n^*) = \omega_0(z_n^*)^{1/\gamma}$ are also exponentially small:

$$\Delta_n(0) \propto \omega_0 e^{-\pi(n+1)/(\gamma\beta_N)}. \quad (84)$$

One can easily verify that $\Delta_n(z)$ changes sign n times between $z = 0$ and $z = \infty$.

The result $z_n^* \propto e^{-\pi n/\beta_N}$ at $n \gg 1$ also follows from a generic reasoning that $\Delta_{\text{ex}}(z)$ should have an extremum at $z \sim z_n^*$ to match with a constant $\Delta_n(z) \approx \Delta_n(0)$ for smaller z . We note however, that the presence of an extremum in $\Delta_{\text{ex}}(z)$ by itself does not guarantee that the solution of the non-linear gap equation exists. Indeed, $\Delta_{\text{ex}}(z)$ for $N = N_{cr}$ has a maximum at $z = O(1)$, but there is no solution with a finite $\Delta(z)$ for this N .

When $\beta_N \gg 1$ (e.g., for $\gamma \ll 1$ and $N = O(1)$), we can still apply the same reasoning for large enough n , when z_n^* is exponentially small in n . However, for $n = O(1)$, $z_n^* \geq 1$, and we should use appropriate expression for $\Delta_{\text{ex}}(z)$ in Eq. (81). Replacing $\Delta_{\text{ex}}(z)$ by $\Delta_{\text{diff}}(z)$ as the two are very close, and using the asymptotic form of $\Delta_{\text{diff}}(z)$ for $z > 1$: $\Delta_{\text{diff}}(z) \sim (1/\sqrt{z})J_1(2\beta_N/\sqrt{z})$, we obtain the condition on z_n^* in the form

$$J_0\left(\frac{2\beta_N}{\sqrt{z_n^*}}\right) = O(1). \quad (85)$$

This equation has a discrete set of solutions $z_n^* = 4\beta_N^2 s_n$, where s_n is a decreasing function of n . The corresponding $\Delta_n(z_n^*) \sim \Delta_n(0) \sim \omega_0(\beta_N^2)^{1/\gamma}$. For small γ , $\beta_N^2 \approx 1/\gamma$, hence $\Delta_n(0) \sim \omega_0(1/\gamma)^{1/\gamma}$. This analysis holds up to $n = n_{\text{max}}$, for which $z_{n_{\text{max}}}^* = O(1)$. For larger n , z_n^* are given by Eq. (83). Still, $\Delta_n(z)$ changes sign n times between $z = 0$ and $z = \infty$.

Note that at small γ , $\Delta_n(0) \propto \omega_0(z_n^*)^{1/\gamma}$ rapidly evolves from $\Delta_n(0) \ll \omega_0$ when $z_n^* < 1$ to $\Delta_n(0) \gg \omega_0$ when $z_n^* > 1$. In Ref.⁵⁸ we solved the non-linear gap equation at small γ and

$N = 1$ for sign-preserving $\Delta_0(z)$. We obtained $\Delta_0(0) = 0.326\omega_0(1/1.4458\gamma)^{1/\gamma}$, consistent with our estimate.

B. The non-linear differential equation

We now corroborate qualitative reasoning by more direct analysis in which we derive and solve the non-linear differential gap equation. To derive this equation, we again depart from the original integral equations for the pairing vertex and the self-energy, Eqs. (5) and (6), or, equivalently, from the non-linear gap equation (7) and approximate the integral over ω'_m in the l.h.s. of (5) by the integrals over $\omega'_m \gg \omega_m$ and $\omega'_m < \omega_m$, each time neglecting either ω'_m or ω_m in the pairing interaction. However, for a finite $\Delta(\omega_m)$ we have to take into account the fact that the self-energy has a more complex form in the presence of Δ . In particular, one can easily verify that if $\Delta(\omega_m)$ tends to a finite value at $\omega_m = 0$, as we assume to be the case, $\Sigma(\omega_m)$ acquires a Fermi liquid form $\Sigma(\omega_m) \sim \omega_m(\omega_0/\Delta(0))^\gamma$ at the smallest ω_m . The non-Fermi liquid $\Sigma(\omega_m) = |\omega_m|^{1-\gamma}\omega_0^\gamma \text{sign}\omega_m = \omega_m/z$ is recovered at frequencies for which $|\omega_m| \gg \Delta(\omega_m)$. These two limiting forms of the self-energy can be combined into the interpolation formula

$$\Sigma(\omega_m) = \omega_m \frac{\omega_0^\gamma}{(\omega_m^2 + \Delta^2(\omega_m))^{\gamma/2}} \quad (86)$$

If we include this self-energy and then follow the same derivation for the linearized differential gap equation, we would obtain

$$\left[\bar{\Delta}(z) \left(z + \frac{1}{(1 + D^2(z))^{\gamma/2}} \right) \right]'' = -\frac{N_{cr}}{4Nz^2} \frac{\bar{\Delta}(z)}{\sqrt{1 + D^2(z)}} \quad (87)$$

where $\bar{\Delta}(z) = \Delta(z)/\omega_0$ and $D(z) = \Delta(z)/z^{1/\gamma}$. There is a second complication, however. One can verify that at non-zero $\Delta(0)$, the r.h.s of the actual, non-linear integral gap equation (7) (with the self-energy contribution kept in the l.h.s) has a regular expansion in powers of ω_m^2 . Indeed, a direct expansion in ω_m yields

$$\frac{\bar{g}^\gamma}{2N} \int d\omega'_m \frac{\Delta(\omega'_m)}{\sqrt{(\omega'_m)^2 + \Delta^2(\omega'_m)}} \frac{1}{|\omega_m - \omega'_m|^\gamma} = A + B\omega_m^2 \quad (88)$$

where A and B are given by convergent integrals:

$$\begin{aligned} A &= \frac{\bar{g}^\gamma}{2N} \int d\omega'_m \frac{\Delta(\omega'_m)}{\sqrt{(\omega'_m)^2 + \Delta^2(\omega'_m)}} \frac{1}{|\omega'_m|^\gamma} \\ B &= -\frac{\gamma(\gamma+1)}{2} \frac{\bar{g}^\gamma}{2N} \int \frac{d\omega'_m}{\sqrt{(\omega'_m)^2 + \Delta^2(\omega'_m)} \left(\Delta(\omega_m) + \sqrt{(\omega'_m)^2 + \Delta^2(\omega'_m)} \right)} \frac{1}{|\omega'_m|^\gamma}. \end{aligned} \quad (89)$$

The combination of Eqs. (86) and (88) then implies that at small ω_m , $\Delta(\omega_m)$ is a regular function of frequency $\Delta(\omega_m) = \Delta_0 + C\omega_m^2$, as is expected in a Fermi liquid regime. Equivalently, $\bar{\Delta}(z) = \bar{\Delta}_0 + \bar{C}z^{2/\gamma}$. This regular expansion of $\bar{\Delta}(z)$ is not reproduced by Eq. (87). The reason can be easily understood by analyzing how the ω_m^2 term appears in the r.h.s. of (88): to get it one has to keep both ω'_m and ω_m in the interaction, i.e., go beyond the approximation used to derive (87). A simple experimentation shows that to reproduce regular behavior of the gap function at small frequencies, one has to multiply the r.h.s. of (87) by the factor $(\sqrt{1+D^2(z)} - |D(z)|)^{1+\gamma}$. This factor reduces to 1 when $D(z)$ is small, but gives additional $z^{(1+\gamma)/\gamma}$ when $D(z)$ is large. With this extra factor, the non-linear differential gap equation takes the form

$$\left[\bar{\Delta}(z) \left(z + \frac{1}{(1+D^2(z))^{\gamma/2}} \right) \right]'' = -\frac{N_{cr}}{4Nz^2} \frac{\bar{\Delta}(z)}{\sqrt{1+D^2(z)}} \left(\sqrt{1+D^2(z)} - |D(z)| \right)^{1+\gamma} \quad (90)$$

One can verify that at small z , the solution of this equation, if it exists, has an asymptotic form $\bar{\Delta}(z) = \bar{\Delta}(0) + \bar{C}z^{2/\gamma}$, consistent with asymptotic form of the solution of the actual integral equation.

The boundary conditions for (90) are a finite $\Delta(0)$ and $\Delta(z) \propto 1/z$ at $z \rightarrow \infty$. The last condition is the same as for the linearized gap equation. According to our qualitative reasoning, this equation should have an infinite, discrete set of solutions $\Delta_n(z)$.

We solve Eq. (90) numerically. We set $\Delta(0)$ to some value, which we vary. For a generic $\Delta(0)$, $\Delta(z)$ evolves with z towards some constant at $z \rightarrow \infty$. We verify whether for some particular $\Delta(0)$, a constant vanishes and $\Delta(z)$ decays as $1/z$. We show the result in Fig. (14) for $\gamma = 0.3$ and $N = 1$ ($N_{cr}/N \approx 13$, $\beta_n \approx 1.75$). We plot the ratio of $\Delta(z \rightarrow \infty)/\Delta(0)$ vs $\Delta(0)$. We see that for a generic $\Delta(0)$, $\Delta(\infty)$ remains finite, but there is a discrete set of $\Delta_n(0)$, for which $\Delta(\infty)$ vanishes. With our numerical accuracy we can clearly identify three such $\Delta_n(0)$. In three inserts in Fig. (14) we show $\Delta(z)$ for these three $\Delta_n(0)$. We see that the gap function changes sign n times as a function of z ($n = 0, 1, 2$), precisely as we anticipated.

In the top right insert in Fig. (14) we plot $\Delta_n(0)$ vs n for $N = 1$ and $\gamma = 0.3$. We clearly see that $\Delta_n(0)$ has exponential dependence on n . We fitted the results to Eq. (83). The best fit yields $\beta_N \approx 1.51$. This is quite consistent with the actual value $\beta_N \approx 1.75$ (we note that Eq. (83) is by itself only valid for $\beta_N < 1$).

In the left panel of Fig. (15) we collect the results for $\gamma = 0.3$ and different N between $N =$

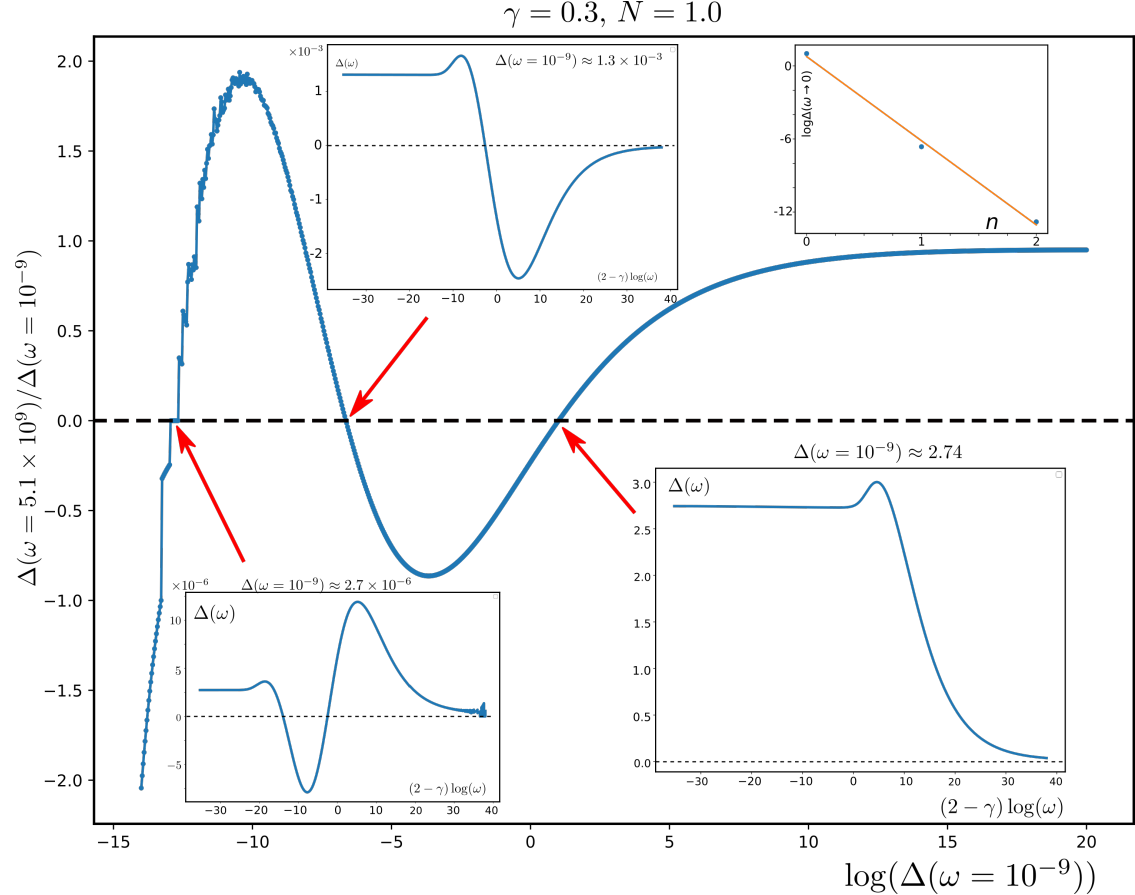


FIG. 14. The ratio of $\Delta(\omega \rightarrow \infty)/\Delta(\omega \rightarrow 0)$ vs $\log \Delta(\omega \rightarrow 0)$.

1 and $N = N_{cr}$, the insert shows compare $\log \Delta_0$ against $\frac{\pi}{\gamma \beta_n}$, where $\beta_N = 0.5(N_{cr}/N - 1)^{1/2}$. We see that the agreement is quite good: the theoretical slope is -1 (see Eq. (84)) and the fitting of numerical data yields the slope -0.95 .

Finally, in the right panel of Fig. (15) we plot Δ_0 vs z for $N \approx N_{cr}/2$, where $\Delta_0(0)$ is already very small. We see that the gap function flattens at $z^* \sim (\Delta_0(0))^\gamma$, which is much smaller than the scale at which $\Delta_0(z)$ has a broad maximum. This is again consistent with our qualitative reasoning.

In the subsequent publication (Paper II) we collaborate the $T = 0$ analysis with the analysis of the linearized gap equation at a finite T . We show that for $N < N_{cr}$, there exists a discrete set of onset pairing temperatures $T_{p,n}$, and the eigenfunction $\Delta_n(\omega_m)$ changes sign n times as a function of Matsubara frequency. We argue that these $\Delta_n(\omega_m)$ grow in magnitude below $T_{p,n}$, but preserve the number of sign changes, and at $T = 0$ coincide with $\Delta_n(\omega_m)$, which we found here.

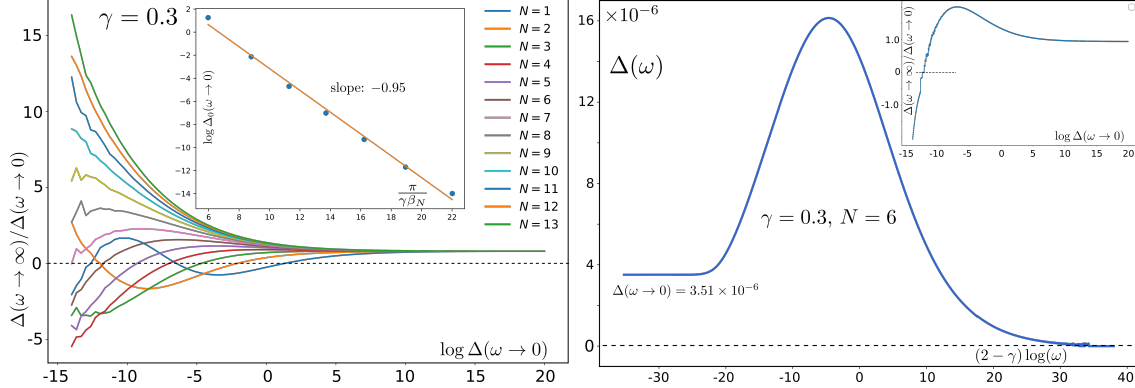


FIG. 15. Left: The ratio of $\Delta(\omega \rightarrow \infty)/\Delta(\omega \rightarrow 0)$ vs $\log \Delta(\omega \rightarrow 0)$. for different N . The insert shows Δ_0 vs $\frac{\pi}{\gamma\beta_N}$, the best fit has the slope of -0.95 . Right Δ_0 vs z for $\gamma = 0.3$ and $N = 6 \approx N_{cr}/2$.

VII. CONCLUSIONS

In this paper we analyzed the competition between two opposing trends in the behavior of interacting fermions near a quantum critical point in a metal: non-Fermi-liquid physics and pairing. Both trends are captured within the model of fermions interacting by exchanging soft bosonic fluctuations of an order parameter, which condenses at the critical point. The non-Fermi liquid behavior is the result of strong, non-analytic self-energy due to boson-mediated scattering near the Fermi surface, the pairing is due to strong attraction in at least one pairing channel, provided by the same soft boson exchange. We considered a class of quantum-critical models with an effective dynamical electron-electron interaction $V(\Omega_m) \propto 1/|\Omega_m|^\gamma$ (the γ -model). In this paper, the first in the series, we considered the case $0 < \gamma < 1$ and restricted the analysis to $T = 0$. The limit $\gamma = 0$ corresponds to BCS theory without the upper cutoff, but for all finite γ the interaction drops off at large Ω and the pairing problem is ultra-violet convergent. To parametrically separate the tendencies towards non-Fermi liquid and pairing, we extended the model and introduced the parameter $1/N$ as additional overall factor in the pairing interaction only. At large N , the tendency towards non-Fermi liquid normal state at $T = 0$ is stronger by N , at small N the tendency towards pairing is stronger by $1/N$.

Our analysis brings two conclusions. First, we found that there indeed exists a critical $N = N_{cr}$, separating non-Fermi liquid normal state at larger N and superconducting state at smaller N . The critical $N_{cr} > 1$ for all $\gamma < 1$, such that the original $N = 1$ model is

superconducting at $T = 0$. Second, we found that the system behavior for $N < N_{cr}$ is rather unconventional in the sense that there exists an infinite set of solutions of the non-linear gap equation, $\Delta_n(\omega_m)$, $n = 0, 1, 2\dots$, all within the same pairing symmetry. The solutions are topologically distinct: $\Delta_n(\omega_m)$ changes sign n times as a function of Matsubara frequency ω_m . All Δ_n emerge at $N = N_{cr}$, but their magnitudes behave differently as functions of $N_{cr} - N$: $\Delta_0 \propto (N_{cr} - N)^{1/2}$, while $\Delta_{n>0} \propto e^{-\pi n/\beta_N}$, where $\beta_N \propto (N_{cr} - N)^{1/2}$. The end point of the set, $\Delta_\infty(\omega_m)$, is the solution of the linearized gap equation at $T = 0$. We obtained the exact analytical solution of the linearized gap equation at $T = 0$ and also a highly accurate simple approximate solution for all $N \leq N_{cr}$. In the subsequent paper we analyze the linearized gap equation at a finite T and show that there is an infinite set of the onset temperatures for the pairing, $T_{p,n}$, and the corresponding eigenfunctions change sign n times as functions of ω_m . We argue that these topologically distinct gap functions grow in magnitude below the corresponding $T_{p,n}$, but largely preserve the functional forms and at $T = 0$ become Δ_n that we found in this work.

The sign-preserving solution with $n = 0$ has the largest condensation energy and is the global minimum of the condensation energy E_c . All other solutions are local minima. Still, the presence of the infinite set of $\Delta_n(\omega_m)$, including the solution of the linear gap equation for all $N \leq N_{cr}$ is a highly non-trivial feature of the pairing at a QCP. In subsequent publications we extend the $T = 0$ analysis to $\gamma > 1$ and argue that the local minima become more closely spaced with increasing γ form a continuous set for $\gamma = 2$. We argue that in this case all solutions have equal condensation energy, and superconducting order gets destroyed already at $T = 0$. As the consequence, the true superconducting T_c terminates at $\gamma = 2$, while the onset temperature for the pairing $T_{p,0} = T_p$ remains finite (see Fig. 2). The two temperatures then must be different for all $0 < \gamma \leq 2$, including $0 < \gamma < 1$, which we considered here. In between T_c and T_p the system displays pseudogap behavior. We emphasize again that the root to this highly unusual behavior is the existence of the solution of the linearized gap equation for all N , rather than only at $N = N_{cr}$.

ACKNOWLEDGMENTS

We thank I. Aleiner, B. Altshuler, E. Berg, D. Chowdhury, L. Classen, R. Fernandes, A. Finkelstein, E. Fradkin, A. Georges, S. Hartnol, S. Karchu, S. Kivelson, I. Klebanov,

A. Klein, R. Laughlin, G. Lonzarich, D. Maslov, M. Metlitski, W. Metzner, A. Millis, D. Mozyrsky, V. Pokrovsky, N. Prokofiev, S. Raghu, S. Sachdev, T. Senthil, Y. Schattner, J. Schmalian, D. Son, G. Tarnopolsky, A-M Tremblay, A. Tsvelik, G. Torroba, E. Yuzbashyan, J. Zaanen, and particularly Y. Wang and Y. Wu for useful discussions. This work by AVC was supported by the NSF DMR-1523036.

Appendix A: The case of small γ and a finite frequency cutoff

The limit $\gamma \rightarrow 0$ of the γ model attracted a lot of attention from various sub-communities in physics^{13,14,16–18,52,58,71} and has been analyzed in both Eliashberg-type and renormalization group approaches. This limit, however, requires extra care because strictly at $\gamma = 0$, the interaction $V(\Omega) \propto |\Omega|^{-\gamma}$ becomes frequency independent, and the pairing problem becomes equivalent to BCS, but without the upper cutoff for the interaction. Meanwhile for any non-zero γ , the gap equation is ultra-violet convergent at ω above $\omega_{max} \sim g/(1.446\gamma)^{1/\gamma}$ (Ref.⁵⁸). This ω_{max} remains finite at any non-zero γ , but grows with decreasing γ faster than the exponent.

In this Appendix we consider how the gap equation gets modified if we introduce the upper cutoff for $V(\Omega)$ at $\Omega = \Lambda$ and consider γ , for which $\Lambda \ll \omega_{max}$. In this situation, we can expand $V(\Omega)$ to first order in γ and express it for $\Omega < \Lambda$ as $V(\Omega) = \gamma \log \Lambda/|\Omega|$. At larger Ω we see $V(\Omega) = 0$. The normal state self-energy is then $\Sigma(\omega_m) = \gamma \omega_m \log \Lambda/|\omega_m|$. Substituting these $V(\Omega)$ and $\Sigma(\omega_m)$ into the equation for the pairing vertex, we obtain

$$\Phi(\omega_m) = \frac{\gamma}{2N} \int \frac{d\omega'_m \log \frac{\Lambda}{|\omega_m - \omega'_m|}}{|\omega'_m|(1 + \gamma \log \frac{\Lambda}{|\omega'_m|})} \quad (A1)$$

Introducing logarithmic variables $x = \log \Lambda/|\omega_m|$, $x' = \log \Lambda/|\omega'_m|$ and restricting with the contributions from $\omega'_m \gg \omega_m$ and $\omega'_m \ll \omega_m$, as we did in the derivation of (43), we reduce (A3) to

$$\Phi(x) = \frac{\gamma}{N} \left[\int_0^x dx' \frac{x' \Phi(x')}{1 + \gamma x'} + \frac{x}{1 + \gamma x} \int_x^\infty dx' \Phi(x') \right] \quad (A2)$$

Differentiating twice over x and introducing $y = \gamma x$, we obtain

$$(\Phi'(z)(1 + z)^2)' = -\frac{\Phi(z)}{N\gamma} \quad (A3)$$

The boundary conditions are $\Phi(z = 0) = 0$ ($\Phi(\omega_m)$ must vanish at $\omega_m = \Lambda$) and $\Phi(z = \infty) = 0$, i.e., $\Phi(\omega_m = 0) = 0$, to avoid the divergence in (A1) at vanishing ω'_m . The solution

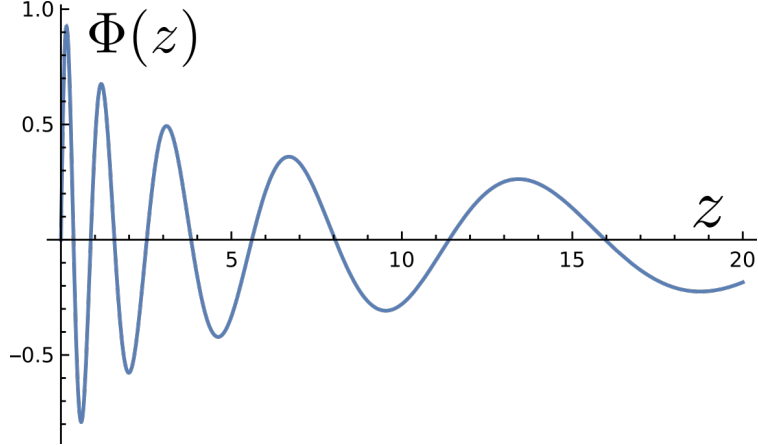


FIG. 16. The function $\Phi(z)$ from Eq. (A4).

of (A1) is

$$\Phi(z) = \frac{C}{\sqrt{1+z}} \cos \left(\phi + \sqrt{\frac{1}{N\gamma} - \frac{1}{4}} \log(1+z) \right) \quad (\text{A4})$$

This $\Phi(z)$ satisfies the boundary condition $\Phi(z = \infty) = 0$ provided $1/N\gamma > 1/4$, i.e., $N < N_{cr} = 4/\gamma$. To satisfy the other boundary condition we choose $\phi = \pi/2$

We plot $\Phi(z)$ in Fig.16 for $N = 1$ and $\gamma = 0.01$. The largest frequency for oscillations (the smallest z is $z \sim 1/\sqrt{\gamma}$, i.e. $\omega_{max} \sim \Lambda e^{-\sqrt{1/(N\gamma)-1/4}}$). This scale determines the magnitude of the gap (the solution of the non-linear gap equation) and the value of T_c . For $N\gamma \ll 1$, $\omega_{max} \sim \Lambda e^{-\sqrt{1/N\gamma}}$. The product $N\gamma$ plays the role of a dimensionless coupling λ , and the result for ω_{max} can be cast into $\omega_{max} \sim \Lambda e^{-1/\sqrt{\lambda}}$. This agrees with Ref.⁷¹.

Comparing ω_{max} obtained with and without the cutoff at Λ we see that the analysis of the γ model without the upper cutoff is valid as long as $g(1/1.446\gamma)^{1/\gamma} \ll \Lambda e^{-\sqrt{1/N\gamma-1/4}}$.

Appendix B: Differential gap equation for arbitrary γ .

The derivation of the differential gap equation, Eq. (43), from the original integral equation is only justified for small γ . In this Appendix we modify the derivation and show that for $N = 1$ the modified gap function $\Delta_{\text{diff}}(\omega_m)$ shows qualitatively the same behavior as the exact $\Delta(\omega_m)$ even for $\gamma \leq 1$.

Specifically, we add to the r.h.s of (43) the additional contribution from $\omega' \sim \omega$, where the interaction is strongly peaked at $\gamma \rightarrow 1$. There is some uncertainty with this contribution as we have to specify the range of integration around $\omega' = \omega$. We choose this range to be

$|\omega' - \omega| \leq a_\gamma \omega$ and keep a_γ as a parameter. We assume that for small γ , $a_\gamma \rightarrow 0$, but for $\gamma \leq 1$, $a_\gamma = O(1)$. Adding this contribution to the r.h.s. of Eq. (43) we find that it becomes

$$\Phi(z) \frac{d+z}{1+z} = \frac{1-\gamma}{N\gamma} \left[\int_z^\infty dy \frac{\Phi(y)}{y(1+y)} + \frac{1}{z} \int_0^z dy \frac{\Phi(y)}{1+y} \right] \quad (\text{B1})$$

where $d = 1 - a_\gamma^{1-\gamma}/N$. Introducing Δ instead of Φ , rescaling z to $\bar{z} = z/d$ and differentiating twice over \bar{z} we obtain differential gap equation in the same form as in (47)

$$(\Delta_{\text{diff}}(\bar{z})(1+\bar{z}))'' = - \left(\beta_N^2 + \frac{1}{4} \right) \frac{\Delta_{\text{diff}}(\bar{z})}{\bar{z}^2}, \quad (\text{B2})$$

once we identify

$$\frac{1-\gamma}{N\gamma - a_\gamma^{1-\gamma}} = \beta_N^2 + \frac{1}{4} \quad (\text{B3})$$

Hence the solution is given by Eq. (52) with \bar{z} instead of z .

Eq. (B3) determines a_γ . At small γ , $\beta_N^2 + 1/4 \approx 1/(N\gamma)$, hence a is small and $\bar{z} \approx z$. However, for larger γ , $a_\gamma = O(1)$, and the rescaling $z \rightarrow \bar{z}$ is essential. Fig. 12 shows that it brings $\Delta_{\text{diff}}(z)$ closer to the exact $\Delta_{\text{ex}}(z)$.

We note in this regard that For $N = 1$ and $\gamma \rightarrow 1$, $a_\gamma^{1-\gamma}/N \approx 1 + (1-\gamma) \log a_\gamma$, and the r.h.s. of (B3) becomes of order one if we choose $a = O(1)$. This is consistent with the fact that $\beta_{N=1}$ tends to a finite value $\beta_{N=1} \approx 0.79$ at $\gamma \rightarrow 1$. Also, the rescaling factor $d = 1 - a^{1-\gamma}/N \approx -(1-\gamma) \log a_\gamma$, hence for $a = O(1)$, $\bar{z} = z/d$ becomes of order $|\omega_m|/g$. As the consequence, the modified $\Delta_{\text{diff}}(\omega_m)$ evolves at a non-singular $\omega_m \sim g$. This is consistent with the behavior of $\Delta_{\text{ex}}(\omega_m)$ at $\gamma \rightarrow 1$ and $N = 1$ (see Fig. 12e).

Appendix C: The exact solution of the linearized gap equation – the computational details.

In this Appendix we present the full details of the computations, leading to the formula for the exact solution of the equation (11). The presentation in this Appendix is self-contained in the sense that it does not use specific notations, introduced in the main text.

1. Reformulation of the equation (11).

We write Eq. (11) as

$$E\Phi(\Omega) = \frac{1-\gamma}{2} \int_{-\infty}^{\infty} \frac{\Phi(\omega) d\omega}{|\omega - \Omega|^\gamma |\omega|^{1-\gamma}} \frac{1}{1 + |\omega|^\gamma} \quad (\text{C1})$$

and use the latter E instead of N to emphasize that this is a continuous variable.⁹⁵

We introduce a set of functions

$$\Phi_\beta(\Omega) = \frac{|\Omega|^{2i\beta+\delta_\Omega}}{|\Omega|^{\gamma/2}} \quad (\text{C2})$$

where β changes from $-\infty$ to $+\infty$ and $\delta_\Omega = +0\text{sign}(1 - |\Omega|)$ is a convergence factor. It is clear that

$$\int \Phi_\beta(\omega) \Phi_\beta^*(\Omega) \frac{d\beta}{2\pi} = \frac{1}{2} |\Omega|^{1-\gamma} \delta(|\Omega| - |\omega|).$$

We now denote

$$a_\beta = \frac{1}{2} \int \frac{d\Omega}{|\Omega|^{1-\gamma}} \Phi_\beta(\Omega) \Phi(\Omega), \quad (\text{C3})$$

multiply (C1) by $\Phi_\beta(\Omega)$, and integrate it over $\frac{d\Omega}{|\Omega|^{1-\gamma}}$. We obtain

$$Ea_\beta = \frac{1-\gamma}{2} \frac{1}{2} \int d\omega \frac{\phi(\omega)}{|\omega|^{1-\gamma}} \frac{1}{1+|\omega|^\gamma} \int \frac{\Phi_\beta(\Omega) d\Omega}{|\Omega|^{1-\gamma} |\Omega - \omega|^{1-\gamma}} = \frac{\epsilon_\beta}{2} \int d\omega \frac{\Phi(\omega) \Phi_\beta(\omega)}{|\omega|^{1-\gamma}} \frac{1}{1+|\omega|^\gamma},$$

where

$$\epsilon_\beta = \frac{1-\gamma}{2} \frac{|\Gamma(\gamma/2 + 2i\beta)|^2}{\Gamma(\gamma)} \left(1 + \frac{\cosh(2\pi\beta)}{\cos(\pi\gamma/2)} \right). \quad (\text{C4})$$

From the definition (C3) (we also use the fact that $\Phi(\omega)$ is taken to be an even function of frequency) we find

$$\int a_\beta \Phi_\beta^*(\omega) \frac{d\beta}{2\pi} = \frac{1}{2} \int \frac{d\Omega}{|\Omega|^{1-\gamma}} \Phi(\Omega) \int \Phi_\beta(\Omega) \Phi_\beta^*(\omega) \frac{d\beta}{(2\pi)} = \frac{1}{2} \Phi(\omega).$$

We then have

$$Ea_\beta = \epsilon_\beta \int \frac{d\beta'}{2\pi} a_{\beta'} \int d\omega \frac{\Phi_{\beta'}^*(\omega) \Phi_\beta(\omega)}{|\omega|^{1-\gamma}} \frac{1}{1+|\omega|^\gamma}.$$

We now compute the integral

$$\int d\omega \frac{\Phi_{\beta'}^*(\omega) \Phi_\beta(\omega)}{|\omega|^{1-\gamma}} \frac{1}{1+|\omega|^\alpha} = 2 \int_0^\infty \frac{d\omega}{\omega} \frac{\omega^{2i(\beta-\beta')+\delta_\omega}}{1+\omega^\gamma} = \frac{2}{\gamma} \int_{-\infty}^\infty dx \frac{e^{ix\frac{2}{\gamma}(\beta-\beta') + x\delta_x}}{1+e^x}$$

where $\delta_x = -0\text{sign}(x)$. At $x \rightarrow \infty$ the integral perfectly converges with or without the convergence factor. At $x \rightarrow -\infty$ we do need the convergence factor, and we assume that δ_x is a small positive number. Evaluating the integral we then obtain

$$\frac{2}{\gamma} \int_{-\infty}^\infty dx \frac{e^{ix\frac{2}{\gamma}(\beta-\beta'-i0)}}{1+e^x} = -\frac{2}{\gamma} \frac{i\pi}{\sinh\left(\frac{2\pi}{\gamma}(\beta-\beta'-i0)\right)}, \quad (\text{C5})$$

and

$$Ea_\beta = -i\epsilon_\beta \frac{1}{\gamma} \int_{-\infty}^\infty \frac{a_{\beta'} d\beta'}{\sinh\left(\frac{2\pi}{\gamma}(\beta-\beta'-i0)\right)}.$$

We now substitute $2\beta/\gamma = k$, and use a_k instead of a_β . Then

$$Ea_k = -\frac{i}{2}\epsilon_{\gamma k/2} \int_{-\infty}^{\infty} \frac{a_{k'} dk'}{\sinh(\pi(k - k' - i0))} \quad (C6)$$

Introducing the new function b_k via

$$a_k = b_k \epsilon_{\gamma k/2}, \quad (C7)$$

we obtain from (C6) the equation for b_k in the form

$$Eb_k = \frac{i}{2} \int_{-\infty}^{\infty} \frac{\epsilon_{\gamma k'/2}}{\sinh(\pi(k' - k + i0))} b_{k'} dk' \quad (C8)$$

2. The functional $F[\phi]$.

For an infinitesimally small $\Phi(\omega)$, the free energy difference between the states with $\Phi(\omega) = 0$ and $\Phi(\omega) \neq 0$ is given by

$$\frac{F[\Phi]}{N_0 \omega_0} = \frac{1}{2} \int \frac{\Phi_\omega^2}{|\omega|^{1-\gamma} (1 + |\omega|^\gamma)} d\omega - \frac{1-\gamma}{4E} \int \frac{\Phi_\omega \Phi_{\omega'} d\omega d\omega'}{|\omega|^{1-\gamma} (1 + |\omega|^\gamma) |\omega - \omega'|^\gamma |\omega'|^{1-\gamma} (1 + |\omega'|^\gamma)}, \quad (C9)$$

where we defined $\Phi(\omega_m) \equiv \Phi_\omega$ to shorten the notations. Taking the first variation of this functional we obtain equation (C1). This functional defines our space of functions, namely we must only consider the functions for which $F[\phi]$ is finite.

3. The normalizability condition.

Now let's take Φ_ω^E to be the solution of (C1) with $E \neq 1$. Then

$$F[\Phi_\omega^\epsilon] = N_0 \bar{g}^2 (1 - \gamma)^{-2/\gamma} \frac{1 - E}{2} \int_{-\infty}^{\infty} \frac{\Phi_\omega^2}{|\omega|^{1-\gamma} (1 + |\omega|^\gamma)} d\omega \quad (C10)$$

We now use

$$\Phi_\omega = 2 \int a_\beta \Phi_\beta^*(\omega) \frac{d\beta}{2\pi},$$

where $\Phi_\beta(\omega)$ is defined in (C2). According to (C5), we have

$$\int \frac{\Phi_\omega^2 d\omega}{|\omega|^{1-\gamma} (1 + |\omega|^\gamma)} = -\frac{4i}{\pi\gamma} \int \frac{a_\beta a_{\beta'}^* d\beta d\beta'}{\sinh\left[\frac{2\pi}{\gamma}(\beta - \beta' - i0)\right]}.$$

Substituting into (C10) and using

$$k = 2\beta/\gamma,$$

we obtain

$$\frac{F[a_k^E]}{N_0\omega_0} = -\gamma(1-E)\frac{i}{2\pi} \int \frac{a_k a_{k'}^* dk dk'}{\sinh [\pi(k - k' - i0)]}. \quad (\text{C11})$$

Using (C7), we rewrite (C11) in terms of b_k as

$$\frac{F[b_k^E]}{N_0\omega_0} = -\gamma(1-E)\frac{i}{\pi} \int \frac{\epsilon_{\gamma k/2} \epsilon_{\gamma k'/2}}{\sinh [\pi(k - k' - i0)]} b_k b_{k'}^* dk dk'.$$

It can be re-expressed as

$$\frac{F[b_k^E]}{N_0\omega_0} = -\gamma(1-E)\frac{i}{\pi} \int \epsilon_{\gamma k/2} \epsilon_{\gamma k'/2} \left[\frac{1}{\sinh [\pi(k - k' + i0)]} + 2i\delta(k - k') \right] b_k b_{k'}^* dk dk'.$$

Comparing to (C8), we finally obtain

$$\frac{F[b_k^E]}{N_0\bar{g}^2(1-\gamma)^{-2/\gamma}\gamma} = -\frac{E(1-E)}{\pi} \int \left[1 - \frac{1}{E} \epsilon_{\gamma k'/2} \right] \epsilon_{\gamma k'/2} b_{k'} b_{k'}^* dk' \quad (\text{C12})$$

Eq. (C12) defines a norm for our solutions. If we manage to solve Eq. (C8) and find b_k for a given E , we will need to verify whether for these b_k , $F[b_k^E]$ is finite. This will give us the spectrum.

4. The solution of Eq. (C8)

We now show that the normalizable solution of Eq. (C8) exists for all $E < \epsilon_0$. We obtain b_k and use them to obtain the pairing vertex $\Phi(\omega_m)$ and the gap function $\Delta(\omega_m)$. For this purpose we need to first find symmetry properties of b_k in (C8).

a. b_k vs b_{-k} .

The equation (C1) is real. So, (i) if an eigenfunction is complex, its complex conjugated must also be an eigenfunction with the same eigenvalue. The eigen value then is double degenerate; (ii) If an eigenvalue is non-degenerate, then the eigenfunction must be real (more precisely, it may have a trivial ω independent phase.) If the eigenfunction of Eq. (C1) is real, then, according to Eqs. (C2) and (C3), we have

$$a_k = a_{-k}^*$$

As the function $\epsilon_{\gamma k/2}$ is real and symmetric under the change $k \rightarrow -k$ we have

$$b_k = b_{-k}^* \quad (\text{C13})$$

b. *Periodicity.*

The equation (C8) has an obvious, but important property. If we change $k \rightarrow k + i$ the r.h.s will turn into itself, but with the opposite sign. So we must have

$$b_{k+in} = (-1)^n b_k. \quad (\text{C14})$$

It means, in particular, that a solution of (C8) is periodic with the period $2i$.

c. *Analytical properties.*

Let's consider equation (C8) for arbitrary complex k , keeping k' to be real. This way we define the analytical function b_k . The integral perfectly converges as long as $\Im k \neq in$ for integer n . So the function b_k can only have singularities on the lines $\Im k = in$. It cannot have poles on these lines, as in this case the integral in the r.h.s. of (C8) would not converge.

Let's return to the equation (C8) and use it to define an analytic function B_k :

$$B_k = \frac{i}{2E} \int_{-\infty}^{\infty} \frac{\epsilon_{\gamma k'/2}}{\sinh(\pi(k' - k))} b_{k'} dk' = \frac{i}{2\pi E} \sum_{n=-\infty}^{\infty} (-1)^n \int_{-\infty}^{\infty} \frac{\epsilon_{\gamma k'/2} b_{k'}}{k' - k + in} dk'$$

(we assume $E \neq 0$). The function b_k is related to B_k as

$$b_k = \lim_{\delta \rightarrow 0} B_{k-i\delta}, \quad \Im k = 0, \quad \delta > 0. \quad (\text{C15})$$

Using the fact that both $\epsilon_{\gamma k/2}$ and $1/\sinh(\pi k)$ are analytic in narrow strip below the real axis, we can express B_k as

$$B_k = \frac{i}{2E} \int_{-\infty-i\tilde{\delta}}^{\infty-i\tilde{\delta}} \frac{\epsilon_{\gamma k'/2}}{\sinh(\pi(k' - k))} B_{k'} dk', \quad \tilde{\delta} > 0 \quad (\text{C16})$$

This formula must be understood in the sense that to compute $b_k = \lim_{\delta \rightarrow 0} B_{k-i\delta}$, for real k , we must first take the limit $\tilde{\delta} \rightarrow 0$ and then $\delta \rightarrow 0$, in which case k in the r.h.s. of (C16) is below the integration path. The function B_k obviously satisfies the periodicity condition, Eq. (C14). It is also clear from (C16) that B_k has branch cuts along the lines $\Im k = in$.

Let's now compute $\lim_{\delta \rightarrow 0} (B_{k+in+i\delta} - B_{k+in-i\delta})$, for real k and positive δ . By Sokhotski-Plemelj theorem: $\frac{1}{x-x_0-i0} = \text{P} \frac{1}{x-x_0} + i\pi\delta(x - x_0)$. Hence

$$\lim_{\delta \rightarrow 0} (B_{k+in+i\delta} - B_{k+in-i\delta}) = -(-1)^n \frac{1}{E} \epsilon_{\lambda k/2} b_k = -\frac{1}{E} \epsilon_{\lambda k/2} B_{k+in-i\delta}, \quad \delta \rightarrow 0, \quad \delta > 0$$

which means that

$$B_{k+in+i0} = \left(1 - \frac{1}{E}\epsilon_{\gamma k/2}\right) B_{k+in-i0}. \quad (\text{C17})$$

This equation is a particular case of the Riemann-Hilbert problem.

Here one has to distinguish between the two cases

- i) $E > \max \epsilon_{\gamma k/2} = \epsilon_0$ – in this case the expression $1 - \frac{1}{E}\epsilon_{\gamma k/2}$ does not change sign, and
- ii) $0 < E < \epsilon_0$ – in this case the expression $1 - \frac{1}{E}\epsilon_{\gamma k/2}$ changes sign twice at $k = \pm k_E$,
where

$$\epsilon_{\gamma k_E/2} = E \quad (\text{C18})$$

We consider the two cases separately.

Case i). $E > \epsilon_0$: In this case we take the logarithms of the both sides of the equation (C17), we then get

$$\log B_{k+in+i0} - \log B_{k+in-i0} = \log \left(1 - \frac{1}{E}\epsilon_{\gamma k/2}\right)$$

So the analytic function $\Phi_k = \log B_k$ has branch cuts along the lines $\Im k = in$ with the jumps given by above formula. According to Sokhotski-Plemelj theorem we have

$$\log B_k = \frac{1}{2\pi i} \sum_{n=-\infty}^{\infty} \int_{-\infty}^{\infty} \frac{\log(1 - \frac{1}{E}\epsilon_{\gamma k'/2})}{k' - k + in} dk' + F_k = \frac{1}{2i} \int_{-\infty}^{\infty} \log(1 - \frac{1}{E}\epsilon_{\gamma k'/2}) \coth(\pi(k' - k)) dk' + F_k,$$

where the analytic function F_k has no branch cuts or singularities, so it must be a polynomial. In order to find this polynomial, we notice, that the first term in the right hand side does not change if we shift $k \rightarrow k + in$, while B_k must acquire a factor of $(-1)^n$ and $\log B_k$ must acquire extra $\pm i\pi n$. There are only two polynomials that have this property, they are are $\pm \pi k$, so there are two solutions:

$$B_k = e^{\pm \pi k + \frac{1}{2i} \int_{-\infty}^{\infty} \log(1 - \frac{1}{E}\epsilon_{\gamma k'/2}) \coth(\pi(k' - k)) dk'}, \quad (\text{C19})$$

Correspondingly, there are two solutions for b_k

$$b_k^{\pm} = B_{k-i0} = e^{\pm \pi k + \frac{1}{2i} \int_{-\infty}^{\infty} \log(1 - \frac{1}{E}\epsilon_{\gamma k'/2}) \coth(\pi(k' - k + i0)) dk'}, \quad (\text{C20})$$

where k is now real.

Notice, that we have two solutions. One can check, that they are indeed complex conjugated.

Now we need to check whether the solutions (C20) are normalizable. From (C20) we find

$$\begin{aligned} b_k b_k^* &= e^{\pm 2\pi k} e^{\frac{1}{2i} \int_{-\infty}^{\infty} \log(1 - \frac{1}{E} \epsilon_{\gamma k'/2}) [\coth(\pi(k' - k + i0)) - \coth(\pi(k' - k - i0))] dk'} \\ &= e^{\pm 2\pi k} e^{-\frac{1}{2i} \int_{-\infty}^{\infty} \log(1 - \frac{1}{E} \epsilon_{\gamma k'/2}) 2i\delta(k - k')} = \cosh^2(\pi k) e^{-\log(1 - \frac{1}{E} \epsilon_{\gamma k/2})} \end{aligned}$$

As the consequence,

$$\frac{F[b_k^E]}{N_0 \bar{g}^2 (1 - \gamma)^{-2/\gamma} \gamma} = -\frac{E(1 - E)}{\pi} \int e^{2\pi k} \epsilon_{\gamma k/2} dk$$

The last integral diverges. The divergence implies that the solutions with $E > \epsilon_0$ are not normalizable and are not the part of the spectrum.

Case ii). $0 < E < \epsilon_0$. In this case there are two points (C18) where the r.h.s of (C17) changes sign. To avoid ambiguity of $\log(-1)$, we first rewrite (C17) as

$$B_{k+in+i0} = \Theta(k - k_E) \Theta(k + k_E) \left| 1 - \frac{1}{E} \epsilon_{\gamma k/2} \right| B_{k+in-i0},$$

where Θ is the step function ($\Theta(x < 0) = -1$ and $\Theta(x > 0) = 1$) Now we take the log of both sides

$$\log B_{k+in+i0} - \log B_{k+in-i0} = \log \left| 1 - \frac{1}{E} \epsilon_{\gamma k/2} \right| + \log \Theta(k - k_E) + \log \Theta(k + k_E).$$

The $\log \Theta(k - k_E)$ is zero for $k > k_E$ and either $+i\pi$ or $-i\pi$ for $k < k_E$. Let's introduce two yet unknown functions χ_n and ξ_n , which have values ± 1 , depending on n , and rewrite the equation above as

$$\log B_{k+in+i0} - \log B_{k+in-i0} = \log \left| 1 - \frac{1}{E} \epsilon_{\gamma k/2} \right| + i\pi \chi_n \frac{1}{2} (1 - \Theta(k - k_E)) + i\pi \xi_n \frac{1}{2} (1 - \Theta(k + k_E)).$$

The Sokhotski-Plemelj theorem now gives

$$\begin{aligned} \log B_k &= \frac{1}{2\pi i} \sum_{n=-\infty}^{\infty} \int_{-\infty}^{\infty} \frac{\log |1 - \frac{1}{E} \epsilon_{\gamma k'/2}|}{k' - k + in} dk' \\ &+ \frac{1}{2} \sum_{n=-\infty}^{\infty} \chi_n \int_{-\infty}^{\infty} \frac{\frac{1}{2}(1 - \Theta(k - k_E))}{k' - k + in} dk' + \frac{1}{2} \sum_{n=-\infty}^{\infty} \xi_n \int_{-\infty}^{\infty} \frac{\frac{1}{2}(1 - \Theta(k + k_E))}{k' - k + in} dk' + F_k. \end{aligned}$$

This can be re-expressed as

$$\begin{aligned} \log B_k &= \frac{1}{2i} \int_{-\infty}^{\infty} \log |1 - \frac{1}{E} \epsilon_{\gamma k'/2}| \coth(\pi(k' - k)) dk' \\ &+ \frac{1}{2} \int_{-\infty}^{k_E} \sum_{n=-\infty}^{\infty} \frac{\chi_n}{k' - k + in} dk' + \frac{1}{2} \int_{-\infty}^{-k_E} \sum_{n=-\infty}^{\infty} \frac{\xi_n}{k' - k + in} dk' + F_k. \end{aligned}$$

According to (C14), the difference $\log B_{k+im} - \log B_k$ should be equal to $i\pi m$ independent on k . For B_k from (C21) we have

$$\log B_{k+im} - \log B_k = \frac{1}{2} \int_{-\infty}^{k_E} \sum_{n=-\infty}^{\infty} \frac{\chi_{n+m} - \chi_n}{k' - k + in} dk' + \frac{1}{2} \int_{-\infty}^{-k_E} \sum_{n=-\infty}^{\infty} \frac{\xi_{n+m} - \xi_n}{k' - k + in} dk' + F_{k+im} - F_k.$$

In order for this expression to be independent of k , the functions χ_n and ξ_n must be independent of n and F_k must be equal to $\pm\pi k + c$, where c is an arbitrary complex constant. We then denote $\chi_n = \chi$, $\xi_n = \xi$, where $\chi = \pm 1$, $\xi = \pm 1$. The signs of χ and ξ can be chosen independently. After this, we obtain

$$\begin{aligned} \log B_k &= \frac{1}{2i} \int_{-\infty}^{\infty} \log \left| 1 - \frac{1}{E} \epsilon_{\gamma k'/2} \right| \coth(\pi(k' - k)) dk' \\ &+ \chi \frac{\pi}{2} \int_{-\infty}^{k_E} \coth(\pi(k' - k)) dk' + \xi \frac{\pi}{2} \int_{-\infty}^{-k_E} \coth(\pi(k' - k)) dk' \pm \pi k + c \end{aligned} \quad (\text{C21})$$

Now we can find the function b_k

$$\begin{aligned} b_k &= B_{k-i0} = \exp \left[\frac{1}{2i} \int_{-\infty}^{\infty} \log \left| 1 - \frac{1}{E} \epsilon_{\gamma k'/2} \right| \coth(\pi(k' - k + i0)) dk' \pm \pi k + c \right. \\ &+ \chi \frac{\pi}{2} \int_{-\infty}^{k_E} [\coth(\pi(k' - k + i0)) - \coth(\pi(k' + i0))] dk' \\ &\left. + \xi \frac{\pi}{2} \int_{-\infty}^{-k_E} [\coth(\pi(k' - k + i0)) - \coth(\pi k')] dk' \right], \end{aligned} \quad (\text{C22})$$

(we redefined the constant c)

Now we need to check if the solution (C22) is normalizable. For this, we need to verify whether the integral in (C12) converges at large $|k|$. This requires us to compute the real part of the exponent in (C22) for $|k| \gg k_E$. We do this on term by term basis

$$\begin{aligned} \Re \left[\frac{1}{2i} \int_{-\infty}^{\infty} \log \left| 1 - \frac{1}{E} \epsilon_{\gamma k'/2} \right| \coth(\pi(k' - k + i0)) dk' \pm \pi k + c \right] &= -\frac{1}{2} \log \left| 1 - \frac{1}{E} \epsilon_{\gamma k/2} \right| \pm \pi k + \Re c, \\ \Re \left[\chi \frac{\pi}{2} \int_{-\infty}^{k_E} [\coth(\pi(k' - k + i0)) - \coth(\pi(k' + i0))] dk' \right] &= \frac{\chi}{2} \log \left| \frac{\sinh(\pi(k' - k))}{\sinh(\pi k')} \right|_{-\infty}^{k_E} \\ &= \frac{\chi}{2} \log \left| \frac{\sinh(\pi(k_E - k))}{\sinh(\pi k_E)} \right| - \chi \frac{\pi}{2} k \rightarrow \chi \frac{\pi}{2} (|k| - k), \quad \text{for } |k| \rightarrow \infty, \\ \Re \left[\xi \frac{\pi}{2} \int_{-\infty}^{-k_E} [\coth(\pi(k' - k + i0)) - \coth(\pi k')] dk' \right] &= \frac{\xi}{2} \log \left| \frac{\sinh(\pi(k' - k))}{\sinh(\pi k')} \right|_{-\infty}^{-k_E} \\ &= \frac{\xi}{2} \log \left| \frac{\sinh(\pi(k_E + k))}{\sinh(\pi k_E)} \right| - \xi \frac{\pi}{2} k \rightarrow \xi \frac{\pi}{2} (|k| - k), \quad \text{for } |k| \rightarrow \infty, \end{aligned}$$

Combining, we find that the real part of the exponent in (C22) is

$$-\frac{1}{2} \log \left| 1 - \frac{1}{E} \epsilon_{\gamma k/2} \right| \pm \pi k + \pi \frac{\chi + \xi}{2} (|k| - k)$$

We see that if we chose $\chi = \xi = -1$, and the minus sign for the term $\pm\pi k$, we get

$$-\frac{1}{2} \log |1 - \frac{1}{E} \epsilon_{\gamma k/2}| - \pi |k|.$$

This guarantees the convergence of the integral in (C12).

With this choice of the constants, the function b_k becomes

$$\begin{aligned} b_k = & \exp \left[\frac{1}{2i} \int_{-\infty}^{\infty} \log |1 - \frac{1}{E} \epsilon_{\gamma k'/2}| \coth(\pi(k' - k + i0)) dk' \right. \\ & - \pi k - \frac{\pi}{2} \int_{-k_E}^{k_E} [\coth(\pi(k' - k + i0)) - \coth(\pi(k' + i0))] dk' \\ & \left. - \pi \int_{-\infty}^{-k_E} [\coth(\pi(k' - k + i0)) - \coth(\pi k')] dk' \right], \end{aligned} \quad (\text{C23})$$

where, we remind, k_E is defined in (C18).

Notice that (i) The normalizability of b_k is due to the $e^{-\pi|k|}$ asymptotic. This absolute value $|k|$ comes from the contribution from the branch cut of the log. This holds only for $E < \epsilon_0$; (ii) There exists only one normalizable solution. This means that this b_k must satisfy the condition (C13). One can check explicitly that it is indeed so.

5. The pairing vertex $\Phi(\omega_m)$

We now use b_k from Eq. (C23) to compute the function $\Phi(\omega_m)$. We recall that $\Phi(\omega_m) \equiv \Phi(\omega)$ is expressed via b_k as

$$\Phi(\omega) = 2 \int_{-\infty}^{\infty} a_{\beta} \Phi_{\beta}^*(\omega) \frac{d\beta}{2\pi} = \frac{\gamma}{2\pi} \int_{-\infty}^{\infty} b_k \epsilon_{\gamma k/2} \Phi_{\gamma k/2}^*(\omega) dk. \quad (\text{C24})$$

We show that this expression is equivalent to

$$\Phi(\omega) = \frac{1 + |\omega|^{\gamma}}{|\omega|^{\gamma/2}} f(\log |\omega|^{\gamma}) \quad (\text{C25})$$

where

$$f(x) = \int_{-\infty}^{\infty} b_k e^{-ikx} dk. \quad (\text{C26})$$

To prove this, we employ the following trick: use

$$\epsilon_{\beta} \Phi_{\beta}(\omega) = \frac{2}{1 - \gamma} \int_{-\infty}^{\infty} \frac{\Phi_{\beta}(\Omega) d\Omega}{|\Omega|^{1-\gamma} |\Omega - \omega|^{\gamma}}$$

and write

$$\Phi(\omega) = \frac{1}{\pi} \frac{\gamma}{1 - \gamma} \int_{-\infty}^{\infty} \frac{d\Omega}{|\Omega|^{1-\gamma} |\Omega - \omega|^{\gamma}} \int b_k \Phi_{\gamma k/2}^*(\Omega) dk$$

or

$$\Phi(\omega) = \frac{1}{\pi} \frac{\gamma}{1-\gamma} \int_{-\infty}^{\infty} \frac{d\Omega}{|\Omega|^{1-\gamma/2} |\Omega - \omega|^{\gamma}} f(\log(|\Omega|^{\gamma})), \quad \text{where } f(x) = \int_{-\infty}^{\infty} b_k e^{-ikx} dk.$$

Comparing this expression with Eq. (C1), we recover (C25). Notice, that this proof does not use an explicit form of the function b_k . It does, however, explicitly uses that fact that $\Phi(\omega)$ is the solution of (66).⁹⁶

The gap function $\Delta(\omega)$ is expressed as

$$\Delta(\omega) = |\omega|^{\gamma/2} f(\log |\omega|^{\gamma}) \quad (\text{C27})$$

6. Summary: the steps to obtain the pairing vertex $\Phi(\Omega)$ and the gap function $\Delta(\omega)$ for $E < \epsilon_0$.

The strategy is the following:

1. Evaluate the integral

$$I(k) = \frac{1}{2} \int_{-\infty}^{\infty} \log \left| 1 - \frac{1}{E} \epsilon_{\gamma k'/2} \right| \tanh(\pi(k' - k)) dk' \quad (\text{C28})$$

Notice, that it is real and antisymmetric.

2. Construct the function

$$b_k = \frac{\sinh(\pi k_E) e^{-iI(k)}}{\sqrt{\cosh(\pi(k - k_E)) \cosh(\pi(k + k_E))}}. \quad (\text{C29})$$

3. Compute

$$f(x) = \int_{-\infty}^{\infty} b_k e^{-ikx} dk. \quad (\text{C30})$$

4. The exact solutions of the linearized equations for the pairing vertex and the gap function are

$$\begin{aligned} \Phi_{\text{ex}}(\omega_m) &= (1 + |\omega|^{-\gamma}) f(\log |\Omega|^{\gamma}) \\ \Delta_{\text{ex}}(\omega_m) &= |\omega|^{\gamma/2} f(\log |\Omega|^{\gamma}) \end{aligned} \quad (\text{C31})$$

Appendix D: Asymptotic expansion at small and large frequencies

To understand the structure of $\Delta_{ex}(\omega_m)$ it is instructive to expand it at small and large ω_m . One can do this in two ways: expand in the formulas for the exact solution, or perturbatively expand the gap equation (10) order by order in ω_m or $1/\omega_m$.

For shortness, we present here the details of the direct perturbative expansion. The point of departure for the expansion in ω_m is the solution of (10) without the last term $1/(1 + |\bar{\omega}'_m|^\gamma)$: $\Phi(\omega_m) = \text{Re}\Phi_0(\omega_m)$, where

$$\Phi_0(\omega_m) = \frac{C_0^<}{\sqrt{|\bar{\omega}_m|^\gamma}} e^{i\phi + \beta_N \log |\bar{\omega}_m|^\gamma} \quad (\text{D1})$$

and, we remind, $\bar{\omega}_m = \omega_m/\omega_0$ and β_N is the solution of $\epsilon(\beta) = N$, where $\epsilon(\beta)$ is given by (38).

Let's expand the r.h.s. of (10) in ω_m and express $\Phi(\omega_m)$ as $\text{Re}[\Phi_0(\omega_m) + \delta\Phi(\omega_m)]$. The equation for $\delta\Phi(\omega_m)$ is

$$\begin{aligned} \delta\Phi(\omega_m) - \frac{1-\gamma}{2N} \int d\omega'_m \frac{\delta\Phi(\omega'_m)}{|\omega'_m|^{1-\gamma} |\omega_m - \omega'_m|^\gamma} = \\ - \frac{1-\gamma}{2N\omega_0^\gamma} \int d\omega'_m \frac{\Phi_0(\omega'_m)}{|\omega'_m|^{1-2\gamma}} \left(\frac{1}{|\omega_m - \omega'_m|^\gamma} - \frac{1}{|\omega'_m|^\gamma} \right) + \frac{1-\gamma}{2N\omega_0^\gamma} \int d\omega'_m \frac{\Phi_0(\omega'_m)}{|\omega'_m|^{1-\gamma}} \end{aligned} \quad (\text{D2})$$

There are two types of terms in the r.h.s of (D2). The first term is local in the sense that the integral over ω'_m is ultra-violet and infra-red convergent and is determined by ω'_m comparable to ω_m . Evaluating this term, we obtain

$$- \frac{1-\gamma}{2\omega_0^\gamma N} \int d\omega'_m \frac{\Phi_0(\omega'_m)}{|\omega'_m|^{1-2\gamma}} \left(\frac{1}{|\omega_m - \omega'_m|^\gamma} - \frac{1}{|\omega'_m|^\gamma} \right) = -|\bar{\omega}|^\gamma \Phi_0(\omega_m) I_1 \quad (\text{D3})$$

where

$$\begin{aligned} I_1 = \frac{1-\gamma}{2N} \int_{-\infty}^{\infty} dy y^{(3\gamma/2-1+i\beta_N\gamma)} \left(\frac{1}{|1-y|^\gamma} - \frac{1}{|y|^\gamma} \right) = \frac{1-\gamma}{2N} \frac{\Gamma(3\gamma/2+i\beta_N\gamma)\Gamma(-\gamma/2-i\beta_N\gamma)}{\Gamma(\gamma)} + \\ \Gamma(1-\gamma) \frac{1-\gamma}{2N} \left(\frac{\Gamma(3\gamma/2+i\beta_N\gamma)}{\Gamma(1+\gamma/2+i\beta_N\gamma)} + \frac{\Gamma(-\gamma/2-i\beta_N\gamma)}{\Gamma(1-3\gamma/2-i\beta_N\gamma)} \right) \end{aligned} \quad (\text{D4})$$

and the integration variable $y = \omega'_m/\omega_m$.

1. Local corrections.

Let's momentarily keep only the local term in the r.h.s. of (D2). We label the corresponding portion of $\delta\Phi(\omega_m)$ as $\delta\Phi_L(\omega_m)$. The functional form of $\delta\Phi_L(\omega_m)$ is determined by

(D3): $\delta\Phi_L(\omega_m) = |\bar{\omega}|^\gamma \Phi_0(\omega_m) C_1$. Substituting into (D2), we find the relation between C_1 and I_1 :

$$C_1^< = C_0^< \left(\frac{I_1}{I_1 - 1} \right) \quad (\text{D5})$$

This analysis can be straightforwardly extended to higher orders in the expansion in $|\bar{\omega}|^\gamma$. At each other we extract infra-red convergent contribution in the source term by subtracting from $1/|\omega'_m - \omega_m|^\gamma$ a proper number of terms ($1/|\omega'_m|^\gamma$, $\omega_m^2/|\omega'_m|^{\gamma+2}$, etc) to make the remaining integral over ω'_m ultra-violet convergent, and solve for $\delta\Phi_L(\omega_m)$ induced by such source terms. The result is

$$\delta\Phi_L(z) = \Phi_0(z) \sum_{n=1}^{\infty} C_n^< z^n \quad (\text{D6})$$

where, we remind, $z = |\bar{\omega}_m|^\gamma$, and

$$C_n^< = C_0^< \left[I_n \prod_{m=1}^n \frac{1}{I_m - 1} \right] \quad (\text{D7})$$

where

$$\begin{aligned} I_m &= \frac{1-\gamma}{2N} Q(m, \gamma, \beta_N), \\ Q(m, \gamma, \beta_N) &= \frac{\Gamma((m+1/2)\gamma + i\beta_N\gamma)\Gamma((1/2-m)\gamma - i\beta_N\gamma)}{\Gamma(\gamma)} + \\ &\quad \Gamma(1-\gamma) \left(\frac{\Gamma((m+1/2)\gamma + i\beta_N\gamma)}{\Gamma(1-(1/2-m)\gamma + i\beta_N\gamma)} + \frac{\Gamma((1/2-m)\gamma - i\beta_N\gamma)}{\Gamma(1-(m+1/2)\gamma - i\beta_N\gamma)} \right) \end{aligned} \quad (\text{D8})$$

Note than $C_n^<$ are complex numbers. Combining $\Delta\Phi_L$ and Φ_0 , we obtain the total local contribution to the pairing vertex $\Phi_L = \text{Re} [\Phi_0 + \delta\Phi_L]$ as

$$\Phi_L(z) = \text{Re} \left[e^{i\phi + \beta_N \log z} \sum_{n=0}^{\infty} C_n^< z^{n-1/2} \right] \quad (\text{D9})$$

Expressing (D9) as the equation for the local contribution to the gap function $\Delta_L(z) = z\Phi_L(z)/(1+z)$, we obtain the first term in (74).

At small γ and $N = O(1)$, $\beta_N \approx \frac{1}{\sqrt{N\gamma}}(1 - N\gamma/8) \gg 1$. Evaluating I_n in two orders in $1/\beta_N$, we find a simple expression

$$I_n = 1 + 2i \frac{n}{\beta_N} - 3 \left(\frac{n}{\beta_N} \right)^2 \quad (\text{D10})$$

Substituting this I_n into (D7) and then into (D6), using the relation between Φ and Δ , and exponentiating the series to order z^3 , we obtain, up to corrections of order z/β_N^2 ,

$$\Delta_L(z) = C_0^< \frac{z^{1/2}}{(1+z)^{3/4}} \cos(\phi + \beta_N Q_1(z)) \quad (\text{D11})$$

where $Q_1(z) = \log z - z/2 + 3z^2/16 + \dots$. Eq. (D11) and the expansion of $Q_1(z)$ coincide with those for $\Delta_{\text{diff}}(z)$, Eqs. (57) and (58). This explicitly confirms that for $\gamma \ll 1$, $\Delta(\omega_m) \approx \Delta_L(\omega_m) \approx \Delta_{\text{diff}}(\omega_m)$.

2. Non-local corrections.

We now look at the other terms, which we had to add and subtract at each order to make local contributions ultra-violet convergent. At the leading order in the expansion the additional term in the r.h.s. of Eq. (D2) is

$$\frac{1-\gamma}{2N\omega_0^\gamma} \int d\omega'_m \frac{\Phi_0(\omega'_m)}{|\omega'_m|^{1-\gamma}} = \frac{1-\gamma}{N\gamma} C_0^< e^{i\phi} \int_0^\infty dx x^{i\beta_N - 1/2} \quad (\text{D12})$$

This integral is ultra-violet divergent, but the divergence is fictitious because the actual $\Phi(\omega_m)$ must drop as $1/|\omega_m|^\gamma$ at large $|\omega_m|$. Accordingly, we cut ultra-violet divergencies at some $|\omega_m| = \omega_{\text{max}}$, which, we argue below, is roughly where x' changes sign. The separation into local and non-local terms obviously holds only for $|\omega_m| < \omega_{\text{max}}$. The non-local term (D12) induces another set of correction to the bare $\Phi(\omega_m) = \text{Re}\Phi_0(\omega_m)$. We label the corresponding non-local part of the full $\Phi(\omega_m)$ as $\Phi_{nL}(\omega_m)$. By construction, $\Phi_{nL}(\omega_m)$ is real. Substituting (D12) into (D2), adding the complex conjugated term, and adding and subtracting $1/|\omega'_m|^\gamma$ to/from $1/|\omega_m - \omega'_m|^\gamma$, we obtain the equation for $\Phi_{nL}(\omega_m)$ in the form

$$\Phi_{nL}(\omega_m) - \frac{1-\gamma}{2N} \int d\omega'_m \frac{\Phi_{nL}(\omega'_m)}{|\omega'_m|^{1-\gamma}} \left(\frac{1}{|\omega_m - \omega'_m|^\gamma} - \frac{1}{|\omega'_m|^\gamma} \right) = K \quad (\text{D13})$$

where

$$K = \frac{1-\gamma}{N} \int_0^{\omega_{\text{max}}} d\omega_m \left(\frac{\Phi_{nL}(\omega_m)}{|\omega_m|^\gamma} - \frac{\text{Re}\Phi_0(\omega_m)}{\omega_0^\gamma} \right) \quad (\text{D14})$$

We first notice that Eq. (D13) without the K term does have the solution $\Phi_{nL}(\omega_m) = E_{0,0}^< |\omega_m|^{(b_0-\gamma)/2}$, where b_0 is the solution of $\epsilon_{b_0/\gamma} = N$ in the interval $[\gamma/2, \gamma/2 + 2]$. For b_0 within this range, the integral in the l.h.s. of (D13) does not diverge in the infra-red and ultra-violet limits. To satisfy (D13) one needs to satisfy also the condition $K = 0$. Substituting our trial solution for $\Phi_{nL}(\omega_m)$ and $\text{Re}\Phi_0(\omega_m)$ into (D14), we find that the condition $K = 0$ is satisfied for some particular ratio $E_{0,0}^</C_0^<$.

This analysis can be extended to higher orders in the perturbation theory. The non-local terms in the r.h.s. of the equation for the pairing vertex appear in the form $A_{10} + A_{11}|\bar{\omega}_m|^\gamma +$

$A_{12}\bar{\omega}_m^{2\gamma} + \dots + A_{20}\bar{\omega}_m^2 + A_{21}|\bar{\omega}_m|^{2+\gamma} + A_{22}|\bar{\omega}_m|^{2+2\gamma} + \dots + A_{30}\bar{\omega}_m^4 + \dots$, where all A_{ij} contain $C_0^<$ as the overall factor. To cancel all these non-local terms, we choose $\Phi_{nL}(\omega_m)$ in the form

$$\Phi_{nL}(\omega_m) = \frac{1}{|\bar{\omega}|^{\gamma/2}} \sum_{n,m=0}^{\infty} D_{n,m} |\bar{\omega}|^{\beta_m + \gamma n} \quad (\text{D15})$$

where $\gamma/2 + 2m < b_m < \gamma/2 + 2(m + 1)$. The terms with $m > 0$ are solutions of the same equation (D14), but with the proper number of terms subtracted from $1/|\omega_m - \omega'_m|^\gamma$ and added to the K term in the r.h.s., to make the integral over ω'_m in the l.h.s. ultra-violet convergent. We see from Fig. 13 that there is one b_n in each interval that satisfies (D14). Substituting this form into the equation for the pairing vertex and collecting non-local terms, we find a set of coupled algebraic equations for $D_{n,m}$ with A_{ij} playing the role of source terms. The precise forms of these equations cannot be obtained within perturbative expansion in ω_m , and we just have to assume that the solution $D_{n,m}$ exists. Re-expressing (D15) as the equation for Δ_{nL} instead of Φ_{nL} , we reproduce $D_{n,m}^<$ series in (74).

Combining (D9) and (D15) we see that the r.h.s. of Eq. (74) is the sum of local and non-local contributions

$$\Delta(z) = \Delta_L(z) + \Delta_{nL}(z). \quad (\text{D16})$$

At the largest ω_m one can expand in $1/z$ and use $\Delta_0(z) = C_0^>/z$ as the zero-order solution. The expansion is straightforward and yields Eq. (75).

¹ P. Monthoux, D. Pines, and G. G. Lonzarich, *Nature* **450**, 1177 (2007); D. J. Scalapino, *Rev. Mod. Phys.* **84**, 1383 (2012).

² M. R. Norman, “Novel superfluids,” (Oxford University Press, 2014) Chap. Unconventional superconductivity.

³ D. J. Scalapino, *Rev. Mod. Phys.* **84**, 1383 (2012).

⁴ S. Maiti and A. V. Chubukov, “Novel superfluids,” (Oxford University Press, 2014) Chap. Superconductivity from repulsive interaction.

⁵ B. Keimer, S. A. Kivelson, M. R. Norman, S. Uchida, and J. Zaanen, *Nature* **518**, 179 (2015).

⁶ T. Shibauchi, A. Carrington, and Y. Matsuda, *Annual Review of Condensed Matter Physics* **5**, 113 (2014).

⁷ R. M. Fernandes and A. V. Chubukov, *Reports on Progress in Physics* **80**, 014503 (2016).

⁸ E. Fradkin, S. A. Kivelson, M. J. Lawler, J. P. Eisenstein, and A. P. Mackenzie, Annual Review of Condensed Matter Physics **1**, 153 (2010).

⁹ K.-Y. Yang, T. M. Rice, and F.-C. Zhang, Phys. Rev. B **73**, 174501 (2006).

¹⁰ L. Fratino, P. Smon, G. Sordi, and A.-M. S. Tremblay, Scientific Reports **6**, 22715 (2016).

¹¹ S. Sachdev, Reports on Progress in Physics **82**, 014001 (2018).

¹² P. Coleman, *Introduction to Many-Body Physics* (Cambridge University Press, 2015).

¹³ D. F. Mross, J. McGreevy, H. Liu, and T. Senthil, Phys. Rev. B **82**, 045121 (2010).

¹⁴ M. A. Metlitski, D. F. Mross, S. Sachdev, and T. Senthil, Phys. Rev. B **91**, 115111 (2015).

¹⁵ R. Mahajan, D. M. Ramirez, S. Kachru, and S. Raghu, Phys. Rev. B **88**, 115116 (2013); A. L. Fitzpatrick, S. Kachru, J. Kaplan, and S. Raghu, Phys. Rev. B **88**, 125116 (2013); Phys. Rev. B **89**, 165114 (2014); G. Torroba and H. Wang, Phys. Rev. B **90**, 165144 (2014); A. L. Fitzpatrick, G. Torroba, and H. Wang, Phys. Rev. B **91**, 195135 (2015), and references therein.

¹⁶ H. Wang, Y. Wang, and G. Torroba, Phys. Rev. B **97**, 054502 (2018).

¹⁷ H. Wang, S. Raghu, and G. Torroba, Phys. Rev. B **95**, 165137 (2017).

¹⁸ A. L. Fitzpatrick, S. Kachru, J. Kaplan, S. Raghu, G. Torroba, and H. Wang, Phys. Rev. B **92**, 045118 (2015).

¹⁹ A. J. Millis, Phys. Rev. B **45**, 13047 (1992).

²⁰ B. L. Altshuler, L. B. Ioffe, A. I. Larkin, and A. J. Millis, Phys. Rev. B **52**, 4607 (1995).

²¹ S. Sachdev, A. V. Chubukov, and A. Sokol, Phys. Rev. B **51**, 14874 (1995).

²² A. Abanov, A. V. Chubukov, and A. M. Finkel'stein, EPL (Europhysics Letters) **54**, 488 (2001).

²³ A. Abanov, A. V. Chubukov, and J. Schmalian, Advances in Physics **52**, 119 (2003); A. Abanov and A. V. Chubukov, Phys. Rev. Lett. **83**, 1652 (1999); A. Abanov, A. V. Chubukov, and J. Schmalian, Journal of Electron Spectroscopy and related phenomena **117**, 129 (2001); A. Abanov, A. V. Chubukov, and M. R. Norman, Phys. Rev. B **78**, 220507 (2008).

²⁴ S. Sachdev, M. A. Metlitski, Y. Qi, and C. Xu, Phys. Rev. B **80**, 155129 (2009); E. G. Moon and S. Sachdev, Phys. Rev. B **80**, 035117 (2009); S. Sachdev, H. D. Scammell, M. S. Scheurer, and G. Tarnopolsky, Phys. Rev. B **99**, 054516 (2019).

²⁵ M. Vojta and S. Sachdev, Phys. Rev. Lett. **83**, 3916 (1999).

²⁶ Y. Wang and A. V. Chubukov, Phys. Rev. Lett. **110**, 127001 (2013).

²⁷ K. B. Efetov, H. Meier, and C. Pepin, Nature Physics **9**, 442 (2013); H. Meier, C. Pépin, M. Einenkel, and K. B. Efetov, Phys. Rev. B **89**, 195115 (2014); K. B. Efetov, Phys. Rev. B

91, 045110 (2015); A. M. Tsvelik, Phys. Rev. B **95**, 201112 (2017).

²⁸ M. A. Metlitski and S. Sachdev, Phys. Rev. B **82**, 075128 (2010).

²⁹ D. Dalidovich and S.-S. Lee, Phys. Rev. B **88**, 245106 (2013); S.-S. Lee, Annual Review of Condensed Matter Physics **9**, 227 (2018).

³⁰ J. Bauer and S. Sachdev, Phys. Rev. B **92**, 085134 (2015).

³¹ C. Castellani, C. Di Castro, and M. Grilli, Phys. Rev. Lett. **75**, 4650 (1995); A. Perali, C. Castellani, C. Di Castro, and M. Grilli, Phys. Rev. B **54**, 16216 (1996); S. Andergassen, S. Caprara, C. Di Castro, and M. Grilli, Phys. Rev. Lett. **87**, 056401 (2001); Y. Wang and A. V. Chubukov, Phys. Rev. B **92**, 125108 (2015).

³² A. V. Chubukov and P. Wölfle, Phys. Rev. B **89**, 045108 (2014); D. Chowdhury and S. Sachdev, Phys. Rev. B **90**, 245136 (2014).

³³ M. Khodas, H. B. Yang, J. Rameau, P. D. Johnson, A. M. Tsvelik, and T. M. Rice, ArXiv:1007.4837 (2010); R. M. Konik, T. M. Rice, and A. M. Tsvelik, Phys. Rev. B **82**, 054501 (2010); M. Khodas and A. M. Tsvelik, Phys. Rev. B **81**, 094514 (2010); A. V. Chubukov and A. M. Tsvelik, Phys. Rev. B **76**, 100509 (2007).

³⁴ D. Vilardi, C. Taranto, and W. Metzner, arXiv:1810.02290 and references therein (2018); T. Holder and W. Metzner, Phys. Rev. B **92**, 245128 (2015); H. Yamase, A. Eberlein, and W. Metzner, Phys. Rev. Lett. **116**, 096402 (2016).

³⁵ G. Sordi, P. Simon, K. Haule, and A.-M. S. Tremblay, Phys. Rev. Lett. **108**, 216401 (2012).

³⁶ B. L. Altshuler, L. B. Ioffe, and A. J. Millis, Phys. Rev. B **52**, 5563 (1995); D. Bergeron, D. Chowdhury, M. Punk, S. Sachdev, and A.-M. S. Tremblay, Phys. Rev. B **86**, 155123 (2012); Y. Wang and A. Chubukov, Phys. Rev. B **88**, 024516 (2013).

³⁷ E.-A. Kim, M. J. Lawler, P. Oreto, S. Sachdev, E. Fradkin, and S. A. Kivelson, Phys. Rev. B **77**, 184514 (2008).

³⁸ M. J. Lawler and E. Fradkin, Phys. Rev. B **75**, 033304 (2007); E. Berg, E. Fradkin, and S. A. Kivelson, Phys. Rev. B **79**, 064515 (2009); R. Soto-Garrido and E. Fradkin, Phys. Rev. B **89**, 165126 (2014).

³⁹ N. E. Bonesteel, I. A. McDonald, and C. Nayak, Phys. Rev. Lett. **77**, 3009 (1996).

⁴⁰ W. Metzner, D. Rohe, and S. Andergassen, Phys. Rev. Lett. **91**, 066402 (2003); V. Oganesyan, S. A. Kivelson, and E. Fradkin, Phys. Rev. B **64**, 195109 (2001); Phys. Rev. B **64**, 195109 (2001); S. Sur and S.-S. Lee, Phys. Rev. B **91**, 125136 (2015); M. Punk, Phys. Rev. B **91**,

115131 (2015), and references therein. L. Dell’Anna and W. Metzner, Phys. Rev. B **73**, 045127 (2006).

⁴¹ J. Rech, C. Pépin, and A. V. Chubukov, Phys. Rev. B **74**, 195126 (2006).

⁴² S.-S. Lee, Phys. Rev. B **80**, 165102 (2009).

⁴³ M. A. Metlitski and S. Sachdev, Phys. Rev. B **82**, 075127 (2010).

⁴⁴ S. Lederer, Y. Schattner, E. Berg, and S. A. Kivelson, Phys. Rev. Lett. **114**, 097001 (2015).

⁴⁵ D. L. Maslov and A. V. Chubukov, Phys. Rev. B **86**, 155137 (2012); A. V. Chubukov and D. L. Maslov, Phys. Rev. B **86**, 155136 (2012); D. L. Maslov and A. V. Chubukov, Phys. Rev. B **81**, 045110 (2010); Phys. Rev. B **79**, 075112 (2009).

⁴⁶ Y. You, G. Y. Cho, and E. Fradkin, Phys. Rev. B **93**, 205401 (2016).

⁴⁷ Z. Wang, W. Mao, and K. Bedell, Phys. Rev. Lett. **87**, 257001 (2001); R. Roussev and A. J. Millis, Phys. Rev. B **63**, 140504 (2001); A. V. Chubukov, A. M. Finkel’stein, R. Haslinger, and D. K. Morr, Phys. Rev. Lett. **90**, 077002 (2003).

⁴⁸ S. Lederer, Y. Schattner, E. Berg, and S. A. Kivelson, Proceedings of the National Academy of Sciences **114**, 4905 (2017).

⁴⁹ A. Klein, Y.-M. Wu, and A. V. Chubukov, npj Quantum Materials **4**, 55 (2019); A. Klein and A. Chubukov, Phys. Rev. B **98**, 220501 (2018).

⁵⁰ J. M. Bok, J. J. Bae, H.-Y. Choi, C. M. Varma, W. Zhang, J. He, Y. Zhang, L. Yu, and X. J. Zhou, Science Advances **2** (2016), 10.1126/sciadv.1501329.

⁵¹ P. A. Lee, Phys. Rev. Lett. **63**, 680 (1989); B. Blok and H. Monien, Phys. Rev. B **47**, 3454 (1993); C. Nayak and F. Wilczek, Nuclear Physics B **417**, 359 (1994); B. L. Altshuler, L. B. Ioffe, and A. J. Millis, Phys. Rev. B **50**, 14048 (1994); Y. B. Kim, A. Furusaki, X.-G. Wen, and P. A. Lee, Phys. Rev. B **50**, 17917 (1994).

⁵² S. Raghu, G. Torroba, and H. Wang, Phys. Rev. B **92**, 205104 (2015).

⁵³ E.-G. Moon and A. Chubukov, Journal of Low Temperature Physics **161**, 263 (2010).

⁵⁴ D. V. Khveshchenko and W. F. Shively, Phys. Rev. B **73**, 115104 (2006).

⁵⁵ J.-H. She and J. Zaanen, Phys. Rev. B **80**, 184518 (2009); J.-H. She, J. Zaanen, A. R. Bishop, and A. V. Balatsky, Phys. Rev. B **82**, 165128 (2010).

⁵⁶ Y. Wang, A. Abanov, B. L. Altshuler, E. A. Yuzbashyan, and A. V. Chubukov, Phys. Rev. Lett. **117**, 157001 (2016).

⁵⁷ T.-H. Lee, A. Chubukov, H. Miao, and G. Kotliar, Phys. Rev. Lett. **1805**, 10280 (2018).

⁵⁸ Y.-M. Wu, A. Abanov, and A. V. Chubukov, Phys. Rev. B **99**, 014502 (2019).

⁵⁹ Y.-M. Wu, A. Abanov, Y. Wang, and A. V. Chubukov, Phys. Rev. B **99**, 144512 (2019); A. Abanov, Y.-M. Wu, Y. Wang, and A. V. Chubukov, Phys. Rev. B **99**, 180506 (2019).

⁶⁰ E. A. Yuzbashyan, A. V. Chubukov, A. Abanov, and B. L. Altshuler, “Non BCS pairing near a quantum phase transition – effective mapping to a spin chain,” In preparation.

⁶¹ A. A. Patel and S. Sachdev, Phys. Rev. Lett. **123**, 066601 (2019).

⁶² I. Esterlis and J. Schmalian, Physical Review B **100** (2019), 10.1103/physrevb.100.115132.

⁶³ Y. Wang, Phys. Rev. Lett. **124**, 017002 (2020).

⁶⁴ D. Hauck, M. J. Klug, I. Esterlis, and J. Schmalian, arXiv 1911.04328 (2019).

⁶⁵ D. Chowdhury and E. Berg, Phys. Rev. Research **2**, 013301 (2020).

⁶⁶ R. Combescot, Phys. Rev. B **51**, 11625 (1995).

⁶⁷ G. Bergmann and D. Rainer, Z. Physik **263**, 59 (1973); P. B. Allen and D. Rainer, Nature **349**, 396 EP (1991); P. B. Allen and R. C. Dynes, Phys. Rev. B **12**, 905 (1975).

⁶⁸ F. Marsiglio, M. Schossmann, and J. P. Carbotte, Phys. Rev. B **37**, 4965 (1988); F. Marsiglio and J. P. Carbotte, Phys. Rev. B **43**, 5355 (1991), for more recent results see F. Marsiglio and J.P. Carbotte, “Electron-Phonon Superconductivity”, in “The Physics of Conventional and Unconventional Superconductors”, Bennemann and Ketterson eds., Springer-Verlag, (2006) and references therein.

⁶⁹ A. Karakozov, E. Maksimov, and A. Mikhailovsky, Solid State Communications **79**, 329 (1991).

⁷⁰ A. V. Chubukov, A. Abanov, I. Esterlis, and S. A. Kivelson, Annals of Physics (2020).

⁷¹ D. T. Son, Phys. Rev. D **59**, 094019 (1999); A. V. Chubukov and J. Schmalian, Phys. Rev. B **72**, 174520 (2005).

⁷² S.-X. Yang, H. Fotso, S.-Q. Su, D. Galanakis, E. Khatami, J.-H. She, J. Moreno, J. Zaanen, and M. Jarrell, Phys. Rev. Lett. **106**, 047004 (2011).

⁷³ M. H. Gerlach, Y. Schattner, E. Berg, and S. Trebst, Phys. Rev. B **95**, 035124 (2017); Y. Schattner, S. Lederer, S. A. Kivelson, and E. Berg, Phys. Rev. X **6**, 031028 (2016); X. Wang, Y. Schattner, E. Berg, and R. M. Fernandes, Phys. Rev. B **95**, 174520 (2017); E. Berg, S. Lederer, Y. Schattner, and S. Trebst, Annual Review of Condensed Matter Physics **10**, 63 (2019).

⁷⁴ K. Haule and G. Kotliar, Phys. Rev. B **76**, 104509 (2007); W. Xu, G. Kotliar, and A. M. Tsvelik, Phys. Rev. B **95**, 121113 (2017).

⁷⁵ A. Georges, L. d. Medici, and J. Mravlje, *Annu. Rev. Condens. Matter Phys.* **4**, 137 (2013); W. Wu, M. Ferrero, A. Georges, and E. Kozik, *Phys. Rev. B* **96**, 041105 (2017).

⁷⁶ G. M. Eliashberg, *JETP* **11**, 696 (1960).

⁷⁷ A. V. Chubukov, A. Abanov, Y. Wang, and Y.-M. Wu, *Annals of Physics* , 168142 (2020).

⁷⁸ O. Simard, C.-D. Hébert, A. Foley, D. Sénéchal, and A.-M. S. Tremblay, *Phys. Rev. B* **100**, 094506 (2019).

⁷⁹ J. Linder and A. V. Balatsky, *Rev. Mod. Phys.* **91**, 045005 (2019).

⁸⁰ K. Yang and S. L. Sondhi, *Phys. Rev. B* **62**, 11778 (2000).

⁸¹ R. Haslinger and A. V. Chubukov, *Phys. Rev. B* **68**, 214508 (2003).

⁸² In obtaining the Eliashberg equations we assumed that states away from the Fermi surface are irrelevant for the pairing and NFL behavior, and extended the integration over momenta to infinite limits. In this situation, fermionic self-energy $\Sigma(\omega_m)$ is real. If the momentum integration over $k - k_F$ holds in finite and non-symmetric limits, $\Sigma(\omega_m)$ has both real and imaginary components. The same holds in SYK-type models at a non-zero chemical potential, see Ref.⁹⁷ and references therein.

⁸³ D. V. Khveshchenko, *Journal of Physics: Condensed Matter* **21**, 075303 (2009).

⁸⁴ D. Chowdhury and S. Sachdev, *Phys. Rev. B* **90**, 134516 (2014).

⁸⁵ A. J. Millis and H. Monien, *Phys. Rev. B* **54**, 16172 (1996).

⁸⁶ M. Eschrig, *Advances in Physics* **55**, 47 (2006), <https://doi.org/10.1080/00018730600645636>.

⁸⁷ A. Abanov, A. V. Chubukov, M. Eschrig, M. R. Norman, and J. Schmalian, *Physical Review Letters* **89**, 177002 (2002).

⁸⁸ A. Abanov and A. Chubukov, *Physica B* **280**, 189 (2000).

⁸⁹ J. M. Luttinger and J. C. Ward, *Phys. Rev.* **118**, 1417 (1960).

⁹⁰ J. Bardeen and M. Stephen, *Phys. Rev.* **136**, A1485 (1964).

⁹¹ A. A. Abrikosov, L. P. Gorkov, and I. E. Dzyaloshinski, *Methods of Quantum Field Theory in Statistical Physics* (Pergamon Oxford, 1965).

⁹² H. Liu, J. McGreevy, and D. Vegh, *Phys. Rev. D* **83**, 065029 (2011).

⁹³ J. Cortez, G. A. Mena Marugán, J. Olmedo, and J. M. Velhinho, *Phys. Rev. D* **83**, 025002 (2011).

⁹⁴ J. Kim, I. R. Klebanov, G. Tarnopolsky, and W. Zhao, *Phys. Rev. X* **9**, 021043 (2019).

⁹⁵ The method, presented in this Appendix, will also work for a generalized version of Eq. (C1)

with $\frac{1}{1+|\omega|^\alpha}$ instead of $\frac{1}{1+|\omega|^\gamma}$.

⁹⁶ There is another way to prove (C26) which does not use the fact that $\Phi(\omega)$ is a solution of (66), instead it uses the analytical properties of the function B_k .

⁹⁷ Y. Gu, A. Kitaev, S. Sachdev, and G. Tarnopolsky, Journal of High Energy Physics **2020**, 157 (2020).